SUBSECTION 2.5.4 TABLE OF CONTENTS

SUBSECTION 2.5.4 LIST OF TABLES

SUBSECTION 2.5.4 LIST OF TABLES (CONTINUED)

SUBSECTION 2.5.4 LIST OF FIGURES

SUBSECTION 2.5.4 LIST OF FIGURES (CONTINUED)

2.5.4 Stability of Subsurface Materials and Foundations

This subsection of the SSAR presents information on the stability of subsurface materials and foundations at the Clinch River Nuclear (CRN) Site for the early site permit application (ESPA). The information has been developed in accordance with the NRC Regulatory Guides (RGs) referenced in the subsections that follow and the guidance presented in Subsection 2.5.4, *Stability of Subsurface Materials and Foundations*, of NUREG-0080, *Standard Review Plan for the Review of Safety Analysis Reports for Nuclear Power Plants: LWR Edition*. This geological, geophysical and geotechnical information is used as a basis to evaluate the stability of subsurface materials and foundations at the CRN Site.

Information presented in this subsection has been developed from a recent subsurface investigation (Reference 2.5.4-1) performed between June 2013 and March 2014 (see Subsection 2.5.4.3.2). The subsurface investigation was performed over a substantial portion of the CRN Site but predominantly within the footprint of the power block area. It was originally designed to support a construction permit application (CPA) and the location of the units being sited at that time (Locations A and B). Reports prepared for the abandoned Clinch River Breeder Reactor Project (CRBRP) including the Preliminary Safety Analysis Report (PSAR) (References 2.5.4-2 and 2.5.4-3) and several reports prepared by Law Engineering (References 2.5.4-4 and 2.5.4-5) were also reviewed. The information from these CRBRP reports; however, is used for comparative purposes only. A list of the reports and geotechnical literature utilized in preparing this subsection is provided in Subsection 2.5.4.14.

Additional site-specific exploration and testing, required to support the combined license application (COLA), will be performed as needed, during detailed engineering when a reactor technology has been selected.

2.5.4.1 Geologic Features

The following discussions focus on geologic features that may affect the CRN Site power block area (a composite that represents the bounding power block area associated with the plant parameter envelope and shown on Figure 2.5.4-1) at the CRN Site. More detailed descriptions of geologic features are presented in Subsection 2.5.1. The information is taken from the recent subsurface investigation program performed at the CRN Site (outlined in Subsection 2.5.4.3). For reference, the existing site elevations in the power block area range from approximately 855 (MP-406) to 780 feet (ft) (MP-207, MP-211) with an average elevation of about 810 ft. A finished plant grade elevation of 821 ft North American Vertical Datum of 1988 (NAVD88) is used for the power block area. Foundation embedment is not expected to exceed a depth of 138 ft below finished grade (Elevation [El.] 683 ft).

All references to elevation given in the following subsections are to NAVD88, with the exception of elevations pertaining to the CRBRP which are with respect to the National Geodetic Vertical Datum of 1929 (NGVD29). In the project area, there is generally a difference of less than 0.5 ft between NAVD88 and NGVD29, with NGVD29 being greater. Likewise, all exploratory point locations are provided relative to Tennessee State Plane Coordinates in North American Datum of 1983 (NAD83) and all references to depth are below the existing ground surface unless stated otherwise.

2.5.4.1.1 Stratigraphy

The stratigraphy at the CRN Site is described in Subsections 2.5.1.1.3.1 and 2.5.1.2.3.2 and a stratigraphic column developed for the site is shown on Figure 2.5.1-28. The stratigraphy at the site is characterized by stratigraphic units that strike northeast and dip relatively steeply to the southeast. The cross-section developed from the subsurface investigation is shown on

Figure 2.5.4-2 and shows the bedrock structure and succession of the stratigraphic units within the footprint of the power block area. Oriented perpendicular to the strike of the bedding planes, rocks belonging to the Knox Group outcrop to the northwest and progressively younger rocks belonging to the Chickamauga Group outcrop to the southeast. The contact between the Knox and Chickamauga Groups is a disconformity. The stratigraphic units within the power block area include from northwest to southeast the Newala Formation, belonging to the Knox Group, the Blackford Formation, the Eidson and Fleanor Members, and the Rockdell and Benbolt Formations belonging to the Chickamauga Group. Detailed descriptions of these units are provided in Subsection 2.5.1.2.3.2. A cross-section that illustrates the depth to Precambrian rock, drawn perpendicular to strike, is shown on Figure 2.5.4-13. Descriptions of these units are provided in Subsection 2.5.1.1.3.1.

Acoustic Televiewer (ATV) logging and outcrop mapping performed at the CRN Site (outlined in Subsection 2.5.1.2.4) reveal the average strike and dip of the bedding planes is N63°E and 33°SE and does not change considerably between the stratigraphic units. A dip angle of 33 degrees is used to project the contacts between the stratigraphic units at depth in the power block area and to estimate the apparent (vertical) thickness of each of the stratigraphic units (Figure 2.5.4-2). Where the stratigraphic contacts were not encountered in the borings, the contacts are projected based on unit thicknesses provided by Hatcher et al. (Reference 2.5.4-6). The true thickness of the stratigraphic units is estimated by multiplying the apparent thickness by the cosine of the dip angle 33 degrees. The true and apparent thicknesses and percent variability are provided in Table 2.5.4-1 for each of the stratigraphic units.

As shown on Figure 2.5.4-2 a foundation embedment depth of approximately 138 ft below finished grade (El. 683 ft) is considered. Because of the dipping beds at the site, various stratigraphic units may be exposed at the foundation level at different locations within the power block area. The implication of this with respect to the evaluation of the foundations for bearing capacity and settlement is discussed in Subsection 2.5.4.10.

2.5.4.1.2 Previous Loading History

Prior to site development for the CRBRP, topography at the site consisted of rolling hills trending northeast-southwest. During site development portions of two of these hills were removed, reportedly by blasting techniques, and excavation for the reactor building extended approximately 100 ft below the ground surface in the center of the site (See Figure 2.5.1-54). The excavation, backfilling and grading associated with the CRBRP was extensive, and once the project was terminated, this area was redressed. This included filling a portion of the excavation (Reference 2.5.4-7).

Table 2.5.4-2 shows the approximate differences between the historic ground surface elevations prior to site development for the CRBRP recent subsurface investigation. The locations of these borings are shown on Figure 2.5.4-1. Based on a comparison of these elevations, up to about 20 ft of fill was placed in the southern portion of the power block area and up to 70 ft of material was removed from the central and northern portions. Outside the power block area as much as 50 ft of fill was placed in areas and approximately the same amount was removed in other areas.

2.5.4.1.3 Discontinuities, Shear-Fracture Zones and Weathered/Fracture Zones

The following subsections discuss discontinuities, shear-fracture zones, and weathered and fractured zones at the CRN Site.

2.5.4.1.3.1 Discontinuities

A detailed discussion on the bedding planes and joints encountered in the borings at the CRN Site is provided in Subsection 2.5.1.2.4. Discontinuities encountered at the CRN Site are related to folding and faulting. Discontinuities include bedding planes and joints. As described previously the orientation of the bedding planes does not change considerably between the stratigraphic units with average strikes ranging between N59°E and N65°E and dips between 32°SE and 35°SE. Two primary joint sets are identified at the site. Both of these joint sets strike parallel to the strike of the bedding planes. The most commonly occurring joint set at the site (Joint Set 1) has an average strike and dip of N60°E and 59°NW and the second (Joint Set 2) has an average strike and dip of N60°E and 38°SE. Three near-vertical secondary joint sets are identified at the site, one that strikes parallel to the strike of the bedding and two that strike parallel to bedding.

ATV data collected during the recent subsurface investigation (Appendix C, Reference 2.5.4-1) indicate that the highest frequency of joints occurs in the upper 100 ft of bedrock. The two primary joint sets are prevalent in all of the stratigraphic units at the site at varying depths while the secondary joint sets are encountered predominantly in the Newala Formation. Most of the joints within each set are described as discontinuous hairline and planar hairline. The joints are generally described as undulating to planar, rough to smooth to slickensided, very tight to open with tightly healed to slightly altered joint walls; the joints are commonly partially or wholly filled with calcite (Reference 2.5.4-1).

Geologic mapping data of the exposed bedrock surface of the CRBRP excavation are available and are discussed in Subsection 2.5.1.2.9. Observations on the occurrence and orientations of the bedding planes and joints are summarized in a technical paper by Kummerle et al. (Reference 2.5.4-8). Observations during mapping reveal that along the west side of the excavation the bedding planes consistently dip at a steeper angle and the concentration of flatter angles observed in some of the rock core are less frequent. Also, the limestone encountered on the east side of the excavation is reported as thinly bedded while the underlying siltstone is reported as more massive and hard. Fewer high angle joints are also reported than had been assumed for rock excavation design and the joints that were mapped in the thinly bedded limestone are reported to be discontinuous. The dip of the high angle joints are reported to be higher, at or near vertical as opposed to the 70- to 75-degree range assumed for design (Reference 2.5.4-8).

2.5.4.1.3.2 Shear-Fracture Zones

A detailed discussion on the shear-fracture zones encountered in the 100- and 200-series borings (Locations A and B, respectively) at the CRN Site is provided in Subsections 2.5.1.2.4 and 2.5.1.2.6.4. Descriptions from the borings indicate that the shear-fracture zones are typically zones of multiple, closely spaced, tightly healed, calcite filled shear fractures (Reference 2.5.4-1). A summary of the shear-fracture zones (greater than or equal to approximately 0.9 ft thick [apparent thickness along boring axis]) encountered in the 100- and 200-series borings is contained in Table 2.5.1-17 and shown on Figure 2.5.1-60. The shear-fracture zones are encountered in the Rockdell and Benbolt Formations (100-series borings) and the Eidson Member (200- and 400-series borings) between elevations of about 750 and 450 ft. The zones range in thickness from about 1 to 22 ft with an average apparent thickness of about 4 ft. The shear-fracture zones encountered are considered to be similar to the shear zone encountered during the CRBRP (Reference 2.5.4-3), as discussed in Subsection 2.5.1.2.6.4.

Shear-fracture zones are likely to be encountered at or below the foundation level. For this reason, the shear-fracture zones are incorporated in the average Geological Strength Index (GSI) rating for each stratigraphic unit for rock mass characterization (See Subsection 2.5.1.2.6).

During excavation for the power block area, detailed geologic mapping provides further characterization of any shear-fracture zones encountered.

Characterization of the shear-fracture zones are based on the 100-, 200-, and 400-series borings drilled at the CRN Site. Further evaluation of these zones is performed at COLA, when a reactor technology has been selected.

2.5.4.1.3.3 Weathered and Fracture Zones

A detailed discussion on the weathered/fracture zones encountered in the 100- and 200-series borings at the CRN Site is provided in Subsection 2.5.1.2.6.3. The fracture zones typically occur along bedding planes or fractures and likely represent early dissolution of the limestone. These zones typically represent poor to fair quality rock consisting of multiple, healed to open, slightly to highly weathered fractures or bedding planes, some calcite or dolomite filled, with occasional core loss and loss of drilling fluid reported (Reference 2.5.4-1). A summary of the fracture zones (greater than or equal to approximately 0.9 ft thick [apparent thickness along boring axis]) encountered in the 100- and 200-series is contained in Table 2.5.1-16 and shown on Figure 2.5.1-59. The fracture zones are typically encountered within approximately 50 ft of the ground surface between elevations of approximately 800 and 750 ft and the apparent thickness of the fracture zones ranges from about 1 to 12 ft with an average apparent thickness of about 3 ft.

The weathered/fracture zones are incorporated in the average GSI rating for each of the stratigraphic units for rock mass characterization. During excavation of the power block area, detailed geologic mapping provides further characterization of any weathered or fracture zones encountered.

Characterization of the weathered and fracture zones are based on the 100- and 200-series borings drilled at the CRN Site. Further evaluation of these zones will be performed as needed in support of the COLA, when a reactor technology has been selected.

2.5.4.1.4 Karst Features

A detailed discussion on the presence of karst features reported for the CRBRP (Reference 2.5.4-3) and encountered at the CRN Site (Reference 2.5.4-1) is provided in Subsection 2.5.1.2.5. Cavities are present in each of the stratigraphic units at the site. These cavities (equal to or greater than 0.1 ft in height) include open- and clay-filled cavities and range in height from less than 1 to about 17 ft, as shown in Table 2.5.1-11 and Figures 2.5.1-51 and 2.5.1-52. These cavities are encountered predominantly in the Rockdell Formation and Eidson Member with fewer cavities encountered in the Benbolt and Blackford Formations and the Fleanor Member. The frequency with which these cavities occur decreases with increasing depth and the majority of the cavities occur within approximately 100 ft of the ground surface.

A discussion on the cavities encountered in the borings drilled as part of the recent subsurface investigation is provided in Subsection 2.5.1.2.6. A number of cavities encountered in the Rockdell Formation (MP-424) are close to and below the deepest foundation embedment depth (El. 683 ft). Four of the five cavities are encountered approximately 5 to 20 ft below the deepest foundation embedment depth. These four cavities range in height from 0.7 to 4.3 ft with cavity bottom elevations ranging from approximately 661 to 676 ft (Table 2.5.1-11).

A mitigation plan to address possible cavities encountered at and below the foundation levels of safety-related structures during excavation is discussed in Subsection 2.5.1.2.6.10. Details of this plan will be developed in support of the COLA.

2.5.4.1.5 Unrelieved Stresses in Bedrock

A discussion on unrelieved stresses in the bedrock at the CRN Site is provided in Subsection 2.5.1.2.6. High residual stresses are not expected in the rock mass at the CRN Site and are not considered to be a hazard during construction or for bearing capacity of the foundation rock mass (see Subsection 2.5.1.2.6.7).

Bedrock at the CRN Site has been subject to normal overburden stress, and thus removal of this stress results in an adjustment in the rock mass in terms of loosening along discontinuities and possibly the development of additional discontinuities. Site development for the power block area at the CRN Site involves the removal of overburden by blasting techniques. As a result of blasting and stress unloading, a disturbed zone of rock adjacent to the foundation occurs. (See Subsection 2.5.1.2.6.7)

As described in Subsection 2.5.4.2.4.4 rock mass strength properties and deformation moduli are estimated for this disturbed zone in addition to the rock below this zone.

2.5.4.2 Properties of Subsurface Materials

This section describes the static and dynamic engineering properties of the CRN Site subsurface materials encountered during the subsurface investigation. An overview of the materials is given in Subsection 2.5.4.2.1. The field investigations, described in Subsection 2.5.4.3, are summarized in Subsection 2.5.4.2.2. The results of laboratory tests performed on soil and rock samples are described in Subsection 2.5.4.2.3. The engineering properties are described in Subsection 2.5.4.2.4.

2.5.4.2.1 Description of Subsurface Materials

The following is a brief description of the subsurface materials and their range in thickness encountered at the site. The information is taken from the borings made for the recent subsurface investigation (outlined in Subsection 2.5.4.3.2) contained in Appendix B of Reference 2.5.4-1. Table 2.5.1-2 summarizes the borings drilled and the subsurface material encountered for the recent subsurface investigation. For reference, the existing site elevations in the areas explored range from about 762 (MP-407) to 855 ft (MP-406) with an average elevation of approximately 806 ft. Finished grade elevation within the power block area is 821 ft.

2.5.4.2.1.1 Existing Fill and Residual Soils

Depths and thicknesses of existing fill and residual soil encountered in the borings are summarized in Table 2.5.4-3. Fill was encountered at the ground surface in most of the borings drilled at the site. The thickest deposit of fill encountered is 51 ft (MP-416). Residual soils are typically encountered immediately below the fill and the thickest deposit of residual soil encountered is 51 ft (MP-418A). With regard to assigning engineering properties, the existing fill and residual soils are considered a single soil unit (existing fill/residual soil). Both the existing fill and residual soils are classified as high plasticity (CH) clay according to the Unified Soil Classification System (USCS), ASTM D2487 (Reference 2.5.4-9). Median Standard Penetration Test (SPT) N_{60}-values indicate that the existing fill and residual soils are medium dense with values of 14 and 19 blows per foot (bpf), respectively.

2.5.4.2.1.2 New Backfill

New granular backfill is used as backfill around structures, to raise grade and as backfill in undercut areas. Backfill surrounding the safety-related structures consists of both lean concrete and granular backfill with lean concrete extending from the foundation level to the top of rock.

Granular backfill is used from the top of rock to finished grade (El. 821 ft). A description of the proposed material is contained in Subsection 2.5.4.5.

2.5.4.2.1.3 Weathered Rock

Depths and thicknesses of weathered rock encountered in the borings are summarized in Table 2.5.4-3. The recent subsurface investigation shows that weathered rock is encountered in most of the borings drilled at the site (Appendix B.1, Reference 2.5.4-1). During the drilling operations, weathered rock was defined as a material having a SPT of 50 blow counts resulting in less than 6 inches (in.) of penetration. (Reference 2.5.4-1)

Subsequent to the recent investigation Rock Quality Designation (RQD) values, ASTM D6032 (Reference 2.5.4-10), shear wave velocity (V_S) values, drill rates and rock core photographs were reviewed to further define the thickness of weathered rock and the corresponding depth to the top of sound rock (hereinafter referred to as rock or bedrock). RQD values equal to or less than 25 percent, representative of very poor quality rock (Reference 2.5.4-10) along with significantly lower-than-average V_S values were also used to define the thickness of weathered rock. The maximum thickness of weathered rock at the CRN Site is approximately 39 ft (MP-415). Weathered rock is excavated from the power block area prior to construction of foundations.

2.5.4.2.1.4 Bowen Formation

The Bowen Formation is a maroon calcareous siltstone. Because of its limited thickness and its distinctive color, Hatcher et al. (Reference 2.5.4-6) describe it as a reliable marker for field and subsurface correlations. The recent subsurface investigation generally describes the bedrock as a reddish brown to olive brown, laminated to very thinly bedded calcareous siltstone. A detailed description of the bedrock is contained in Subsection 2.5.1.2.3.

The Bowen Formation was encountered in two borings (MP-415 and MP-428) for a total linear footage of 41 ft (see Table 2.5.4-1). The top of the formation was encountered in the two borings at elevations of 773 and 765 ft (see Table 2.5.1-2). The thickness of the Bowen Formation is illustrated on the subsurface profile on Figure 2.5.4-2. The average apparent (vertical) thickness of the formation based on the borings is estimated at 30 ft (see Table 2.5.4-1). The Bowen Formation is outside of the footprint of the power block area (see Figure 2.5.4-2).

RQD values for the Bowen Formation range from 14 to 53 percent with average and median values of 26 and 20 percent, respectively, indicative of poor to very poor quality rock.

2.5.4.2.1.5 Benbolt Formation

The Benbolt Formation comprises interbedded fossiliferous nodular limestone, unfossiliferous amorphous micrite within a dark gray siltstone matric, and unfossiliferous calcarenite (Reference 2.5.4-6). The recent subsurface investigation describes the bedrock as a gray limestone (micrite/wackestone), strong, very thinly to thinly bedded, locally moderately bedded, and nodular limestone interbedded with little to some laminated to thinly bedded calcareous siltstone. A detailed description of the bedrock is contained in Subsection 2.5.1.2.3.

The Benbolt Formation is encountered in the southeastern portion of the power block area, predominantly in the 100-series borings but also in a few of the 400-series borings. Twenty-five borings penetrated into the Benbolt Formation for a total linear footage of 3254 ft (see Table 2.5.4-1). The top of the formation encountered in the borings ranges in elevation from about 794 to 739 ft (determined from Table 2.5.1-2). The thickness of the Benbolt Formation is illustrated on the subsurface profile on Figure 2.5.4-2. The average apparent (vertical) thickness of the formation based on the borings is estimated at 330 ft. (see Table 2.5.4-1).

RQD values for the Benbolt Formation range from 0 to 100 percent with average and median values of 88 and 98 percent, respectively, indicative of good to excellent quality rock. Rock core recovery and RQD values obtained from the borings are summarized in Table 2.5.4-4 and shown on Figure 2.5.4-3.

2.5.4.2.1.6 Rockdell Formation

The Rockdell Formation is a thick limestone with bedded and nodular chert that transitions with depth to a calcareous siltstone, a fossiliferous nodular limestone and a micritic limestone (Reference 2.5.4-6). The recent investigation generally describes the bedrock as two units, Unit C and Unit D, based on an 11 to 32 ft thick calcareous siltstone layer that forms the contact between the two units (Reference 2.5.4-1). Units C and D are generally described as gray and brownish-gray, strong, laminated to moderately bedded limestone (micrite/wackestone/grainstone), interbedded with few to little, laminated to very thinly bedded calcareous siltstone. A detailed description of the bedrock is contained in Subsection 2.5.1.2.3. With regard to assigning engineering properties, the Rockdell Formation is considered as a single unit.

The Rockdell Formation is encountered in the central and southeastern portions of the power block area, predominantly in the 100-series borings but also in some of the 400-series borings. Sixteen borings penetrated into the Rockdell Formation for a total linear footage of 1794 ft (see Table 2.5.4-1). The top of the formation encountered in the borings ranges in elevation from about 801 to 577 ft (determined from Table 2.5.1-2). The thickness of the Rockdell Formation is illustrated on the subsurface profile on Figure 2.5.4-2. The average apparent (vertical) thickness of the formation based on the borings is estimated at 287 ft (see Table 2.5.4-1).

RQD values range from 0 to 100 percent with average and median values of 88 and 96 percent, respectively, indicative of good to excellent quality rock. Rock core recovery and RQD values obtained from the borings are summarized in Table 2.5.4-4 and shown on Figure 2.5.4-3.

2.5.4.2.1.7 Fleanor Member (Lincolnshire Formation)

The upper member of the Lincolnshire Formation, the Fleanor Member, comprises maroon, calcareous and shaly siltstone with numerous light gray limestone beds (Reference 2.5.4-6). The recent investigation generally describes the bedrock as a red, medium strong, laminated to medium bedded, calcareous siltstone with few to little gray micritic limestone layers. A detailed description of the bedrock is contained in Subsection 2.5.1.2.3.

The Fleanor Member is encountered in the central portion of the power block area, predominantly in the 200-series borings but also in some of the 400-series borings. Twenty nine borings penetrated into the Fleanor Member for a total linear footage of 2953 ft (see Table 2.5.4-1). The top of the Fleanor Member encountered in the borings ranges in elevation from 809 to 381 ft (determined from Table 2.5.1-2). The thickness of the Fleanor Member at the CRN Site is illustrated on the subsurface profile on Figure 2.5.4-2. The average apparent (vertical) thickness of the member based on the recent investigation is estimated at 257 ft (see Table 2.5.4-1).

RQD values range from 0 to 100 percent with average and median values of 89 and 98 percent, respectively, indicative of good to excellent quality rock. Rock core recovery and RQD values obtained from the borings are summarized in Table 2.5.4-4 and shown on Figure 2.5.4-3.

2.5.4.2.1.8 Eidson Member (Lincolnshire Formation)

The lower member of the Lincolnshire Formation, the Eidson Member, comprises massive to nodular limestone with bedded and nodular chert (Reference 2.5.4-6). The recent investigation generally describes the bedrock as a gray, medium strong and strong, laminated to thinly bedded, fresh, argillaceous micritic limestone.

The Eidson Member is encountered in the central and northwestern portions of the power block area, predominantly in the 200-series borings but also in some of the 400-series borings. Seventeen borings penetrated into the Eidson Member for a total linear footage of 1027 ft (see Table 2.5.4-1). The top of the Eidson Member encountered in the borings ranges in elevation from about 809 to 604 ft (determined from Table 2.5.1-2). The thickness of the Eidson Member at the CRN Site is illustrated on the subsurface profile on Figure 2.5.4-2. The average apparent (vertical) thickness of the member based on the borings is estimated at 102 ft (see Table 2.5.4-1).

RQD values range from 0 to 100 percent with average and median values of 79 and 88 percent, respectively, indicative of good quality rock. Rock core recovery and RQD values obtained from the borings are summarized in Table 2.5.4-4 and shown on Figure 2.5.4-3.

2.5.4.2.1.9 Blackford Formation

The Blackford Formation comprises purplish to dark maroon calcareous siltstone interbedded with light gray calcarenite (Reference 2.5.4-6). The recent investigation describes the bedrock as two units, the Lower and Upper Blackford. The contact between the Lower Blackford and the underlying Newala Formation is a disconformity. The Lower Blackford is generally described as a gray, locally mottled, strong, laminated to thickly bedded, micritic limestone. The Upper Blackford is generally described as a gray, calcareous siltstone, laminated to moderately bedded, interbedded with little to some limestone with few to little chert beds, lenses and nodules. A detailed description of the bedrock is contained in Subsection 2.5.1.2.3. With regard to assigning engineering properties, the Blackford Formation is considered as a single unit.

The Blackford Formation Member is encountered in the central and northwestern portions of the power block area, in the 200-series and 400-series borings. Fifteen borings penetrated into the Blackford Formation for a total linear footage of 1554 ft (see Table 2.5.4-1). The top of the Blackford Formation encountered in the borings ranges in elevation from 840 to 507 ft (determined from Table 2.5.1-2). The thickness of the formation at the CRN Site is illustrated on the subsurface profile on Figure 2.5.4-2. The average apparent (vertical) thickness of the formation based on the borings is estimated at 254 ft (see Table 2.5.4-1).

RQD values range from 0 to 100 percent with average and median values of 81 and 92 percent, respectively, indicative of good to excellent quality rock. Rock core recovery and RQD values obtained from the borings are summarized in Table 2.5.4-4 and shown on Figure 2.5.4-3.

2.5.4.2.1.10 Newala Formation

The Newala Formation is the uppermost unit of the Knox Group and comprises predominantly fine to medium grained dolomite with some chert nodules (Reference 2.5.4-6). Hatcher et al. (Reference 2.5.4-6) report that the thickness of the Newala Formation is variable due to the erosional unconformity (disconformity) and indicates the relief on this surface is a minimum of about 230 ft. The recent investigation generally describes the formation as a fresh, fine to medium grained, gray, locally mottled red, strong to very strong, moderately to thickly bedded crystalline dolomite, with few irregular chert nodules and chert beds. A detailed description of the bedrock is contained in Subsection 2.5.1.2.3.

The Newala Formation is encountered in the northwestern portion of the power block area, predominantly in the 400-series borings and one 200-series boring (MP-201). Sixteen borings penetrated into the Newala Formation for a total linear footage of 2501 ft (see Table 2.5.4-1). The top of the formation encountered in the borings ranges in elevation from approximately 815 to 481 ft (determined from Table 2.5.1-2). Regionally, the thickness of the formation is estimated to range between 900 and 1200 ft (Reference 2.5.4-11). The thickness of the formation at the CRN Site is unknown as none of the borings drilled at the site penetrated the full thickness of the unit (see Figure 2.5.4-2).

RQD values range from 0 to 100 percent with average and median values of 93 and 98 percent, respectively, indicative of excellent quality rock. Rock core recovery and RQD values obtained from the borings are summarized in Table 2.5.4-4 and shown on Figure 2.5.4-3.

2.5.4.2.1.11 Subsurface Profiles

Figure 2.5.4-2 illustrates a typical subsurface profile through the footprint of the power block area. The profile is constructed perpendicular to the strike of the bedding planes (parallel to the dip direction). The location of this profile is shown on Figure 2.5.4-1. This profile is presented with respect to excavation within the power block area to a foundation embedment depth of 138 ft below finished grade (El. 683 ft).

2.5.4.2.2 Field Investigations

The field investigation programs performed previously for the CRBRP and the recent field investigation performed at the CRN Site are described in Subsection 2.5.4.3. A summary of the investigations performed for the CRBRP is in Table 2.5.4-5. A summary of the field work performed for the recent subsurface investigation is in Table 2.5.4-6. A summary of the soil and rock strata encountered in the borings is in Table 2.5.1-2. Geophysical surveys performed for the CRBRP and at the CRN Site are described in Subsection 2.5.4.4. The field investigation at the CRN Site was performed in accordance with guidance presented in RG 1.132, *Site Investigations for Foundations of Nuclear Power Plants*.

2.5.4.2.3 Laboratory Testing

As with the field exploration, laboratory tests of soil and rock samples were performed previously for the CRBRP and have been performed as part of the recent subsurface investigation. Previous test results are summarized in the CRBRP PSAR (Reference 2.5.4-2). The types and numbers of tests completed during the recent subsurface investigation are shown in Table 2.5.4-7 and the test results are contained in Reference 2.5.4-1.

The laboratory testing was performed in accordance with the guidance presented in RG 1.138, Rev. 2, *Laboratory Investigations of Soils and Rocks for Engineering Analysis and Design of Nuclear Power Plants*. The laboratory work was performed under an approved quality program with work procedures developed specifically for the project. Soil and rock samples were shipped under chain-of-custody protection from the storage area (described in Subsection 2.5.4.3.2) to the testing laboratory. If required, samples were further divided and/or shipped to the appropriate testing laboratory under chain-of-custody rules. Laboratory testing was performed at the AMEC laboratories in Durham, North Carolina and Atlanta, Georgia (all soil testing) and Charlotte, North Carolina (rock core testing). Testing was also performed at AMEC QA-approved laboratories at GeoTesting Express in Acton, Massachusetts (rock core testing) and TestAmerica, Inc. in St. Louis, Missouri (geochemical testing).

The tests performed on the soil samples focused primarily on obtaining the basic characteristics of the soil (grain size, natural moisture content and plasticity) and the shear strength and

compaction characteristics. The tests performed on the rock core samples focused on obtaining the basic characteristics of the rock (unit weight and specific gravity), compressive strength, shear and elastic moduli, Poisson's ratio, slake durability and calcium carbonate content.

The details and results of the laboratory testing are included in Appendices F through H of Reference 2.5.4-1. These appendices include references to the industry standard used for each specific laboratory test. The results of the tests on soil samples are shown on Tables 2.5.4-9, 2.5.4-10, and 2.5.4-12. The results of the tests on the rock core samples are summarized for each of the stratigraphic units on Tables 2.5.4-13 to 2.5.4-15, 2.5.4-19 and 2.5.4-20.

2.5.4.2.4 Engineering Properties

The engineering properties for the existing fill/residual soil, granular backfill, weathered rock and the bedrock within the footprint of the power block area are derived from the recent subsurface investigation and laboratory testing programs and are provided in Table 2.5.4-21.

The engineering properties for the bedrock are developed for each of the stratigraphic units, independent of depth. Field and laboratory test results indicated no appreciable variation in the intact rock and rock mass properties with depth. Engineering properties are developed for the Benbolt and Rockdell Formations, the Eidson and Fleanor Members of the Lincolnshire Formation and the Blackford and Newala Formations. The engineering properties are developed to evaluate the stability of the foundation materials.

The following subsections briefly describe the sources and/or methods used to develop the selected properties shown in Table 2.5.4-21.

2.5.4.2.4.1 Soil Properties

The following paragraphs describe the properties of the existing fill/residual soil. The properties are developed based on the results of the laboratory testing program unless stated otherwise. The properties of the proposed granular backfill are discussed in Subsection 2.5.4.5.3.

The recommended SPT N_{60}-value in Table 2.5.4-21 is based on corrected field measured N-values using the relationship given in Coduto (Reference 2.5.4-12). A summary of the field measured N-values and the calculated N_{60}-values is provided in Table 2.5.4-8. The recommended value shown in Table 2.5.4-21 is based on the combined median N_{60}-value for the existing fill and residual soil. Field measured N-values are adjusted with various correction factors to improve their repeatability and account for variations in test procedures (Reference 2.5.4-12). The values are corrected for energy (N_{60}) where 60 is the percentage of the theoretical free-fall hammer energy, boring diameter, sampler type and rod length. The following equation was used to calculate the N_{60}-values.

$$N_{60} = E_R \times C_B \times C_S \times C_R \times N \qquad \text{Equation 2.5.4-1}$$

where:

- N_{60} = N-value adjusted for field procedures
- E_R = energy correction factor = ETR/60%; where ETR = energy transfer ratio
- C_B = borehole diameter correction; where diameter = 2.5 to 4.5 in., C_B = 1.00
- C_S = sampler correction factor for soil sampler; C_S = 1.20 for split-spoon sampler without a liner
- C_R = rod length correction; C_R ranges from 0.75 for lengths less than 10 ft to 1.00 for lengths greater than 30 ft
- N = field SPT value (bpf)

Sieve analyses of 34 existing fill/residual soil samples were performed, the results of which are summarized in Table 2.5.4-9. The recommended fines content in Table 2.5.4-21 for the existing fill/residual soils is the average of these test results.

The results for the natural moisture contents and Atterberg limits of the existing fill/residual soil are shown in Table 2.5.4-9. As described in Subsection 2.5.4.2.1.1, both the existing fill and residual soil are high plasticity clays (CH) based on the USCS, ASTM D2487 (Reference 2.5.4-9). The recommended values shown in Table 2.5.4-21 are taken as the average of the test results from the existing fill.

The dry unit weight and moisture content results for the existing fill are contained in Table 2.5.4-10. The average dry unit weight and average moisture content are used to determine the total unit weight in Table 2.5.4-21. Specific gravity values are contained in Table 2.5.4-10. The recommended value is shown in Table 2.5.4-21.

The undrained shear strength of the existing fill was determined from unconsolidated undrained (UU) triaxial tests, the results of which are contained in Table 2.5.4-10. The undrained shear strength is also estimated from the unconfined compressive strength of the soil using the relationship that the undrained shear strength is approximately one-half of the unconfined compressive strength. The unconfined compressive strength is estimated based on SPT N_{60}-values (Reference 2.5.4-13). The recommended value shown in Table 2.5.4-21 is the smaller of these two values computed.

The drained shear strength, effective cohesion and angle of internal friction of the existing fill were determined from consolidated undrained (CU) triaxial tests, the results of which are contained in Table 2.5.4-10. The recommended values shown in Table 2.5.4-21 are based on the average of these test results but are adjusted (downward adjustment) to account for the small number of laboratory tests performed.

Shear (V_s) and compression (V_p) wave velocity measurements were taken in three borings in the existing fill/residual soil as part of the recent field testing program. The measurements were taken using suspension P-S velocity methods (Appendix C, Reference 2.5.4-1). The results are summarized in Table 2.5.4-11. The average V_s and V_p values are shown in Table 2.5.4-21. Using these average V_s and V_p values, a Poisson's ratio is calculated using Equation 2.5.4-2 (Reference 2.5.4-14) and is shown in Table 2.5.4-11. This value is considered high for cohesive soil and is adjusted (downward adjustment) as shown in Table 2.5.4-21.

$$\mu = \frac{((V_p/V_s)^2 - 2)}{2 \cdot ((V_p/V_s)^2 - 1)}$$ Equation 2.5.4-2

where:

μ = Poisson's ratio

V_s = Shear wave velocity

V_p = Compression wave velocity

The low strain (strains of 10^{-4} percent or less) shear modulus is derived using the relationship between V_s, total unit weight and acceleration due to gravity given in Equation 2.5.4-3 from Bowles (Reference 2.5.4-14). The low strain elastic modulus is derived using the relationship between the shear modulus and the modulus of elasticity given in Equation 2.5.4-4 from Reference 2.5.4-14. The values are shown in Table 2.5.4-21.

$G_L = (\gamma/g)\cdot V_s^2$ Equation 2.5.4-3

$E = 2(1+\mu)\cdot G$ Equation 2.5.4-4

where:

G = Shear modulus

E = Elastic modulus

γ = Total unit weight

g = Acceleration due to gravity

V_s = Shear wave velocity

The high strain or static modulus of elasticity is derived using the relationship with the undrained shear strength in Equation 2.5.4-5 given in Reference 2.5.4-16. The high strain shear modulus is derived using the relationship between elastic modulus, shear modulus and Poisson's ratio given in Equation 2.5.4-4. The recommended values are shown in Table 2.5.4-21.

$E_H = 600 \times S_u$ Equation 2.5.4-5

where:

E_H = High strain elastic modulus

S_u = Undrained shear strength

Maximum dry density and optimum moisture content were determined as part of the recent laboratory testing program. Bulk samples of the existing fill were taken for testing from two test pits, TP-1 and TP-2. The results of the modified Proctor compaction tests, ASTM D1557 (Reference 2.5.4-15) are shown in Table 2.5.4-12. The values shown in Table 2.5.4-21 are based on the average of the results from TP-1 and TP-2 (with oversize correction applied).

2.5.4.2.4.2 Weathered Rock Properties

Weathered rock is described in Subsection 2.5.4.2.1.3. Although the weathered rock will be excavated during construction, it is considered in site response analysis and selected engineering properties of the weathered rock are developed from in situ testing and material correlations.

The total unit weight in Table 2.5.4-21 is assumed based on the mid to upper range of unit weights for a silty sand and gravel (90 to 155 pcf) (Reference 2.5.4-13).

A limited number of V_s and V_p measurements were taken in the weathered rock as part of the field testing program. The measurements were taken using suspension P-S velocity methods (Appendix C, Reference 2.5.4-1). The results are summarized in Table 2.5.4-11. The average V_s and V_p values are shown in Table 2.5.4-21. Using these average V_s and V_p values, a Poisson's ratio is calculated using Equation 2.5.4-2, and is shown in Table 2.5.4-21.

2.5.4.2.4.3 Intact Rock Properties

The following paragraphs describe the intact rock properties developed for the stratigraphic units encountered within the footprint of the power block area. These include the Benbolt, Rockdell, Blackford and Newala Formations and the Fleanor and Eidson Members. The properties are

developed based on the results of the laboratory and field testing programs performed for the CRN Site.

The total unit weight and specific gravity of the stratigraphic units were determined from the laboratory test results. The results are summarized in Table 2.5.4-13. The values in Table 2.5.4-21 are the average total unit weight and specific gravity.

Moisture content tests were conducted on rock core samples retrieved from the Fleanor Member. The results are summarized in Table 2.5.4-14 and show the average and median values for the samples that were handled with special care and the average and median values for the samples that were handled with routine care (Reference 2.5.4-17). Some of the rock core samples were handled with special care to determine if the handling method influenced the moisture content of the rock; no noticeable differences in moisture content were observed. The moisture content in Table 2.5.4-21 is the rounded average and median value.

Unconfined compressive strength tests were conducted as part of the laboratory testing program. The corrected measurements (corrected based on the length/diameter ratio) are summarized for each of the stratigraphic units in Table 2.5.4-15 and plotted against depth on Figure 2.5.4-4. The recommended unconfined compressive strength values in Table 2.5.4-21 are based on the lowest (most conservative) rounded median or average value.

V_s and V_p measurements for each of the stratigraphic units are summarized in Table 2.5.4-16 and plotted against depth on Figures 2.5.4-5 and 2.5.4-6. The average V_s and V_p values have been selected as shown in Table 2.5.4-21. Using these average V_s and V_p values, a Poisson's ratio is calculated using Equation 2.5.4-2, and is shown in Table 2.5.4-21.

The low strain (strains of 10^{-4} percent or less) shear modulus is derived using the relationship between V_s, total unit weight and acceleration of gravity in Equation 2.5.4-3. The low strain elastic modulus is derived using the relationship between the shear modulus and the modulus of elasticity in Equation 2.5.4-4. The results are summarized in Table 2.5.4-21.

The high strain shear modulus of elasticity is derived from laboratory test results. The high strain shear modulus is derived using the relationship between elastic modulus, shear modulus and Poisson's ratio in Equation 2.5.4-4. The results are summarized in Table 2.5.4-21.

For sound rock, shear and elastic moduli typically remain constant at both small and large strains, as is indicated by the similar results for the low strain and high strain shear and elastic moduli of the stratigraphic units. The results of the low strain shear and elastic moduli are selected as shown in Table 2.5.4-21. Pressuremeter testing performed as part of the recent field investigation program provides shear moduli at various loadings and thus various levels of strain. The results indicate a strain-hardening (ductile) behavior suggesting that the use of the low strain values is conservative. The results of the pressuremeter tests are summarized in Tables 2.5.4-17 and 2.5.4-18 and discussed in more detail in Subsection 2.5.4.3.

The coefficient of sliding is derived from the tangent of the angle of friction between the foundation material and the bedrock. The value in Table 2.5.4-21 is from Reference 2.5.4-13 and is for mass concrete founded on clean, sound rock.

Slake durability index tests were performed as part of the laboratory testing program. Slake durability indices provide an indication of the susceptibility of the rock to slaking. The results are summarized in Table 2.5.4-19. The slake durability indices in Table 2.5.4-21 are the average values for each of the bedrock units.

Calcium carbonate content tests (calcite equivalent, percent) were conducted as part of the laboratory testing program. The results are summarized in Table 2.5.4-20. The values in Table 2.5.4-21 are average values unless only one test was performed in which case this value is the recommended value.

2.5.4.2.4.4 Rock Mass Properties

Rock mass properties differ from intact rock properties in that they account for discontinuities and features such as weathered and fracture zones and shear-fracture zones in the stratigraphic units. The following paragraphs describe the rock mass strength and deformation properties developed for the stratigraphic units encountered within the power block area.

The properties are developed using the GSI. The application of the GSI classification and Hoek-Brown failure criterion assumes that the rock mass contains several sets of discontinuities that are closely spaced relative to the proposed structure, such that it behaves as a homogeneous and isotropic mass and that a predetermined failure plane does not exist. In other words, while the behavior of the rock mass is controlled by the movement and rotation of the rock blocks separated by intersecting discontinuities, there are no preferred failure directions (Reference 2.5.4-18). The size of the power block area excavation is expected to be much larger than the rock blocks that make up the rock mass at the site (Figure 2.5.4-2).

Rock core and geophysical data regarding discontinuities and fractures zones were reviewed for the presence of continuous weathered or fractured zones that provide a predetermined failure plane. As discussed in Subsection 2.5.1.2.6.3, data indicate that weathered or fractured zones are, for the most part, encountered in the uppermost 100 ft. The rock mass below this zone typically is tighter and contains less frequent and less persistent (shorter) discontinuities. Observations from a grouting program conducted within the excavation footprint of the CRBRP and excavation for the CRBRP foundation supports this conclusion (Reference 2.5.4-2, Appendix 2-C, and Reference 2.5.4-61). The grouting program demonstrated very little grout take and the excavation observations reported very little groundwater inflow. Both observations support the conclusion that the discontinuities below the weathered zone are tight, less frequent and shorter and do not result in predetermined failure surfaces.

As described in detail, in Subsection 2.5.1.2.6, the GSI for each stratigraphic unit is represented as a range rather than a single value. The range in GSI is used to estimate the rock mass strength and deformation properties. The GSI results for each of the stratigraphic units are summarized in Table 2.5.1-15. The GSI values for the stratigraphic units are used in the computer program RocData to determine the strength and deformation characteristics of the rock mass.

The rock mass strength and deformation properties are developed for the stratigraphic units within a disturbed zone adjacent to the foundation to account for stress relief and blast damage of the rock mass immediately adjacent to the foundation and a zone below this zone, an undisturbed zone. Reference 2.5.4-19 provides guidelines on the use of a disturbance factor, D, which ranges from D = 0 for undisturbed rock masses to D = 1 for very disturbed rock masses. Reference 2.5.4-19 recommends D = 0.7 for damage from controlled blasting.

The rock mass strength and deformation properties are developed using the GSI classifications of the stratigraphic units that are based on a select number of 100-, 200- and 400-series borings drilled at the CRN Site.

Rock Mass Strength

The rock mass strength is developed using the Generalized Hoek-Brown failure criterion. The Hoek-Brown failure criterion is an empirical criterion which relates strength in terms of the major and minor principal stresses. Its nonlinear form distinguishes it from the well-known linear Mohr-Coulomb failure criterion. Originally developed by Hoek and Brown (Reference 2.5.4-20) the fundamental idea of the Hoek-Brown criterion starts with the properties of the intact rock and reduces these properties due to the existence of discontinuities in the rock (GSI). It assumes that failure is controlled by interlocked blocks and pieces of intact rock, with no preferred failure planes. The GSI classification system has been developed for the estimation of rock mass properties and is a key input parameter in the Hoek-Brown failure criterion.

As described in Subsection 2.5.1.2.6.2, the GSI has evolved and has been expanded to include poor quality rock mass and the development of the GSI chart which is based on the blockiness of the rock mass and the condition of the discontinuity surfaces in the rock mass (Reference 2.5.4-21) (Figure 2.5.1-58). The data presented in Subsection 2.5.1.2.6 and shown on the set of figures comprising Figure 2.5.1-38 indicate that the rock mass at the CRN Site contains five distinct joint sets that define the blockiness of the rock mass, making GSI applicable to the site as supported by Hoek et al. (Reference 2.5.4-50, Figure 4).

The rock mass strength properties are developed using the Generalized Hoek-Brown criterion given in the computer program RocData. The Hoek-Brown material constants (m_i, m_b, s and a) are derived using the GSI and/or D and a combination of these constants is used with the uniaxial compressive strength of the intact rock to develop the tensile and uniaxial compressive strengths of the rock mass and the global compressive strength of the rock mass (overall strength of the rock mass).

To determine the equivalent using (best-fit) Mohr Coulomb parameters (c' and ø') for the Hoek-Brown strength criterion in RocData, the maximum principal stress at failure (σ_{3MAX}) is set equal to the compressive strength of the intact rock divided by four. The maximum principal stress at failure (σ_{3MAX}) is the maximum principal stress over which the equivalent Mohr-Coulomb parameters are calculated.

The RocData input and output parameters are summarized for each stratigraphic unit in Table 2.5.4-22, for D = 0, and Table 2.5.4-23, for D = 0.7. The rock mass strength properties for each of the stratigraphic units are summarized in Table 2.5.4-24. Comparing rock mass compressive strength against intact compressive strength for the stratigraphic units with GSI greater than or equal to 80 indicates that the rock mass compressive strengths of approximately 1500 to 6600 pounds per square inch (psi) are approximately one-third of the intact compressive strengths of 4500 to 20,000 psi, which appears reasonable for the CRN Site for an undisturbed rock mass (D = 0).

Rock Mass Deformation Modulus

The deformation modulus (Young's Modulus) of the rock mass is developed using three empirical equations in RocData. The Generalized Hoek-Diederichs method given in Reference 2.5.4-22 uses the elastic modulus of the intact rock and GSI and D. The Simplified Hoek-Diederichs method, given in Reference 2.5.4-22, uses GSI and D. The Hoek, Carranza-Torres and Corkum method given in Reference 2.5.4-19 utilizes the compressive strength of the intact rock and GSI and D. The RocData input and output parameters are summarized for each of the stratigraphic units in Table 2.5.4-22, for D = 0, and Table 2.5.4-23, for D = 0.7.

In addition to the methods available in RocData, the deformation modulus of the rock mass is derived using the empirical equation proposed in Reference 2.5.4-23. Reference 2.5.4-24

compares estimates of deformation moduli calculated from a number of other empirical equations to measured settlements and found that moduli estimated as a function of GSI given in Reference 2.5.4-19, and empirical equations given in Reference 2.5.4-23 provide an acceptable fit. The method given in Reference 2.5.4-23 utilizes only GSI.

The rock mass deformation moduli estimated using these empirical equations for each of the stratigraphic units are summarized in Table 2.5.4-25. Also in this table for comparison purposes are the moduli obtained from the in situ pressuremeter tests and developed from the low strain V_s data. Rock mass deformation moduli for low strain are frequently overestimated using V_s data and frequently underestimated using in situ pressuremeter test method. This is shown in Table 2.5.4-25 where estimates of the deformation moduli derived from the V_s range from approximately 5000 to 11,400 ksi and from in situ pressuremeter testing range from about 900 to 2400 ksi. Estimates of the rock mass deformation moduli given by Reference 2.5.4-22 (Generalized Hoek-Diederichs method), Reference 2.5.4-19 and Reference 2.5.4-23 for both disturbed (D = 0.7) and undisturbed (D = 0.0) rock masses generally occur between these ranges and appear to confirm that these empirical methods provide reasonable values for the CRN Site.

2.5.4.3 Foundation Interfaces

Subsection 2.5.4.3.1 summarizes previous subsurface investigations performed for the CRBRP while Subsection 2.5.4.3.2 summarizes the recent subsurface investigation program implemented for the CRN Site.

2.5.4.3.1 Subsurface Investigation Program for the CRBRP

The subsurface investigation program performed and the results obtained for the CRBRP are described in detail in the PSAR (References 2.5.4-2 and 2.5.4-3). Table 2.5.4-5 summarizes the studies performed for the CRBRP and the following paragraphs provide a brief description of the exploration program.

Over 100 soil and rock core borings were completed for the CRBRP for siting the safety-related structures. A selection of these boring locations is shown on Figure 2.5.4-1. These existing borings are designated as the B-series borings (Reference 2.5.4-3). The soil borings were advanced using rotary wash drilling techniques and SPTs were performed at 5-ft intervals in accordance with ASTM D1586 (Reference 2.5.4-3). The rock core borings were advanced in accordance with ASTM D2113-70 using NQ-, HQ-, and NX-size core barrels. Rock core recovery and RQD values were recorded.

Observation wells were installed in select borings at the CRBRP site to measure groundwater levels and to obtain groundwater samples. Permeability tests were conducted and piezometers were installed in a number of the wells. In situ deformation characteristics of the intact rock were measured using a Goodman Jack. (Reference 2.5.4-3)

2.5.4.3.2 Recent Subsurface Investigation Program for the CRN Site

The recent subsurface investigation was performed between June 2013 and March 2014. The investigation was performed over a substantial portion of the CRN Site but predominantly within the footprint of the power block area. The investigation consisted of a substantial number of exploration points and was originally designed to support the CPA and the locations of the units (Locations A and B) being sited at that time. These exploration point locations are identified as the MP-series and are shown on Figures 2.5.4-1 and 2.5.4-2.

The scope of the work is listed below:

- 82 exploratory borings
- Three test pits
- 44 observation wells
- Two surface geophysical tests – reflection and refraction
- Downhole geophysical tests in 28 borings
- Field permeability and pumping tests
- Groundwater level monitoring in the observation wells
- Rock pressuremeter tests in two borings.
- Survey of all exploration points
- Laboratory testing of boring soil and rock core samples.

The exploration program was performed following the guidelines in RG 1.132, *Site Investigations for Foundations of Nuclear Power Plants*. The field work was performed under an audited and approved quality program and work procedures developed specifically for the project. Soil and rock core samples were stored in an onsite storage facility during the subsurface investigation. The samples were transported to and stored in the sample storage facility following the method in ASTM D4220 (Reference 2.5.4-27). (Reference 2.5.4-1)

Details and results of the exploration program are contained in Appendices A through I of Reference 2.5.4-1. The borings, test pits, observation wells, and rock pressuremeter testing are summarized below. The laboratory tests are summarized and the results presented in Subsection 2.5.4.2. The geophysical tests are summarized and the results presented in Subsection 2.5.4.4.

2.5.4.3.2.1 Borings and Soil Samples/Rock Cores

The 82 borings drilled at the CRN Site ranged in depth from about 20 to 540 ft. The deep borings, drilled to depths greater than or equal to about 350 ft, are at least 200 ft deeper than the deepest foundation embedment depth which is not expected to exceed 138 ft (El. 683 ft). Borings include the MP-series borings (100-, 200-, and 400-series) and the CC-B series borings. With the exception of six of the borings (MP-111 PS; MP-111 UD; MP-122 PS-A; MP-122 PS-B; MP-122 UD-A, and MP-122 UD-B) that were drilled in soil only, all of the borings were drilled in soil and extended into the bedrock.

The 100- and 200-series borings drilled at the site are located within the footprint of the CRN Site power block area in Locations A and B, respectively. A number of the 400-series borings are also within the footprint of the power block area, while the majority is in the surrounding areas. Seven of the borings (MP-112, -113, -212, -213, -424, -425, and -425) were drilled at inclinations of between 25 and 29 degrees from the vertical. (See Figure 2.5.4-1 Sheet 2)

The borings were advanced in soil using rotary wash drilling techniques until SPT refusal occurred (the PS and UD designated soil borings were advanced using air rotary techniques and hollow-stem auger, respectively). Steel casing was then set into the rock, and the holes were advanced using wireline rock coring equipment consisting of 5-ft long HQ3 core barrels with a split inner barrel. The soil was sampled using an SPT sampler at 2.5-ft intervals to about 15 ft

deep and at 5-ft intervals below 15 ft. The SPTs were performed with automatic hammers in accordance with ASTM D1586 (Reference 2.5.4-29). The automatic hammers were calibrated in accordance with ASTM D4633 (Reference 2.5.4-28). The recovered soil samples were visually described and classified by the onsite geologist. A selected portion of the soil sample was placed in a glass sample jar with a moisture proof lid. The sample jars were labeled, placed in boxes and transported to the onsite storage area. SPT refusal was defined as a SPT N-value of 50 blow counts resulting in less than 6 in. of penetration. SPT N-values were not obtained in the inclined borings or the PS or UD designated borings. However, soil samples were recovered using the SPT sampler for classification purposes. (Reference 2.5.4-1)

Intact soil samples were taken in borings MP-111 UD, MP-122 UD-A, and MP-122 UD-B. Samples were retrieved using 3-in. thin-walled tube samples in accordance with ASTM D1587 (Reference 2.5.4-25). (Section 2.7.3 of Reference 2.5.4-1)

Rock coring was performed in accordance with ASTM D2113 (Reference 2.5.4-26). Rock coring was typically conducted upon SPT refusal and rock was recovered in 5-ft long core runs. After removal from the split inner barrel, the recovered rock was carefully placed in wooden core boxes then photographed. The onsite geologist visually described the core, noting the presence of joints and fractures and distinguishing natural breaks from mechanical breaks, and recorded this information on the field logs. The geologist also computed the percentage recovery and RQD. Filled core boxes were transported to an onsite sample storage facility. Here, a senior geologist reviewed the field logs against the rock core and re-photographed the core. (Reference 2.5.4-1)

The borings were backfilled with cement-bentonite slurry once all testing and sampling was completed. All casing was removed from the borings during grouting except for three designated PS holes where the PVC casing was grouted in place to enable P-S velocity logging. At boring MP-219 approximately 59 ft of drill tools were left in place due to the core barrel becoming locked in the hole. (Section 2.5 of Reference 2.5.4-1)

The boring logs and the photographs of the rock cores are contained in Appendix B of Reference 2.5.4-1. Boring locations and depths etc. are summarized in Table 2.5.1-2.

2.5.4.3.2.2 Observation Wells/Well Tests

Forty-four groundwater wells were installed at the CRN Site. Thirty-four of the wells are used as groundwater observation wells for monitoring of groundwater levels and, in select wells, water quality sampling. The observation wells were installed as two or three well-clusters; eight two-well clusters and six three-well clusters. Additional wells installed at the CRN Site were for aquifer performance testing and consisted of one pumping test well and six adjacent pumping-test-specific observation wells (see Subsection 2.4.12). (Section 3.0 of Reference 2.5.4-1)

The site observation and pumping test wells were installed based on information from adjacent geotechnical borings that were drilled prior to installing the wells. This included conducting downhole geophysical logging and packer permeability tests in many of the geotechnical borings identified for installation of adjacent observation groundwater wells. (Section 3.0 of Reference 2.5.4-1)

The observation wells were screened in the weathered rock and/or bedrock between elevations of about 796 and 492 ft (Table 3.1 of Reference 2.5.4-1). Borings for the observation wells were advanced using a rotary air-percussion drill rig. After the designated depth of each well was reached, the PVC well screen and casing were set in the boring, the sand pack and bentonite seal were placed, followed by a grout plug which was placed from the top of the bentonite seal to

the ground surface. Each well was capped with a protective locked steel cover and surrounded with a concrete pad. (Section 3.0 of Reference 2.5.4-1)

Each well was developed by pumping and surging. Field permeability slug tests were performed in most of the observation wells in accordance with ASTM D4044 (Reference 2.5.4-30). Both rising and falling head tests were performed when possible. Pneumatic or mechanical testing equipment was used for the slug testing. Slug testing was not performed in a few of the observation wells due to low or variable groundwater levels (see Subsection 2.4.12). Electronic transducers and data loggers were used to measure the water levels and times during the test. (Reference 2.5.4-1)

The pumping test was performed to obtain estimates of transmissivity, storage coefficient, and hydraulic conductivity at the test location. The test is described in detail in Appendix 2.4.12B.

Observation well installation and field permeability records are contained in Appendix E of Reference 2.5.4-1.

2.5.4.3.2.3 Groundwater Levels/Sampling

Water level measurements were initially taken in the completed observations wells on a weekly basis between September 24 and December 20, 2013 using an electronic water level meter. Thereafter, water levels were collected on a monthly basis for the remainder of the 12-month duration followed by collection on a quarterly basis for the second year of monitoring. Pressure transducers were installed in 13 of the observation wells (OW-101 well series, OW-202 well series, OW-409 well series, OW-417 well series, and the OW-423 well series) for continuous groundwater level monitoring. The results of the groundwater monitoring are discussed in detail in Subsection 2.4.12. (Section 3.5 of Reference 2.5.4-1)

Groundwater samples were obtained from selected observation wells for geochemical characterization including pH, specific conductance, turbidity, dissolved oxygen, temperature, redox potential, and for major anions and cations (Section 3.6 of Reference 2.5.4-1). Tables 2.4.12-15 and 2.4.12-16 present the results of the geochemical tests. Subsection 2.5.4.6.3 discusses the results of the geochemical analysis regarding the durability of foundation materials.

Groundwater level monitoring readings are contained in Appendix I of Reference 2.5.4-1. Geochemical test results are contained in Appendix H of Reference 2.5.4-1.

2.5.4.3.2.4 Test Pits

Three test pits (TP-1, TP-2, and TP-3) were excavated at the CRN Site, the locations of which are shown on Figure 2.5.4-1. Test pits TP-1 and TP-2 are located in the footprint of the power block area while TP-3 is located to the south, close to the CC-B-series borings. The test pits were excavated using a track mounted CAT 314C-LCR excavator to depths ranging between 3 and 12 ft. The excavated soil was visually described and classified by the onsite geologist and recorded on a field log. Bulk samples of representative soil types were taken using 2 or 3 5-gallon plastic buckets and 2 glass jars with moisture proof lids for each sample. Upon completion of the excavation, each test pit was backfilled with the excavated soil. The test pit logs are contained in Appendix B of Reference 2.5.4-1. (Section 2.9 of Reference 2.5.4-1)

2.5.4.3.2.5 Rock Pressuremeter Testing

Rock pressuremeter testing was performed by a specialty contractor in two borings, MP-105 and MP-205. Three test intervals were selected per boring and each test interval was approximately

1.4 ft long. In boring MP-105 the tests were performed in the Benbolt and Rockdell Formations between depths of approximately 82 and 188 ft. In MP-205 the tests were performed in the Fleanor and Eidson Members between depths of about 72 and 210 ft. The tests were performed with an initial loading and three unload/reload cycles at pressure increments of approximately 500, 1000, and 1500 psi. Table 2.5.4-17 summarizes the results of the pressuremeter tests and the shear modulus determined from the test results. (Appendix B.3 of Reference 2.5.4-1)

For the CRBRP, in situ Goodman Jack tests were conducted and the elastic moduli derived from the results of these tests are presented in the PSAR (Reference 2.5.4-3). The results are summarized in Table 2.5.4-18. As shown in this table, the range of elastic moduli for the Fleanor and Eidson Members derived from the in situ Goodman Jack tests (Reference 2.5.4-3) is large. The elastic moduli calculated from the average pressuremeter test results for the Fleanor and Eidson Members fall within this range.

2.5.4.3.2.6 Direct Shear Tests

Direct shear strength tests were performed on nine rock core samples in accordance with ASTM D5607 (Reference 2.5.4-31). Intact shear strength tests were performed on five rock core samples and sliding friction tests were performed on four rock core samples. The tests were conducted to determine the shear strength of discontinuities for rock slope design during excavation and construction.

2.5.4.4 Geophysical Surveys

Subsection 2.5.4.4.1 summarizes previous geophysical investigations performed for the CRBRP, while Subsection 2.5.4.4.2 summarizes the recent geophysical program implemented at the CRN Site.

2.5.4.4.1 Previous Geophysical Surveys for CRBRP

The geophysical surveys performed and the results obtained for the CRBRP are described in the PSAR (Reference 2.5.4-3). These surveys included a suite of downhole geophysical testing performed in a number of the borings for the CRBRP and included, but was not limited to, electrical resistivity, spontaneous potential, gamma, and V_s and V_p. The downhole V_s and V_p measurements from the CRBRP subsurface investigation program are compared to the recent measurements obtained for the CRN Site in Table 2.5.4-16. (Reference 2.5.4-3)

2.5.4.4.2 Geophysical Surveys for the CRN Site.

Subsection 2.5.4.4.2.1 summarizes the methods used and results of surface geophysical testing that were performed at the CRN Site. Subsection 2.5.4.4.2.2 summarizes the methods used and results of the downhole geophysical testing that were performed at the CRN Site.

2.5.4.4.2.1 Surface Geophysical Testing

Surface geophysical testing at the CRN Site consisted of performing a seismic refraction and reflection survey. The following paragraphs summarize the methods used and the results obtained. The results are contained in Appendix D of Reference 2.5.4-1.

Seismic Refraction Survey

The seismic refraction survey was performed at the CRN Site in June 2013 to map the depth to bedrock beneath six seismic refraction profiles, designated SRS-1 through SRS-6. The locations of these lines are shown on Figure 2.5.4-1. Seismic refraction lines SRS-1 though SRS-5 are

located in the footprint of the power block area while SRS-6 is located west of the power block area in the former CRBRP excavation.

The seismic refraction survey was conducted using the P-wave seismic refraction technique. Details of the seismic refraction method and equipment used are given in Appendix D of Reference 2.5.4-1, which also contains a detailed description of the results.

Seismic tomography models for SRS-1 through SRS-6 are shown on Figure 2.5.4-7. The three color schemes in the models (blue-green, yellow-orange, and red-pink) represent low, intermediate and high velocities that occur at 3000 feet per second (fps), 6500 fps and 10,000 fps, respectively. Also shown on the models as a dotted line is the interpreted-seismic-bedrock-interface (7000 fps), the locations of borings that are within approximately 50 ft of each line and the depths to the top of weathered rock and bedrock from the borings logs.

In the central portion of the power block area the tomographic models for SRS-1, SRS-2 and SRS-5 show that the interpreted depth to bedrock is between approximately 9 and 42 ft. In the southern portion of the power block area the tomographic models for SRS-3 and SRS-4 show that the interpreted depth to bedrock is between approximately 16 and 43 ft. In both areas there is reasonable consistency between the depth to bedrock from the interpreted seismic-bedrock interface and the depth interpreted from the boring logs. Any differences in the depth to bedrock from the interpreted seismic-bedrock interface and from the boring logs are considered to reflect the degree of weathering of the bedrock and/or the presence of saturated soil (Appendix D, Reference 2.5.4-1).

The tomographic model for SRS-6, located in the former excavation for the CRBRP, shows that the interpreted depth to bedrock is about 54 ft. Beneath the westernmost and easternmost portions of the line, the interpreted depths to bedrock are shallower at about 3 and 30 ft, respectively.

Seismic Reflection Survey

The seismic reflection survey was performed at the CRN Site in November 2013 within the bedrock beneath two reflection profiles, designated SRL-1 and SRL-2, to interpret the following: the contact (disconformity) between the stratigraphic units of the Chickamauga Group and underlying Knox Group; the general inclination of the bedding planes in the stratigraphic units between the borings; and the presence of any anomalies, such as faults or cavities. The locations of the SRL-1 and SRL-2 lines are shown on Figure 2.5.4-1. Seismic reflection survey line SRL-1 is located in the power block area, while SRL-2 is located west of the power block area. (Section 2.11.2 of Reference 2.5.4-1)

The seismic reflection survey was conducted using the P-wave seismic reflection technique based on the procedure outlined in ASTM D7128 Reference 2.5.4-32. Details of the seismic reflection method and equipment used are given in Appendix D of Reference 2.5.4-1, which also contains a detailed description of the results. Data processing included enhanced stack options such as spectral whitening; an FX predictive deconvolution enhancement filter; and, finite difference time migration. Because there are always issues with data quality at the end of survey lines due to reduction in fold, the survey lines were extended beyond the proposed plant area so that data migration was not needed to obtain high quality data in the survey target area beneath the potential power block locations. The lengths of the survey lines were constrained by the Clinch River to the south and Chestnut Ridge to the north and could not have been easily extended to obtain the additional data required to resolve the anomalies or artifacts described below.

The uninterpreted and interpreted, nonmigrated, P-wave seismic reflection sections for SRL-1 are shown on Figure 2.5.1-36. The interpretable regions of the section are delineated by orange/yellow lines at the end of each section. Three horizons shown as yellow, blue and green lines on the section represent the zone within which the contact between the stratigraphic units of the Chickamauga Group and underlying Knox Group is inferred. Anomalies in the section are represented by annotated blue dashed lines. Interpretation of these data is discussed in Subsection 2.5.1.2.4.2.1.

Within the interpreted portion of SRL-1, the reflectors generally show continuous, moderately steeply dipping beds. Three anomalous zones are identified on the section. Two of these zones (A-1 and A-3) reflect areas where there is a change in dip of the beds and are interpreted as being artifacts associated with out-of-plane reflectors or special aliasing. The zone designated A-2 reflects a distortion in the reflectors in the zone within which the contact between the stratigraphic units of the Chickamauga Group and underlying Knox Group is inferred and is interpreted to represent the effects of tuning or the interference from events outside of the plane of the seismic profile. No other anomalies such as offsets or structural features are interpreted within the section.

The results for SRL-2 are similar to the results for SRL-1. Two anomalous areas are interpreted on the section where the reflectors appear to be disrupted; however, neither of them displays disruptions in the overlying or underlying horizons that are indicative of a fault-like feature (Reference 2.5.4-1).

2.5.4.4.2.2 Downhole Geophysical Testing

Downhole geophysical testing was performed at the CRN Site between June and October 2013. Downhole geophysical measurements were collected in 27 uncased and 3 cased borings. The purpose of the downhole testing was to obtain the following: (Section 2.12.1 of Reference 2.5.4-1)

- V_p and V_s (Suspension P-S velocity logging)
- Acoustic televiewer (ATV) and deviation data
- Conductivity and natural-gamma data
- Caliper and natural-gamma data
- Fluid temperature, fluid conductivity and natural-gamma data

Downhole testing was performed in borings drilled using rotary wash drilling and wireline rock coring techniques. An exception to this was a number of borings where the upper portions of the borings collapsed. Attempts to keep the borings open long enough to allow testing included sequencing the removal of casing, circulating thick drilling mud, and the use of weak grout mixes followed by re-drilling. However, after several attempts with little success it was decided that only downhole P-S logging and deviation testing would be performed in the overburden in a select number borings. These borings, MP-111PS, MP-122PS-A, and MP-122PS-B were drilled using rotary air drilling techniques and P-S velocity logging and deviation data were obtained through grouted-in-place PVC casing. (Section 2.12.1 of Reference 2.5.4-1)

Details of the methods and equipment used to perform the downhole geophysical tests are provided in Appendix C of Reference 2.5.4-1, which also contains a detailed description of the results. The method and results are summarized briefly in the following paragraphs.

Suspension P-S Velocity Logging

The purpose of the suspension P-S velocity logging was to obtain V_s and V_p for the various stratigraphic units. It was used to obtain in situ measurements of vertically propagating horizontally polarized shear and compressional wave velocities at 1.64 ft intervals. The borings were filled with water during logging. The acquired data were analyzed and the profiles of velocity versus depth for each boring were produced for both compressional and horizontally polarized shear waves. The profiles are contained in Appendix C of Reference 2.5.4-1.

V_s and V_p profiles compiled for each of the stratigraphic units are shown on Figures 2.5.4-5 and 2.5.4-6. The velocity measurements are grouped by stratigraphic unit based on their recorded mid-point depth in the boring and the stratigraphic contacts identified for each unit. Compilation of the profiles did not include velocity measurements from the inclined borings or from boring MP-420 (considered too far from the power block area) and measurements within the weathered rock were omitted. A summary of the minimum, maximum and average V_s and V_p for each of the stratigraphic units is contained in Table 2.5.4-16.

Table 2.5.4-16 shows that V_s and V_p are typically higher for the limestone- and dolomite-dominant lithologies. The Newala Formation exhibits the highest average V_s and V_p of 10,800 fps and 19,900 fps, respectively. The Rockdell Formation and Eidson Member exhibit similar velocities with average V_s of 9000 fps and V_p of about 17,000 fps. Likewise, the Benbolt and Blackford Formations exhibit similar V_s and V_p with average V_s of 8000 and 8200 fps and average V_p of 15,400 and 15,700 fps, respectively. The Fleanor Member exhibits the lowest average V_s and V_p of 7200 fps and 14,500 fps, respectively.

Also contained in Table 2.5.4-16 are the minimum, maximum and average V_s and V_p for the Fleanor and Eidson Members and Blackford Formation obtained for the CRBRP. These measurements are similar to those obtained for the CRN Site.

The velocity profiles on Figures 2.5.4-5 and 2.5.4-6 show that V_s and V_p do not change appreciably with depth.

Acoustic Televiewer (ATV) Logging

The purpose of the ATV logging was to obtain boring deviation/inclination data and to collect images of the borings walls in accordance with ASTM D5753 (Reference 2.5.4-33). The data and images were collected using a HiRAT model High Resolution Acoustic Televiewer probe (HIRAT). (Section 2.12.5 of Reference 2.5.4-1)

The ATV data were processed to produce sinusoidal projections of planar and semi-planar discontinuities over the televiewer images. The sinusoidal projections were processed to calculate an apparent dip angle using the nominal boring diameter for each boring. True dip was calculated and is presented on the logs in arrow format with true dip indicated by the arrow position across the plot. Azimuth of dip (not strike) is indicated by the direction of the arrow tail. The true dip and azimuth are presented with the comments on the right-hand side of the log. The televiewer data were processed for deviation data, and three dimensional plots produced. (Appendix C of Reference 2.5.4-1)

The televiewer images and the dip and azimuth of the dip data are produced on multi-page logs in Appendix C of Reference 2.5.4-1. ATV and boring deviation data were collected in all of the borings with the exception of MP-111PS, MP-122PSA and MP-122PSB where only deviation data were collected. Depths on all of the vertical logs are referenced to ground surface while depths for the inclined borings are along the boring axis. Rose diagrams of the discontinuity dip

azimuths are also produced in Appendix C of Reference 2.5.4-1. (Appendix C of Reference 2.5.4-1)

With the exception of the inclined borings that were drilled between 25 and 29 degrees from the vertical, the deviation data show that all of the borings were inclined 3 degrees or less from the vertical (with a mean dip of 1.3 degrees) and the greatest error in depth due to this dip was 0.08 ft in 58 ft (0.15 percent of depth) (Appendix C of Reference 2.5.4-1). The dip and dip azimuths of the discontinuities collected from ATV logging are used to analyze the discontinuity orientations, prepare scatter and contour plots of the discontinuity poles and determine discontinuity sets and their average orientations, as discussed in Subsection 2.5.1.2.5.

Induction/Natural-Gamma; Caliper/Natural-Gamma; Fluid Temperature/Fluid Conductivity/Natural-Gamma

The purpose of the induction/natural-gamma (gamma) logging was to identify the lithostratigraphic units at the CRN Site. The logging was performed in accordance with ASTM D5753 (Reference 2.5.4-33), ASTM D6274 (Reference 2.5.4-34), and ASTM D6726 (Reference 2.5.4-35) using a DUIN model dual induction probe. Gamma logs provide a record of natural gamma radiation emitted from the boring walls. Induction logs measure conductivity and when combined with gamma logs can provide high-resolution information on lithology. (Appendix C of Reference 2.5.4-1)

The purpose of the caliper/natural-gamma (gamma) logging was primarily to measure the diameter of the boring and to identify anomalous structures in the walls of the boring such as cavities, fissures etc. Caliper measurements were collected concurrently with natural-gamma emissions in accordance with ASTM D5753 (Reference 2.5.4-33), ASTM D6167 (Reference 2.5.4-36), and ASTM D6274 (Reference 2.5.4-34) using a Model 3ACS 3-leg caliper probe. (Appendix C of Reference 2.5.4-1)

The purpose of the fluid temperature/fluid conductivity/natural-gamma logging was primarily to identify the lithostratigraphic units and the presence of salt or fresh groundwater (for observation well siting) at the CRN Site. Fluid temperature and conductivity measurements were collected concurrently with the natural-gamma emissions in accordance with ASTM D5753 (Reference 2.5.4-33) and ASTM D6274 (Reference 2.5.4-34) using a Model TCGS temperature/conductivity/gamma probe. (Appendix C of Reference 2.5.4-1)

Single plots combining induction/natural-gamma with caliper and caliper-based natural-gamma and fluid temperature/conductivity are contained in Appendix C of Reference 2.5.4-1. All of the depths on the plots or logs are referenced to the ground surface with the exception of the inclined borings that are measured along the boring axis. Mechanical caliper data in the inclined borings are considered erroneous as the weight of the probe reportedly prevented the opening of the caliper arms against the boring wall.

The multiple parameter logs, contained in Appendix C of Reference 2.5.4-1, show that changes in conductivity correspond with changes in natural-gamma and that the natural-gamma data agree well with natural-gamma data collected with the caliper data. Comparison between the data sets provides an almost exact match verifying the performance of the natural-gamma measuring system. Gamma signatures are typically higher in mud-supported rocks such as mudstones and siltstones. The natural-gamma logs reveal that gamma signatures are highest in the Fleanor Member, followed by the Benbolt and Blackford Formations and lowest in the Eidson Member and Rockdell and Newala Formations.

Caliper logs show consistent gauge below the bedrock surface and also the presence of open and clay-filled fractures by an increase in boring diameter and corresponding increase in natural-gamma. Caliper and natural gamma plots correspond well with changes in velocity.

Fluid temperature and conductivity changes generally correspond with fractures identified on the acoustic televiewer logs.

2.5.4.5 Excavation and Backfill

This section discusses the excavation and backfill for safety-related structures at the CRN Site and includes the following topics:

- The extent (horizontally and vertically) of anticipated safety-related excavations, fills and slopes
- Excavation methods and stability
- Backfill sources
- Quality control and Inspections, Tests, Analyses, and Acceptance Criteria (ITAAC)
- Construction dewatering impacts
- Retaining walls

2.5.4.5.1 Extent of Excavations, Fill and Slopes

Existing elevations within the power block area range from 855 (MP-406) to 780 ft (MP-207, MP-211). Topography generally slopes gently downward from northwest to southeast as shown on Figure 2.5.4-1. The approximate ground surface and site stratigraphy are shown on Figure 2.5.4-2, a cross-section through the power block area orientated approximately perpendicular to strike. Finished plant grade elevation for the power block area is 821 ft. The bottom of the basemat of the most deeply embedded safety-related power block structures are expected not to exceed a depth of 138 ft below finished grade, elevation 683 ft.

Existing fill/residual soil and weathered rock vary in thickness within the power block area and are generally thickest in the central and southern portions of the power block area as shown on Figure 2.5.4-2. Bedrock is shallowest at the northern portion of the power block area. At the center of Locations A and B, the top of bedrock is encountered approximately 20 and 30 ft below the existing ground surface. Strata thicknesses and variability at Locations A and B are given in Table 2.5.4-26. Construction of the basemat at these locations requires a substantial amount of excavation in both soil and rock. Excavation sidewalls are expected to be vertical or near-vertical due in part to the depth of excavation, requiring the use of surface mounted cranes. The lateral extents of the excavation are expected to be limited, on the order of 15 ft beyond the exterior face of the perimeters walls, sufficient to provide working room for construction and backfilling of the exterior walls. The floor of the excavation is expected to be irregular due to the different stratigraphic units that are encountered, requiring the use of dental concrete to establish a level grade.

Concrete backfill and compacted granular backfill are used in filling the excavation. Concrete backfill is used for dental concrete as well as backfilling around the structure from the basemat to the top of rock. Compacted granular backfill is used above the elevation of rock to finished grade. Compacted granular backfill is also used for general site grading in the power block area to raise the grade to El. 821 ft.

Construction of the safety-related structures requires a temporary excavation on the order of approximately 120 ft below existing grade at Location A and 130 ft below existing grade at Location B. The excavation slopes are made in existing fill/residual soil, weathered rock, and bedrock. Excavation of these slopes is discussed in the following paragraphs. Design of the excavation and backfill is done during the detailed design stage of the project.

2.5.4.5.2 Excavation Methods and Stability

2.5.4.5.2.1 Excavation in Soil

Excavation in existing fill/residual soil can be made with conventional earthmoving equipment. Excavation must adhere to regulations from Occupational Safety and Health Administration (OSHA), 29 CFR 1926, Safety and Health Regulations for Construction. Due to the final excavation depth, the excavations in soil likely include vertical cuts supported with tied-back sheet piles or soldier pile and lagging walls. The side slopes of the ramp for construction access made in soil can likely be excavated at slope angles of 2 (horizontal) to 1 (vertical).

2.5.4.5.2.2 Excavation in Weathered Rock

Between approximately 9 and 10 ft of weathered rock underlies the existing fill/residual soil at Locations A and B within the power block area. Excavation in this weathered rock can be achieved using conventional excavating equipment. Excavation support methods similar to those used for soil can be used for weathered rock. As described in Subsection 2.4.12, groundwater is generally encountered above the top of bedrock, within the weathered rock. Groundwater control as described in Subsection 2.5.4.6.2 is required during excavation and for excavation support.

2.5.4.5.2.3 Excavation in Rock

Excavation in rock is likely made using controlled blasting techniques. As noted by Reference 2.5.4-8 the majority of rock excavation (1.1 million cubic yards of primarily laminated siltstone and limestone) for the CRBRP was made by blasting. To minimize rock excavation and provide crane access to the bottom of the excavation, 75-ft high near-vertical rock slopes in the north, south and east portions of the excavation were required. Methods included production and perimeter blasting. Production blasting, to remove the bulk of the excavation, was conducted in 13-ft lifts with burden distances of 5 to 7 ft and spacing between holes of 6 to 8 ft. Perimeter blasting was conducted to form the finished excavation face and foundation grade. Perimeter blast holes were spaced on 2-ft intervals.

The near-vertical rock slope was stabilized with rock bolts. Reference 2.5.4-8 reports that the original rock bolt design for the foundation and excavation support system was based on subsurface data. As the excavation proceeded, geologic mapping of exposed rock surfaces enabled a redesign of the rock bolting program.

Slope movement and foundation performance was monitored with an extensive instrumentation program during and after the excavation. Instrumentation included 20 inclinometers to monitor slope movement around the perimeter of the excavation, 34 horizontal extensometers to monitor deep seated wedge movement of the rock slopes, two vertical extensometers to measure heave and settlement, and 25 piezometers to measure hydrostatic levels behind the excavation slopes and at foundation grade (Reference 2.5.4-8).

The blasting program for the CRN Site varies depending on where within the power block area the safety-related structure(s) are located and in which stratigraphic unit they are embedded. The stratigraphy of the site is described in Subsection 2.5.4.2.1. The northwest portion of the power block area is underlain by the Newala Formation which belongs to the Knox Group and is

described predominantly as a dolomite. The southeast portion of the power block area is underlain by stratigraphic units belonging to the Chickamauga Group which are described predominantly as interbedded siltstone and limestone. The differing rock and rock mass characteristics of these stratigraphic units may require different blasting methods. Likewise, the design of the excavation support system depends on where within the power block area the safety-related structures are located.

Depending on the technology selected at the time of the COLA, additional subsurface data may be required to further characterize the underlying stratigraphic bedrock units for the final plant layout. Design of the excavation support system, including rock bolting, is developed during detailed design. This design accounts for the specific rock units encountered in the excavation, including the dip angle of these units.

2.5.4.5.3 Backfill Sources

As previously discussed, backfill around the safety-related structures will be made with concrete from the basemat to the top of rock and compacted granular backfill from top of rock to finished grade. Granular backfill consists of a processed graded aggregate meeting the gradation requirements of Type A aggregate of the Tennessee Department of Transportation (TDOT) Standard Specifications for Road and Bridge Construction (Reference 2.5.4-37) Section 303, Table A2.6. Given the large amount of rock that needs to be excavated, it may be advantageous to set up a crushing and blending plant onsite to produce the crushed aggregate to the required gradation specification. Otherwise, the graded aggregate is imported from nearby quarries.

A detailed field and laboratory test program is conducted, during the COLA design stage, to evaluate backfill sources and their engineering properties. This program evaluates the use of onsite excavated rock as well as imported backfill. The test program considers gradation (grain size distribution), density, soundness, durability, strength, and the dynamic properties of the backfill. A test pad is constructed to establish placement and compaction methods. It is expected that the granular backfill is compacted to at least 95 percent of the maximum dry density as determined by the modified Proctor test (ASTM D1557, Reference 2.5.4-15) and that the moisture content of the compacted fill is within 3 percent of its optimum moisture content.

2.5.4.5.4 Quality Control and ITAAC

Details, including identification of quality requirements and industry standards, regarding safety-related backfill material and placement specifications are developed during the COLA stage, once a specific technology has been selected. ITAAC related to backfill will also be developed during the COLA stage. General requirements for backfill and subgrade quality control are provided in the following paragraphs.

2.5.4.5.4.1 Granular Backfill

A quality assurance and quality control program for the backfill is established to verify that the granular backfill is constructed to the design requirements. This program is developed in an earthwork specification prepared during the detailed design phase of the project. A testing subcontractor, independent from the earthwork contractor, is used to perform testing as part of the quality control program for backfill. The testing subcontractor has an approved quality program. The backfill quality control program covers all aspects of the backfill testing program from qualification of the borrow material to verification of compaction. Qualification of the borrow material include classification tests, slake durability, LA abrasion, grain size distribution tests, and laboratory compaction (modified Proctor) tests. These tests determine the acceptability of borrow material and optimum moisture content for compaction. Field density testing is performed to verify compaction requirements are met as the backfill is placed.

For limited earthwork, where fill is compacted with hand equipment, one density test is conducted for every 2000 ft^2 per foot of fill placed. Otherwise, field density tests are performed a minimum of one per 10,000 ft^2 of fill placed, with at least one test per lift.

2.5.4.5.4.2 Concrete Backfill

Concrete backfill may be used for dental repair to create a level, uniform surface for installation of the concrete basemat foundation. The concrete backfill is also used for side fill surrounding the safety-related structures from the basemat elevation to the top of rock.

Concrete fill mix designs are developed in a design specification prepared during the detailed design phase of the project. Field observations are performed to verify that approved mixes are used and test specimens are obtained to verify that specified design parameters are reached.

2.5.4.5.4.3 Foundation Bedrock

Properties of foundation materials are discussed in Subsection 2.5.4.2.4. Methods and procedures used for verification and quality control of foundation materials are discussed herein. Visual inspection of the final bedrock excavation surface is performed to confirm material is in general conformance with the expected foundation materials based on boring logs. Visual inspection of exposed bedrock foundation subgrade is performed to confirm that cleaning and surface preparations are completed in accordance with the specification. Geologic mapping of the final exposed excavated bedrock surface is performed before placement of concrete (dental) backfill and foundation concrete. The geologic mapping program includes photographic documentation of the exposed surface and documentation for significant geologic features and is conducted under the guidelines presented in Reference 2.5.4-38.

The details of the quality control and quality assurance programs for foundation bedrock is addressed in the design specifications prepared during the detailed design phase of the project.

2.5.4.5.5 Control of Groundwater During Excavation

Construction dewatering is discussed in Subsection 2.5.4.6.2.

2.5.4.6 Groundwater Conditions

Groundwater measurements, construction dewatering, and chemical properties are discussed in the following sections.

2.5.4.6.1 Groundwater Measurements and Elevations

Groundwater is present in the existing fill/residual soil and weathered rock at the CRN Site. A detailed discussion of groundwater conditions is presented in Subsection 2.4.12. The groundwater generally occurs at depths ranging from near surface to approximately 25 ft depending on the location and depth of the observation wells. The weathered rock generally acts as a water table aquifer and most of the groundwater flow occurs within this zone. Groundwater flow also occurs through discontinuities and openings in the underlying bedrock predominantly in the upper 100 to 150 ft of bedrock where the highest frequency of open discontinuities is reported to occur.

Groundwater observation wells were installed at the CRN Site as part of the recent subsurface investigation program. The locations of these wells are shown on Figure 2.4.12-4 and the logs and details of tests performed in the wells are contained in Appendix E of Reference 2.5.4-1. As described in Subsection 2.5.4.3, the observation wells at the site were installed in two- and three-

well clusters with screened intervals of upper (between 15 to 105 ft), lower (between 89 to 178 ft) and deeper (between 176 to 297 ft) zones. Between September 2013 and March 2014, three observation well clusters installed in the power block area (OW-101, OW-202, and OW-409) exhibited groundwater level elevations ranging from approximately 800 to 738 ft in the upper zone, from about 779 to 706 ft in the lower zone and from about 765 to 739 ft in the deeper zone (only OW-101 and OW-202). (See Subsection 2.4.12, Table 2.4.12-9).

Groundwater movement at the site is generally to the southeast and southwest toward the Clinch River arm of the Watts Bar Reservoir. Horizontal hydraulic gradients range from 0.03 to 0.11 ft/ft and average vertical hydraulic gradients range from -0.71 ft/ft (upward) to 1.15 ft/ft (downward) for the observation well clusters. Hydraulic conductivity values for the bedrock stratigraphic units are estimated to range from 0.04 to 3 ft/day based on the results of the packer permeability tests while average hydraulic conductivity values are estimated to range from 0.00055 to 7.6 ft/day based on the results of the slug tests (see Tables 2.4.12-10 and 2.4.12-11). Results of an aquifer pumping test are presented in Subsection 2.4.12.

2.5.4.6.2 Construction Dewatering

Groundwater levels at the site are likely to result in the need for temporary dewatering of the foundation excavations extending below the water table during construction. Dewatering is performed in a manner that minimizes drawdown effects on the surrounding environment. Solution openings or cavities, and open bedding planes and fractures are likely controlled by blocking off the structures or be filled with cement grout to reduce groundwater inflow to the excavation and reduce the extent of dewatering.

Dewatering for excavations is achieved by gravity-type systems. Groundwater is extracted by pumping from sumps in the lowest working levels of the excavation and transferred to an impoundment facility. Horizontal relief wells are installed in the rock excavation walls to prevent hydrostatic pressure buildup behind the walls and the water is collected in sumps from which it is pumped.

The response to groundwater extraction is assessed using a network of observation wells installed at the site plus stream gauges if necessary.

2.5.4.6.3 Groundwater Chemical Properties

Geochemical tests were done on groundwater samples and the results are presented in Tables 2.4.12-15 and 2.4.12-16. From Table 2.4.12-15, the pH of the groundwater ranges from 6.97 to 9.58 with an average pH of 7.53. From Table 2.4.12-16, the sulfate concentration of the groundwater ranges from 6.9 milligrams per liter (mg/L) to 150 mg/L with an average sulfate concentration of 42 mg/L and the chloride concentration ranges from 1.3 mg/L to 24 mg/L with an average chloride concentration of 4.5 mg/L.

Reference 2.5.4-51 provides Exposure Category S for guidance on the exposure of concrete in contact with soil or water containing deleterious amounts of water-soluble sulfate ions. Four exposure categories, S0 to S3 are identified. The average concentration of 42 mg/L results in an Exposure Category of S0 which is assigned for conditions where the water-soluble sulfate concentration in contact with concrete is low and injurious sulfate attack is not a concern.

Reference 2.5.4-51 also provides Exposure Category C for guidance on the exposure of nonprestressed and prestressed concrete to conditions that require additional protection against corrosion of reinforcement. Three exposure categories, C0 to C2, are identified. An Exposure Category C1 is assigned since the foundations will be exposed to moisture but will not be in contact with external sources of chlorides; where external sources of chlorides, as noted in

Section R19.3.1 of Reference 2.5.4-51, include direct contact with deicing chemicals, salt, salt water, brackish water, and sea water. Table 19.3.2.1 of Reference 2.5.4-51 provides the requirements for concrete by exposure class.

2.5.4.7 Response of Soil and Rock to Dynamic Loading

This section presents response of soil and rock to dynamic loading and includes the following discussions:

- Effects of past earthquakes
- Development of velocity profiles
- Dynamic laboratory tests
- Variation of shear modulus and damping with strain

2.5.4.7.1 Effects of Past Earthquakes

The historical earthquake events are described in Subsection 2.5.2.1. The effects of prior earthquakes including potential paleoseismic features at the site are described in Subsection 2.5.1.2.6.6.

2.5.4.7.2 Velocity Profiles

Various geophysical surveys were conducted at the CRN Site to characterize in situ dynamic properties of the soil and rock, including seismic refraction and reflection, and P-S Suspension logging as described in Subsection 2.5.4.4.2. The P-S Suspension logging method was used to collect V_s and V_p measurements in the soil and rock. Figures 2.5.4-5 and 2.5.4-6 present V_s and V_p profiles for each stratigraphic unit. These unit V_s and V_p profiles are assembled as described in the following paragraphs according to the corresponding stratigraphy to provide unique V_s and V_p profiles for Locations A and B.

2.5.4.7.2.1 Shear Wave Velocity Profiles

The stratigraphy at Locations A and B is developed by first considering the depth to the Newala Formation (Knox Group), which underlies the Chickamauga Group at the site. The Knox Group outcrops in the northwest portion of the power block area. Projecting the Knox/Chickamauga Group contact southeast at a dip angle of 33 degrees, provides an elevation of 296 ft, or 514 ft below existing grade (using an existing grade elevation of 810 ft) at the center of Location B. Extending the projection to the center of Location A provides an elevation of -267 ft, or 1067 ft below existing grade (using an existing grade elevation of 800 ft). While two borings (MP-201 and MP-423) penetrated into the Knox Group in the area of Location B, the Newala Formation was beyond the depth of exploration (540.6 ft in boring MP-101) at Location A.

With the depth to the Newala Formation established, the overlying stratigraphy at Locations A and B is completed using average thicknesses of the corresponding Knox and Chickamauga Group stratigraphic units (Table 2.5.4-1). At Location A, these units include the Blackford Formation, Eidson Member, Fleanor Member, Rockdell Formation, and Benbolt Formation. At Location B, these units include from deepest to shallowest, the Newala Formation, Blackford Formation, and Eidson and Fleanor Members. Weathered rock and existing fill/residual soil are located above the Chickamauga Group. These weathered and soil materials are approximately 20 ft thick at Location A and 30 ft thick at Location B.

The V_s profiles at Locations A and B are developed using site-measured V_s data, V_s data measured in similar nearby geologic units, and estimated V_s values from literature from the top of unweathered rock to Precambrian basement rock. The geologic cross-section illustrating the shallow portion of these profiles is shown on Figure 2.5.4-12 with the full depth shown on Figure 2.5.4-13. The best estimate (mean) basecase V_s profile for the shallow geologic units was developed for each area by computing the lognormal mean profile for the measured V_s data from the boreholes taken in the area, or just outside the area (within 100 ft), as shown in Figure 2.5.4-11 where the V_s data for each borehole was normalized to the top of unweathered rock, zero depth. The associated borehole data and lognormal average V_s profile for Location A and Location B are shown on Figures 2.5.4-14 and 2.5.4-15, respectively with the top of the profile (depth = 0) at the top of unweathered rock. Below the measured data and extending into the Newala, average V_s values provided in Table 2.5.4-21 were assigned to the underlying geologic units. Unless supported by measured data, the Newala Formation and the remainder of the Knox Group were assigned a V_s of 11,000 fps. These profiles are shown on Figures 2.5.4-16 and 2.5.4-17 for Locations A and B, respectively.

Limited V_s data is available for the deep geologic units. Measured data from spectral analysis of surface waves (SASW) surveys in the Conasauga shale, Pumpkin Valley shale, and Rome Formation at the nearby Watts Bar facility were used. These data were taken from depths of 500 and 1500 ft and adjusted to the CRN Site using generic V_s profiles for central and eastern U.S. hard rock (Reference 2.5.4-58) and applied to the deeper geologic units of the profiles. These profiles are shown on Figures 2.5.4-18 and 2.5.4-19 for Locations A and B, respectively.

Epistemic uncertainty in the mean basecase (best estimate) profiles for Locations A and B is accounted for with upper- and lower-range basecase profiles developed using a depth-independent scale factor of 1.25, providing a plus or minus 25 percent variation about the mean basecase profiles. The V_s values for the upper-range basecase profiles are capped at about 11,500 fps. Note that prior to developing the upper- and lower-range profiles, the shallow portion of the profiles, where the lognormal mean V_s values were used, is converted to a layered model with uniform velocities. The uncertainty associated with a scale factor of 1.25 is considered sufficient to account for potential complexity of wave propagation associated with the dipping stratigraphy at the site. The best estimate (P1), lower-range (P2) and upper-range (P3) profiles for Locations A and B are shown on Figures 2.5.4-20 and 2.5.4-21, respectively. These profiles are tabulated in Tables 2.5.4-30 and 2.5.4-31, respectively.

2.5.4.7.2.2 Compression Wave Velocity Profiles

The V_p profiles at Locations A and B are developed in a similar manner to the V_s profiles. The unit V_p profiles as presented on Figure 2.5.4-6 are developed based on the site stratigraphy corresponding to Location A and Location B for the corresponding stratigraphic units, weathered rock, and existing fill/residual soil.

2.5.4.7.3 Dynamic Laboratory Tests

Two resonant column torsional shear tests were conducted on intact samples of the existing cohesive fill, samples MP-122UDA ST-2 and MP-111UD ST-5. Normalized shear modulus reduction and damping vs. shear strain relationships are obtained for each sample. These results are plotted on Figures 2.5.4-8 and 2.5.4-9 and are compared to the Electric Power Research Institute (EPRI) curves (Plasticity Index [PI] = 30, 40 and 50 percent) (Reference 2.5.4-39). This comparison shows that the shear modulus test data aligns reasonably well with the EPRI curves. The EPRI PI = 30 percent curve is the best fit for averaging the two test results, which is supported by the measured PIs of 32 and 33 percent for the test samples. However, since the onsite clay soils have an overall average PI of 40 percent and the test data reasonably conform to the EPRI curves, the EPRI PI = 40 percent curve for both shear modulus reduction and

damping are recommended. (Note that the damping values from the test data from MP-111UD suggest nearly double the damping ratio as compared to the EPRI values.)

2.5.4.7.4 Variation of Shear Modulus and Damping with Strain

The variation of damping and shear modulus in rock under dynamic loading is evaluated in this section. The variation of damping and shear modulus for weathered rock, in situ soils, and granular backfill are not utilized in the rock column amplification/attenuation analysis and thus are not discussed here. Site attenuation, kappa, is briefly discussed here with additional discussion provided in Subsection 2.5.2.5.1.

2.5.4.7.4.1 Material Damping and Shear Modulus

The dynamic performance of the firm rock material in the upper 500 ft is evaluated under linear and nonlinear behavior with respect to dynamic material properties, specifically the variation of damping and shear modulus with shear strain. In order to represent both possible behaviors, two sets of hysteretic damping and shear modulus reduction curves are used for the upper 500 ft of the site. A subset of the EPRI rock curves (Reference 2.5.4-39) is used to represent the upper range nonlinearity (M1) in the materials at the site and linear analyses (M2) to represent an equally plausible alternative rock response. The original depth dependent curves were provided over depths of 51 to 120 ft and 2001 to 5000 ft. The curves are modified for the M1 profile to depths of 0 to 21 ft and 21 to 500 ft. The damping curves are further revised reducing the original 3 percent low strain hysteretic damping to 2 percent damping. These EPRI rock curves are provided in Figure 2.5.4-26. A damping value of 1.25 percent is used to represent a linear response. For rock layers greater than 500-foot depth, a linear response is used with a damping adjusted such that the site attenuation (kappa) of the entire profile matches the target kappa described in the subsequent section and in more detail in Subsection 2.5.2.5.1. Damping values for the nonlinear (M1) and linear (M2) analyses for each of the best estimate (P1), lower-range (P2) and upper-range (P3) profiles for Locations A and B are presented Tables 2.5.4-30 and 2.5.4-31, respectively.

2.5.4.7.4.2 Kappa

The site attenuation, kappa, specified at the ground surface and zero epicentral distance from the seismic source, is thought to include all mechanisms of in situ damping and reduces the need to rely solely on laboratory testing to estimate seismic energy dissipation at a given site. Kappa is not dependent on frequency or level of motion at rock (very stiff) sites, which makes it possible to estimate a range of kappa values from small local or regional earthquakes. The estimated kappa (or range of kappa) is applicable and important to characterizing strong ground motions, which have significant impact on engineering design.

Two methods are used to estimate a range of kappa values for use at the CRN Site, both of which employ the use of an analogue site, Tellico Dam, and are discussed further in Subsection 2.5.2.5.1. The Tellico Dam site is considered similar to the CRN Site based on the geologic structure but the depth to basement is somewhat deeper at the Tellico Dam site, by about 2400 ft.

The first kappa estimation method is an estimate derived from the peak frequency and normalized response spectral shapes. The analyses of response spectral shape for kappa are shown in Figures 2.5.4-22 through 2.5.4-25. Each figure shows the average, minimum, and maximum of the recorded 5 percent damped acceleration response spectral shape for several earthquakes of similar magnitude at Tellico Dam. A fourth curve is shown on each figure, representing a point-source model to fit these data, resulting from a best-estimate kappa. The magnitude and distance parameters for the point-source model are taken as the average from

the recorded data at Tellico Dam. Corrections are made for attenuation from source and crustal amplification. Fourteen sets of recordings over the magnitude range **M** 0.9 to **M** 3.2 and hypocentral distance range of 15.3 kilometers (km) to 54.2 km were used to estimate the kappa. Using the normalized spectral shape method the best fit kappa values were 0.006 second (s) and 0.009 s.

The second kappa estimation method is an estimate derived from direct measurement of the high-frequency decay of the S-wave Fourier amplitude spectrum (FAS). The steps and adjustments necessary (such as attenuation and crustal amplification) to compute kappa from the S-wave FAS data are described in Subsection 2.5.2.5.1. Considering two crustal models and 14 recorded earthquakes from the Tellico Dam site, a lower range kappa of 0.010 s and an upper range kappa of 0.016 s are estimated. Results of this method are given in Table 2.5.4-32.

Summarizing, kappa values ranging from 0.006 to 0.016 s for the CRN Site are based on the analyses of response spectral shapes (5 percent damped) and the slopes of the S-wave FAS at high-frequency. A best-estimate value for kappa is taken as the median of 0.010 s. Subsection 2.5.2.5.1 provides a discussion of how kappa is distributed throughout the profiles and relative weights for Locations A and B.

2.5.4.7.5 Rock Column Amplification/Attenuation Analysis

The rock column amplification/attenuation analysis is described in Subsection 2.5.2.5. This analysis considers a deep rock profile, from Elevation 683 ft to the Precambrian basement rock, with the stratigraphy shown on Figures 2.5.4-12 and 2.5.4-13. The V_s profiles, material damping, shear modulus, and kappa values used in this analysis are described in Subsections 2.5.4.7.4 or 2.5.2.5.1.

Unit weights of the geologic units for use in these analyses were taken from Table 2.5.4-21 for units above and including the Newala. Unit weights of 170 pcf for the Conasauga shale and 175 pcf for the Pumpkin Valley shale and Rome Formation are assigned to the rock units below Newala. These values are presented for each of the profiles in Tables 2.5.4-30 and 2.5.4-31.

2.5.4.8 Liquefaction Potential

This section presents the evaluation of the liquefaction potential of the materials adjacent to and under safety-related structures at the CRN Site. This section conforms to the guidelines in RG 1.198, *Procedures and Criteria for Assessing Seismic Soil Liquefaction at Nuclear Power Plant Sites*.

Soil liquefaction is a process by which loose, saturated, granular deposits lose a significant portion of their shear strength due to pore pressure buildup resulting from cyclic loading, such as that caused by an earthquake. Soil liquefaction can lead to foundation bearing failures and excessive settlements.

Reference 2.5.4-40 defines liquefaction as the transformation of a granular material from solid to liquefied state as a consequence of increased pore-water pressure and reduced effective stress. Increased pore-water pressure is induced by the tendency of granular materials to compact when subjected to cyclic shear deformations. The change of state occurs most readily in loose to moderately dense granular soils with poor drainage, such as silty sands or sands and gravels capped by or containing seams of impermeable sediment. As liquefaction occurs, the soil stratum softens, allowing large cyclic deformations to occur.

The safety-related structures at the CRN Site are embedded at a depth expected not to exceed 138 ft below final grade (El. 683 ft). Sound rock (bedrock/rock below the weathered rock) is

located at an average elevation of approximately 780 ft at Locations A and B, approximately 100 ft above the foundation level. Furthermore, if any dental work is required to prepare the foundation surface, dental concrete is used. Liquefaction cannot occur in sound rock or concrete; therefore, there is no potential for liquefaction in the foundation materials.

Subsection 2.5.4.5 describes the plan for backfilling around safety-related structures. Concrete is used from the foundation level to the top of rock. Here again, there is no potential for liquefaction of the concrete backfill. Granular backfill is used around the structures from the top of rock to finished grade. The granular backfill is compacted to at least 95 percent of the modified Proctor value. Based on the gradation and degree of compaction, this backfill is not considered to be susceptible to liquefaction.

The liquefaction potential of existing fill/residual soil at the site is also evaluated here. Since liquefaction occurs in granular materials, the standard methods for determining liquefaction resistance apply to soils that classify as sands or gravels. Since the existing fill/residual soil at the CRN Site do not classify as sands or gravels, as described in Subsection 2.5.4.2, the SPT methods available to quantify resistance to liquefaction are not applicable and Cone Penetration Test data were not collected. Fine grained soils are typically not considered susceptible to liquefaction and it is generally accepted that cohesive soils are not susceptible to liquefaction. Nevertheless, the CRN Site soils are evaluated in a qualitative manner using criteria for fine grained soils proposed by Polito (Reference 2.5.4-41) and Seed et al. (Reference 2.5.4-42).

Test results from Atterberg limits conducted on representative soils are plotted on Figure 2.5.4-10 along with the Polito criteria for liquefiable soils (Reference 2.5.4-41), whereby plasticity is the key factor. If this requirement, whether measured in terms of liquid limit or PI, is met, the soil does not appear to be susceptible to flow liquefaction. A PI of 10 and a liquid limit of 30 are used as threshold values. All of the CRN Site soils plotted on Figure 2.5.4-10 fall outside the proposed zone of liquefiable soils and therefore are not susceptible to liquefaction by the Polito criteria.

In summary, safety-related structures are founded on rock, backfilled with concrete and compacted granular backfill and these materials are not susceptible to liquefaction. The CRN Site soils, which include the existing fill and residual soil, consist predominately of cohesive fine-grained material and are not susceptible to liquefaction.

2.5.4.9 Earthquake Design Basis

The development of the site-specific GMRS for Locations A and B is described in Subsection 2.5.2.5.8. The associated vertical GMRS is computed with the V/H ratios as described in Subsection 2.5.2.5.8.

2.5.4.10 Static and Dynamic Stability

This section presents the evaluation of static and dynamic stability of safety-related structures including bearing capacity, heave, settlement, and lateral earth pressures in the power block area at the CRN Site. The geologic features at the site are summarized in Subsection 2.5.4.1 (described in detail in Subsection 2.5.1) and the subsurface investigation and laboratory testing programs are described in Subsection 2.5.4.3. Description of the subsurface materials, including the engineering properties of the existing fill/residual soil and bedrock units, are described in Subsection 2.5.4.2.

Subsection 2.5.4.1.1 describes the stratigraphy at the site and Figure 2.5.4-2 presents a cross-section through the power block area. The site is underlain with a succession of stratigraphic units that generally strike N63°E with a dip angle of 33 degrees. Rocks belonging to the Knox Group outcrop to the northwest and progressively younger rocks belonging to the

Chickamauga Group outcrop to the southeast. The stratigraphic units within the power block area include, from northwest to southeast, the Newala Formation, the Blackford Formation, the Eidson and Fleanor Members, the Rockdell Formation, and the Benbolt Formation. The average thickness of these units is presented in Table 2.5.4-1.

Subsection 2.5.4.1.3 describes the discontinuities, shear-fracture zones and weathered/fracture zones encountered in the stratigraphic units. These discontinuities may impact the stability of foundations and are accounted for by considering the effect of rock mass properties on the performance of the foundations. Subsection 2.5.4.2.4.4 describes the rock mass strength and deformation properties.

Overlying the dipping bedrock units, a layer of weathered rock and existing fill/residual soil is encountered at the CRN Site. These materials are described in Subsection 2.5.4.2.4. Existing site grades vary within the power block area with an average elevation of approximately 810 ft. The finished grade elevation is 821 ft. Compacted granular fill is used to replace weathered rock, residual soil, and existing fill beneath structures and to establish finished grade.

Due to the dipping strata at the CRN Site, the stratigraphic units underlying the power block area vary depending on location. At the northwest end of the power block area the Newala Formation outcrops at the ground surface while to the southeast, this formation is estimated to be well over 1000 ft below the ground surface. For this reason, the two specific locations in the power block area, Location A and Location B are evaluated for static and dynamic stability of safety-related structures with a foundation embedment of 138 ft below finished grade (El. 683 ft). The existing ground surface elevation at Location A is approximately 800 ft, while the elevation at Location B is approximately 810 ft.

Reference 2.5.4-50 provides a GSI chart that suggests rock with a rock quality designation (RQD) above 80 percent is representative of intact or massive rock and is controlled by material properties rather than discontinuities. As noted in Table 2.5.4-21, the average RQD values of the bedrock at the CRN Site range from 80 to 93 percent. Nevertheless, the application of the GSI classification and the Hoek-Brown relationship is based on observations that the rock mass contains several sets of discontinuities that are closely spaced relative to the dimensions of the proposed structure and a predetermined failure plane does not exist. The applicability of GSI in rock mass characterization is discussed in Subsection 2.5.4.2.4.4.

A simplified stratigraphic model along with empirical relationships are used for the evaluation of bearing capacity in Subsections 2.5.4.10.1.1 and 2.5.4.10.1.2, and settlement and heave in Subsection 2.5.4.10.2. The stratigraphy underlying the CRN Site consists of an inclined layered system of alternating siltstones and limestones. The similarity of the engineering properties of these rock units, in both strength and stiffness, suggests that, for evaluation purposes, the individual rock units may be considered separately to develop a range of results. Material properties of intact rock and rock mass properties based on GSI are considered in evaluating bearing capacity and settlement and heave. A finite element model, presented in Subsection 2.5.4.13, is used to validate the assumptions and empirical relationships used.

2.5.4.10.1 Bearing Capacity

The materials encountered beneath the foundation, within the depth of influence (D_i), are considered in the evaluation of bearing capacity. A depth of 2 times the width of the foundation (2B) is a general approach to calculate D_i and is based on Boussinesq's stress distribution and the depth at which the foundation contact pressure is reduced to 10 percent. Beyond the depth of influence, the applied load is considered insignificant from a bearing capacity perspective. While several technologies are being considered for the CRN Site, a foundation width of 220 ft is a reasonable assumption, resulting in a D_i of 440 ft at elevation 381 ft.

The rock units encountered at the foundation level and within the D_i vary between Locations A and B. At Location A, the Rockdell and Benbolt Formations are encountered at the foundation level with the underlying Fleanor Member encountered within the D_i. The Newala Formation is over 1000 ft below the foundation level at this location. At Location B, the Eidson and Fleanor Members are encountered at the foundation level with the underlying Blackford and Newala Formations encountered within the D_i. For bearing capacity analyses, each stratigraphic unit within the depth of influence of a respective foundation is considered separately, as a single infinite rock layer below the foundation. Therefore, the Newala, Blackford, Eidson, Fleanor, Rockdell, and Benbolt units are considered separately. This approach provides a range of bearing capacity values and the most reasonably conservative value is considered.

The evaluation of bearing capacity of rock is well documented in the literature (References 2.5.4-43, 2.5.4-44, 2.5.4-45, 2.5.4-47, 2.5.4-48, and 2.5.4-49). While authors present different methods, each method generally considers intact rock properties and rock mass properties. The intact rock properties, obtained from laboratory testing, are described in Subsection 2.5.4.2.4.3 and include unit weight, specific gravity, Poisson's ratio, unconfined compressive strength, elastic modulus, and shear modulus. The rock mass properties which account for the in situ condition of the rock mass are described in Subsection 2.5.4.2.4.4. These properties include rock mass strength and rock mass deformation modulus. The rock mass strength is developed using the Hoek-Brown failure criteria (Reference 2.5.4-19) and the GSI classification system. The rock mass deformation modulus is developed using empirical equations and a combination of the intact elastic modulus, GSI and a disturbance factor (D). Both of these approaches are described in detail in Subsection 2.5.1.2.6.2. For the bearing capacity analysis, the lower- and upper-bound GSI and disturbance factors of D = 0.7 and D = 0 are considered. D = 0.7 accounts for the potential of a disturbed zone, due to blasting during construction beneath the foundation and D = 0 for an undisturbed zone below this.

2.5.4.10.1.1 Ultimate Bearing Capacity

Ultimate bearing capacity (q_u) is estimated using the following three empirical equations. Two of these methods utilize the Hoek-Brown rock mass constants (m_i, m_b, s, a) and the other method utilizes a bearing capacity factor based on the friction angle (Φ) of the rock mass.

Wyllie, Reference 2.5.4-49, provides the following equation for ultimate bearing capacity on a rock mass.

$$q_u = C_{f1} \cdot s^{0.5} \cdot \sigma_{ci} \cdot [1 + (m_b \cdot s^{-0.5} + 1)^{0.5}] \qquad \text{Equation 2.5.4-6}$$

where:

C_{f1} = correction factor based on foundation dimensions (length (L)/base (B)) from Table 5.4 of Reference 2.5.4-49, where C_{f1} = 1.12 corresponding to L/B = 2.

σ_{ci} = intact uniaxial compressive strength (unconfined compressive strength in Table 2.5.4-21)

Equation 2.5.4-6 is applicable when the following criteria are met:

1. Loading is vertical and concentric
2. Foundation rock is uniform to depth below the maximum expected shear surface
3. Water level is lower than depth of the shear surface

4. Foundation rock has strength parameters defined by friction angle and cohesion

5. Friction and adhesion on the vertical sides of the footing are neglected (if any)

Each of these criteria are satisfied by the estimated conditions at the CRN Site, with the exception of number 3, which is not satisfied by the groundwater estimated at 15 ft below finished grade and higher than the depth of the shear failure. It is also worth pointing out that Criterion 2 is met by assuming a homogeneous rock mass. Although the CRN Site does not meet Criterion 3, this method is adequately suited to calculate bearing capacity. Results are compared to the other methods described in this section.

The U.S. Army Corps of Engineers (USACE), Reference 2.5.4-43, provides the following equation for ultimate bearing capacity on a rock mass.

$$q_u = 0.5 \cdot \gamma \cdot B \cdot N_\gamma + \gamma \cdot D \cdot N_q$$ Equation 2.5.4-7

where:

D = depth of foundation below ground level

$N\gamma$ = bearing capacity factor = $N_\phi^{0.5} \cdot (N_\phi^2 - 1)$

N_q = bearing capacity factor = N_ϕ^2

N_ϕ = bearing capacity factor = $\tan^2 \cdot (45 + \frac{\phi}{2})$

ϕ = friction angle of the rock mass

B = foundation width

γ = total unit weight

Equation 2.5.4-7 is applicable to a foundation bearing on a moderately dipping (20 to 70 degrees from foundation plane) jointed rock mass with general shear failure along joints or a highly jointed rock mass with general shear failure on irregular failure surface through the rock mass. With the dipping bedrock and identifiable joint sets, Equation 2.5.4-7 is adequately suited to calculate bearing capacity.

Reference 2.5.4-46 provides the Kulhawy and Carter (Reference 2.5.4-47) equation for ultimate bearing capacity on a rock mass assuming a strip footing and weightless rock mass:

$$q_u = \sigma_{ci} \cdot (s^a + (m_b \cdot s^a + s)^a)$$ Equation 2.5.4-8

Equation 2.5.4-8 is very similar to Equation 2.5.4-6 and is adequately suited for the estimated conditions of the CRN Site, with the exception of a strip load footing.

2.5.4.10.1.2 Allowable Bearing Capacity

Allowable bearing capacity (q_a) is defined as the ultimate bearing capacity divided by a factor of safety (FS). An FS of 3 is applied to each of the methods described above. A summary of q_a values computed for the various stratigraphic units within the disturbed (D = 0.7) and undisturbed

(D = 0) zones and for the lower- and upper-bound GSI underlying Locations A and B is provided in Table 2.5.4-27.

Bowles (Reference 2.5.4-48) presents a method for estimating q_a of a rock mass by applying a large FS to the σ_{ci} value with the FS ranging from 6 to 10 depending on the RQD of the rock. Since each of the stratigraphic units being considered here have high RQD values, ranging from 80 to 93 as described in Subsection 2.5.4.2.1, an FS of 6 is used. The unconfined compressive strength, σ_{ci} values for each unit from Table 2.5.4-21 is divided by 6 to calculate the allowable bearing capacity. Results are summarized in Table 2.5.4-27. This method of calculating q_a describes failure due to the material properties of the rock and is adjusted for RQD. Given the relatively high RQD and depth of the foundations, the Reference 2.5.4-48 method is well suited to the estimated foundation conditions at the CRN Site.

A general bearing failure of the foundation is ruled-out due to a net decrease in the bearing pressure at the foundation level. The change in pressure at the foundation level is computed as the assumed new building load (q) minus the existing overburden (σ_o). The amount of unloading (σ_o) is computed for a safety-related structure founded 120 ft below existing grade, resulting in σ_o = 18.7 kilopounds per square foot (ksf). A value of 9 ksf is assumed for the safety-related foundation load, q. Thus, the net change in pressure at the foundation level is expected to be negative – an unloading condition. With a decrease in pressure, general shear failure, including sliding along a predetermined failure plane, such as a bedding plane, is not likely to occur.

Subsection 2.5.1.2.6.3 describes weathered or fracture zones as typically occurring along bedding planes or fractures, and typically represent poor to fair quality rock, consisting of multiple, healed to open, slightly to highly weathered fractures or bedding planes, some calcite or dolomite filled, with occasional core loss and loss of drilling fluid reported. However, below the uppermost weathered zone (depth of 100 ft or less), rock mass discontinuities (including bedding joints) become tighter, less frequent, and shorter as depth increases. The site investigation data indicate that few bedding fractures have weathering or weakening below the power block foundation level. Therefore, weathering and fractures along bedding planes below the foundation are not likely to result in continuous planar discontinuities. GSI is applicable to rock masses with many joint sets (Reference 2.5.4-50), and therefore GSI is appropriate to estimate rock mass properties for foundation stability analysis.

Given that a general shear failure, including sliding along a bedding plane or joint surface, is not likely, the material properties of the rock units (rock mass) are expected to control failure. The U.S. Army method (Reference 2.5.4-43) and Bowles method (Reference 2.5.4-48) rely more directly on the material properties of the rock than do the Wyllie method (Reference 2.5.4-49) or the Kulhawy and Carter method (Reference 2.5.4-47) thus are more suited to the conditions at the CRN Site.

The results of these four bearing capacity methods are summarized in Table 2.5.4-27. Note that lower-bound GSI and D=0.7, to account for disturbed rock mass from blasting and stress relief, are used to calculate minimum values for three of the four methods. The Bowles method does not incorporate GSI or D thus there are no associated minimum values. The extent of this disturbed zone is unknown and dependent upon the blasting technique used. However, it is unlikely to extend to depths beyond 10 to 15 ft below the foundation level. Minimum allowable bearing capacity estimates from the three methods are based on a uniformly (full depth) disturbed rock mass and are overly conservative, considering the anticipated conditions at the CRN Site. Therefore, the allowable bearing capacities estimated using Bowles (Reference 2.5.4-48) are the recommended values for design guidance and the rounded low-formation value (110 ksf) is the recommended q_a for the PPE (Table 2.5.4-27). Note that the Bowles' values is less than the average value (135 ksf) of the calculated minimum values for the other three methods.

2.5.4.10.1.3 Allowable Bearing Capacity of Concrete

Lean concrete may be used for purposes of dental repair/filling of the exposed foundation. The allowable bearing capacity assigned to the underlying stratigraphic units should not exceed the q_a of the dental concrete.

The American Concrete Institute (Reference 2.5.4-51) gives the following equation for q_a of concrete:

$$q_a \leq \phi \cdot 0.7 \cdot \lambda \cdot f'_c \qquad \text{Equation 2.5.4-9}$$

where:

Φ	=	reduction factor = 0.65 for bearing on concrete
λ	=	modification factor = 1 for normal weight concrete
f'_c	=	specified compressive strength of concrete
With f'_c	=	2500 psi, q_a = 1138 psi = 164 ksf

Thus the q_a of dental concrete is greater than the assigned q_a for the underlying rock.

2.5.4.10.1.4 Dynamic Bearing Capacity

No guidance is given in Reference 2.5.4-51 for increasing the design bearing strength of concrete for dynamic loading. Similarly, no increase in the allowable bearing capacity for the underlying rock is provided. Thus, 110 ksf is recommended for both the static and dynamic allowable bearing capacity for rock.

2.5.4.10.2 Settlement and Heave Analysis

As previously discussed safety-related foundations embedded 120 ft below existing grade are expected to result in an unloading (heave) of the underlying bedrock with little if any settlement. Nevertheless, settlement and heave analyses using rock mass properties are considered. Rock mass deformation modulus, E_{rm}, values for combinations of D and GSI (E_{rm} values using the Reference 2.5.4-22 and Reference 2.5.4-23 methods as described in Subsection 2.5.4.2.4.4) were used in the analyses. The Hoek and Diederichs method (Reference 2.5.4-22) incorporates both GSI and D while the Gokceoglu (Reference 2.5.4-23) method incorporates only GSI. This results in three E_{rm} values for each of the upper-bound and lower-bound GSI with D = 0 and D = 0.7 (two are Hoek and Diederichs, Reference 2.5.4-22, and one is Gokceoglu Reference 2.5.4-23). Using these six E_{rm} values leads to six estimations of settlement and heave for the foundation and stratigraphic unit, representing the three E_{rm} calculation methods and the conditions for an undisturbed and a disturbed rock mass.

For settlement and heave analyses, each stratigraphic unit within the depth of influence of a respective foundation is considered separately, as a single infinite rock layer below the foundation, similarly to what was done for the bearing capacity analyses discussed in Subsection 2.5.4.10.1.

2.5.4.10.2.1 Settlement Analysis

For the large mat foundation that supports the power block structures, general considerations indicate that total settlement should be limited to 6 in., while differential settlement should be limited to 3 in. (Reference 2.5.4-52). For footings that support smaller plant components, the total

settlement is generally limited to 1 in., while the differential settlement is limited to 0.5 in. (modified from Reference 2.5.4-57).

The safety-related structures at the CRN Site have an embedment depth that is expected not to exceed 138 ft below finished grade; thus these structures are founded directly on bedrock and settlement, if any, is expected to be small. Settlement is individually calculated for each of the stratigraphic units being considered. A foundation contact pressure of 9 ksf is assumed for the analysis.

Total settlement, δ, is estimated for a flexible foundation using the following equation from the USACE *Rock Foundations* engineering manual (Reference 2.5.4-43), assuming an elastic infinite homogeneous material.

$$\delta = \frac{1.12 \cdot q \cdot B \cdot (1-\mu^2) \cdot (\frac{L}{B})^{0.5}}{E_d} \text{ x RF}$$

Equation 2.5.4-10

where:

E_d = modulus of deformation, taken here as (see Table 2.5.4-25).

q = applied load, 9 ksf

L/B = 1.4

RF = reduction factor for rigid foundation = 0.78

A summary of the estimated settlements for each of the stratigraphic units, considering the range E_{rm} values is provided in Table 2.5.4-28. This summary shows that the estimated total settlements are below 0.5 in for all cases and range from 0.01 to 0.28 in. Recall that the E_{rm} values were calculated using upper- and lower-bound GSI values and D values of 0 and 0.7. Further analysis of settlement, including differential settlement, is performed at COLA. The analysis must take into account construction practices, and the specific technology selected accounting for foundation dimensions, foundation loads, embedment depth and construction sequence.

2.5.4.10.2.2 Heave Analysis

Total heave due to stress relief during the excavation is predicted using an empirical method suggested by Christian and Carrier (Reference 2.5.4-53) for elastic deformation of an isotropic material. The equation assumes an infinite homogeneous material. For application to the CRN Site, the elastic modulus (E) is replaced with E_{rm}. Heave is evaluated for each stratigraphic unit extending to the full depth of influence and the range of predicted heave is considered.

$$\text{Heave} = u_0 \cdot u_1 \cdot (\frac{qB}{E})$$

Equation 2.5.4-11

where:

u_0 = 0.96, based on embedment depth and foundation width

u_1 = 0.60 based on foundation length and width

B = foundation width ≈ 220 ft

E = E_{rm} = varies per stratigraphic unit (see Table 2.5.4-25)

q = amount of unloading, (30 ft x 0.12 ksf) + (90 ft x 0.168 ksf) = 18.7 ksf

Table 2.5.4-29 shows that total heave ranges from 0.01 in. to 0.36 in. and the largest estimated total heave is less than 0.5 in. The measured heave is likely closer to the heave value given for the larger GSI since the lower heave value represents a disturbed zone (D = 0.7) for the full depth of influence beneath the foundation; in practice, the disturbed zone due to excavation is considerably less than this, but further analysis is performed during the COLA detailed design. The analysis must take into account construction practices, and the specific technology selected accounting for foundation dimensions, foundation loads, embedment depth and construction sequence.

2.5.4.10.2.3 Settlement and Heave Summary

The amount of unloading from excavation versus the amount of reloading from the new structures results in a net decrease in bearing pressure. The calculated settlement and heave values are very small and differences in magnitude are due to the different analytical approaches available to calculate settlement and heave. The settlement is largely attributed to recompression of the material as opposed to new elastic or consolidation settlement. The estimated heave and settlement are expected to be instantaneous, occurring during and shortly after construction. No long-term settlement is expected after construction.

2.5.4.10.3 Lateral Earth Pressure

Lateral earth pressure exerted on below grade walls is determined by considering the state of stress of the soil/rock behind the wall which develops as a result of wall movement. Reference 2.5.4-14 provides Rankine's solution for determining the static lateral earth pressure assuming the ground surface behind the top of the wall is level and there is no friction between the wall and backfill:

$$\sigma'_h = \gamma' \cdot z \cdot K \qquad \text{Equation 2.5.4-12}$$

where:

σ'_h = effective lateral pressure exerted on a wall at depth z

γ' = effective unit weight of the soil/material below groundwater table and moist unit weight above the groundwater table

z = depth below surface

K = coefficient of static earth pressure

With an embedment depth expected not to exceed 138 ft below grade, the below grade walls of the safety-related structures at the CRN Site will behave as non-yielding walls thus the materials behind the walls are in an at-rest condition and the at-rest earth pressure coefficient is used to determine lateral pressure. Reference 2.5.4-14 provides the at-rest lateral earth pressure coefficient:

$$K_0 = 1 - \sin\Phi' \qquad \text{Equation 2.5.4-13}$$

where:

Φ' = effective friction angle of the material behind the wall

As described in Subsection 2.5.4.5.1, at Locations A and B within the power block area, the excavation is expected to include about 40 ft of soil and 100 ft of rock. Backfill below the bedrock

level is made with concrete and above the bedrock level is made with granular backfill. Where concrete backfill is used, the lateral forces exerted on the below grade wall are considered negligible. Where granular backfill is used a K_0 = 0.5 is used, based on Φ' = 30 degrees rather than 36 degrees for granular backfill to determine the lateral force. If the annular space between the wall and backfill is less than 20 ft, the in situ soils may contribute to the lateral earth pressures, therefore K_0 = 0.66 (Φ' = 20 degrees) should also be considered in determining the lateral force.

Additional components contribute to the lateral pressure exerted on below grade walls:

- Hydrostatic pressure
- Surcharge-induced (equipment and adjacent structures) pressure
- Seismic induced pressure

Evaluation of these components and a full assessment of lateral earth pressure is conducted during the COLA stage, once a specific technology has been selected. This evaluation includes finite element modeling using site-specific foundation input response spectra to determine the seismic component of lateral earth pressure.

2.5.4.11 Design Criteria

The criteria summarized below are considered geotechnical criteria. While these criteria have been initially addressed for ESPA, they will be reevaluated at the COLA stage, once a specific technology has been selected.

- The liquefaction potential of cohesive residual soils at the CRN Site is evaluated in Subsection 2.5.4.8. RG 1.198 provides that cohesive soils with fines content greater than 30 percent that are either classified as clays or have a PI greater than 30 percent should generally not be considered susceptible to liquefaction. The residual soils are characterized with a fines content of 80 percent and a PI of 40 percent and are thus not considered susceptible to liquefaction. Methods to evaluate the liquefaction potential of fine grained soils (References 2.5.4-41 and 2.5.4-42) confirm this conclusion. The proposed granular backfill, based on the gradation and level of compaction, was also not considered susceptible to liquefaction.
- Bearing capacity and settlement criteria are presented in Subsection 2.5.4.10. Generally acceptable total and differential settlements are limited to 6 in. and 3 in., respectively, for large mat foundations, and 1 in. and 0.5 in., respectively, for footings.
- Subsection 2.5.5 discusses the stability of slopes at the site; however, because site grading has not yet been established, the presence of any safety-related slopes has not been determined.

Other geotechnical-related criteria that pertain to structural design (such as wall rotation, sliding, and overturning) are addressed at the COLA stage, specific to the selected technology.

2.5.4.12 Techniques to Improve Subsurface Conditions

The presence of karst at the CRN Site and in the power block area specifically is described in Subsection 2.5.1.2.5. The impact of any karst features on safety-related structures must be evaluated once the locations of these structures have been established. Assuming these structures are deeply embedded in rock, the use of geophysical methods from the surface to

evaluate the presence of karst at depth is difficult. Instead, a subsurface investigation using geophysical methods to evaluate the presence of karst is recommended once the floor of the excavation is reached. The goal of this investigation is to detect any potential voids below the foundation level within a certain zone of influence (void zone of influence). The void zone is developed considering the minimum size and location (both areal and depth) of a potential void beneath the foundation that does not detrimentally impact the foundation. The particular geophysical method(s) used depends on the depth of the zone of influence and the resolution required to detect potential voids. If anomalies are identified during the geophysical investigation, core drilling is conducted to validate the anomalies and identify remedial needs. Remediation may include grouting.

Due in part to the dipping stratigraphic units and adjustment of the rock mass due to excavation, it is likely to be difficult to obtain a smooth flat excavation surface. Instead, the surface is likely to be jagged where bedding planes contribute to the removal of irregularly shaped rock blocks. Dental concrete is used to create a smooth and level foundation surface. This dental work requires careful cleaning of the rock surface. Placement of dental concrete should not exceed 18 in. in thickness.

Excavation mapping is conducted during the entire excavation as described in Reference 2.5.4-38.

The excavation slopes and side walls are expected to be bolted as discussed in Subsection 2.5.4.5.

An instrumentation plan is developed to monitor lateral and vertical displacement during excavation and construction. Slope inclinometers and horizontal extensometers are installed to monitor slope movement. Extensometers are installed to monitor heave in subsurface materials due to the excavation associated relaxation of the rock mass. Settlement monitors are installed to monitor the vertical movement during and after construction. Piezometers are installed to monitor changes in pore pressures during excavation and dewatering, and settlement due to construction of the structures. The power block area is underlain by hard rock, where heave and settlement due to construction activities are expected to be minimal and to take place simultaneously with construction. Any monitoring is developed and implemented prior to start of construction.

2.5.4.13 Foundation Assessment Model

A PLAXIS 2D model was developed to determine potential karstic cavity impacts on SMR foundations. The details of the analysis are contained within Reference 2.5.4-59. Cases were performed at 40 ft, 90 ft, and 140 ft depths for 5 foot, 10 foot, and 15 foot cavity sizes at varying locations under the foundation. Table 2.5.4-33 provides the cases for Location A and B.

The PLAXIS model for Location A and B was performed at two different cross-sections, to account for varying dip of the stratigraphic layers. The model included a disturbed zone around the simulated cavity to include the appropriate material properties for cohesion and friction angle. The model also included initial conditions, dewatering assumptions, excavation assumptions and loading similar to currently approved Large Light Water Reactor designs. The results of the foundation assessment model are provided in Table 2.5.4-34.

The results of the FE models were evaluated with one primary goal: to identify a cavity size that may potentially collapse under static excavation, dewatering, and structural loads. Anticipated foundation host rocks, namely the Fleanor Member of the Lincolnshire Formation and the Benbolt and Rockdell formations, are all relatively stiff/competent rocks. Excluding potential cavity collapses, these rock formations are not expected to undergo large strains or deformations

under excavation, dewatering, or structural static loads (i.e., foundation deformations are expected to be negligible). As such, the foundations should be safe provided that potential postulated critical (large enough size) cavities do not collapse.

The collapse potential of cavities is evaluated in terms of relative shear. Relative shear is the ratio of induced shear stress (due to static loads) to shear strength. If this ratio reaches 100 percent, a plastic zone (Mohr-Coulomb failure) starts to develop around a cavity, and collapse is initiated. Initiation of plastic zone does not denote impending failure, and further loading is needed to propagate the failure zone to the surface. Therefore, this approach provides additional conservatism. For Location A and B modeling purposes, a critical relative shear ratio value of 0.85 (85 percent) was conservatively selected to provide a margin of safety of at least 15 percent.

All model results after loading phase were specifically evaluated in terms of relative shear and vertical formation, with consideration for cavity diameters, depths, locations, and foundation embedment depths.

For model scenarios featuring 15 ft cavity diameters, relative shear values are about 10 percent higher relative to models utilizing 5 ft cavity diameter. Vertical deformation resulting from a 15 ft cavity diameter is also about 2 percent higher than the vertical deformations resulting from a 5 ft diameter cavity.

The computational results suggest that models of 15 ft cavity diameters represent the most critical case of failure, relative to models of 10 ft and 5 ft cavity diameters. However, the effect of cavity size on deformation is negligible given that calculated critical ratios indicate that collapse is not initiated, and is only near the critical limit for the 15 ft cavity size.

Relative shear values are about 10 percent higher for PLAXIS 2D models of cavities located 30 ft below foundation basemat, relative to models featuring cavity depths 5 ft below the basemat. However, vertical deformations resulting from cavities located 5 ft below the foundation basemat are approximately 6 percent higher than vertical deformations resulting from cavities located 30 ft below the foundation basemat.

Models of cavities located below the center of the foundation or below the edge of foundation exhibit nearly comparable relative shear values. In contrast, models featuring cavities positioned on a stratigraphic contact (i.e., a bedding plane) demonstrate relative shear values about 40 percent higher. With regards to vertical deformations, models of cavity location 5 ft below foundation basemat levels exhibit deformations roughly 50 percent higher than models of cavities located on bedding plane discontinuities.

Postulated collapse of karstic cavities is a geologic hazard to be addressed for the proposed SMR Units 1 and 2 and 3 and 4 at the CRN Site. Accordingly, the impact of various postulated cavity sizes and locations on SMR foundation performance were evaluated using a PLAXIS 2D model. Specifically, the PLAXIS 2D model developed for Units 1 and 2 (Location A) and 3 and 4 (Location B) considered:

- cavity diameters equal to 5 ft, 10 ft, and 15 ft (selected based on what size is likely to fail and based on observed cavity sizes),
- cavity depths of 5 ft and 30 ft below foundation embedment depths,
- foundation embedment depths of 40 ft, 90 ft, and 140 ft,
- cavity locations on the edge of the nuclear island, the center of the nuclear island, and on or along bedding planes conservatively assumed to feature significant discontinuities or fracture zones.

For all cases considered, the following main conclusions can be drawn:

1. For all model simulations, the largest cavity diameter (15 ft) was determined to be most critical as expected.

2. Deeper cavities produce increased relative shear around the cavity, which is attributed to the larger initial in situ stresses.

3. Relative shears around the cavities are comparable for individual embedment depths. However, vertical deformation increases with decreasing depth of a cavity relative to foundation embedment depths/excavation surfaces.

4. Cavities located on bedding plane discontinuities or in bedding plane fracture zones are most critical and result in highest relative shear around the cavity.

Approximately 99 percent of the cavities observed in Location A and B borings are significantly less than 11 ft in inferred height. Maximum observed cavity height does not exceed 17 ft. Moreover, cavity development in CRN Site areas is generally limited to the most markedly weathered zone immediately below ground surface, to depths less than 100 ft; 75 percent of reported cavities in Location A and B borings occur at depths less than 55 ft. Consequently, cavity-related failure has a higher potential to occur at relatively shallow depth, less than about 30 ft. Given that foundation embedment depths are deeper than 30 ft and that the 15 ft critical cavity diameter determined by PLAXIS 2D modeling is significantly larger than the 11 ft height that bounds 99 percent of the cavities observed in CRN Site borings, Location A and B are generally suitable for SMR foundation.

Nonetheless, at COLA, foundation performance will be re-evaluated on selection of a final technology, taking into account specific plant design, specific plant loads, and any potential ground improvement or grouting plans. Final foundation locations will also be re-evaluated using specific plant information, with consideration for specific site stratigraphy, subsurface layering orientation, and specific fracture or bedding plane discontinuity zonation.

In addition to the karst evaluation performed in the PLAXIS 2D analysis, an additional analysis of the site bearing capacity was performed for Location A and B at 80 and 138 foot depths. This finite-element analysis is provided to confirm the validity of the simplified model used for bearing capacity and settlement in Subsection 2.5.4.10. The analysis is provided in Reference 2.5.4-60. The ultimate bearing capacity for the CRN Site is high, ranging from 320 kips per square foot to 526 kips per square foot for the sections and embedment depths evaluated. The ultimate bearing capacity of Location A is estimated as 441 kips per square foot, and the ultimate bearing capacity for Location B is estimated as 320 kips per square foot. Geometry modifications were made to allow the PLAXIS model to be more consistent with the bearing capacity calculations presented in Subsection 2.5.4.10.1.2 and Table 2.5.4-27. When a factor of safety of 3 is considered to determine the allowable bearing capacity, the values from this analysis compare very well with the previously performed allowable bearing capacity analysis as presented in Subsection 2.5.4.10. For Location A, the PLAXIS bearing capacity is 147 kips per square foot as compared to the SSAR bearing capacity of 149 kips per square foot. For Location B, the PLAXIS bearing capacity is 107 kips per square foot as compared to the SSAR bearing capacity of 108 kips per square foot. In general, the comparison of these two methodologies and the subsequent results demonstrates a reasonable agreement for the allowable bearing capacity.

2.5.4.14 References

2.5.4-1. AMEC Environment and Infrastructure Inc., *Data Report Rev. 4. Geotechnical Exploration and Testing, Clinch River SMR Project, Oak Ridge, Tennessee*, AMEC Project No. 6468-13-1072, October 16, 2014.

2.5.4-2. Project Management Corporation, *Clinch River Breeder Reactor Project Preliminary Safety Analysis Report*, Vol. 3, 1982.

2.5.4-3. Project Management Corporation, *Clinch River Breeder Reactor Project Preliminary Safety Analysis Report*, Vol. 2, 1982.

2.5.4-4. Law Engineering Testing Company, *Low Water and Groundwater Hydrology, Geology, and Seismology Report*, Clinch River Breeder Reactor Plant, Atlanta, Georgia, May 1974.

2.5.4-5. Law Engineering and Environmental Services, *Report of Cut Site Exploration, Former Clinch River Breeder Reactor Site, Roane County, Tennessee*, June 1998.

2.5.4-6. Hatcher et al., *Status Report on the Geology of the Oak Ridge Reservation*, Oak Ridge National Laboratory, Environmental Sciences Division, Publication No. 3860, October 1992.

2.5.4-7. Department of Energy, TVA, and Project Management Corporation, “Site Redress Planning Task Force Report,” January 1984.

2.5.4-8. Kummerle, R.P., and D.A. Benvie, *Exploration, Design and Excavation of Clinch River Breeder Reactor Foundations,* 28th U.S. Symposium on Rock Mechanics, Tucson, June 1987.

2.5.4-9. ASTM D2487-11, “Standard Practice for Classification of Soils for Engineering Purposes (Unified Soil Classification System).”

2.5.4-10. ASTM D6032-08, “Standard Test Method for Determining Rock Quality Designation (RQD) of Rock Core.”

2.5.4-11. Lemiszki, P.J., R.D. Hatcher, and R.H. Ketelle, *Preliminary Detailed Geologic Map of the Oak Ridge, TN Area*, DRAFT, scale 1:24,000, 2013.

2.5.4-12. Coduto, D.P., *Geotechnical Engineering Principles and Practices*, 2nd ed., Prentice Hall, NJ, 2010.

2.5.4-13. Naval Facilities Engineering Command, “Foundation and Earth Structures, Design Manual 7.02,” September 1986.

2.5.4-14. Bowles, J.E., *Foundation Analysis and Design*, 4th ed., McGraw-Hill Book Company, New York, 1988.

2.5.4-15. ASTM D1557-12. “Standard Test Methods for Laboratory Compaction Characteristics of Soil Using Modified Effort (56,000 ft-lbf/ft^3 (2,700 kN-m/m^3)).”

2.5.4-16. Davie, J.R., and M.R. Lewis, *Settlement of Two Tall Chimney Foundations*, Proceedings, 2nd International Conference on Case Histories in Geotechnical Engineering, St. Louis, MO, June 1988.

2.5.4-17. ASTM D5079-08, “Standard Practices for Preserving and Transporting Rock Core Samples.”

2.5.4-18. Hoek, E., P.G. Marinos, and V.P. Marinos, *Characterization and Engineering Properties of Tectonically Undisturbed but Lithologically Varied Sedimentary Rock Masses*, International Journal of Rock Mechanics and Mining Sciences, Vol.42, pp. 277–285, 2005.

2.5.4-19. Hoek, E. et al., *Hoek-Brown Failure Criterion*, Proceedings of the North American Rock Mechanics Symposium and 17th Tunneling Association of Canada Conference, Toronto, Vol. 1, pp. 263–273, 2002.

2.5.4-20. Hoek, E., and E.T. Brown, *Underground Excavations in Rock*, The Institution of Mining and Metallurgy, London, 1980.

2.5.4-21. Deere, D.U., *Technical Descriptions of Rock Cores for Engineering Purposes, Rock Mechanics and Engineering Geology*, Vol. 1, No. 1, pp. 16–22, 1963.

2.5.4-22. Hoek, E., and M.S. Diederichs, *Empirical Estimation of Rock Mass Modulus*, International Journal of Rock Mechanics and Mining Science, Vol. 43, pp. 203–215, 2006.

2.5.4-23. Gokceoglu C. et al., *Predicting the Deformation Moduli of Rock Masses*, International Journal of Rock Mechanics and Mining Sciences, Vol. 40, pp. 701–710, 2003.

2.5.4-24. Justo, J.L. et al., *The Use of Rock Mass Classification Systems to Estimate the Modulus and Strength of Jointed Rock*, Rock Mechanics and Rock Engineering, Vol. 43, pp. 287–304, 2010.

2.5.4-25. ASTM D1587-08, “Standard Practice for Thin-Walled Tube Sampling of Soils for Geotechnical Purposes.”

2.5.4-26. ASTM D2113-14, “Standard Practice for Rock Core Drilling and Sampling of Rock for Site Exploration.”

2.5.4-27. ASTM D4220/D4220M-14, “Standard Practices for Preserving and Transporting Soil Samples.”

2.5.4-28. ASTM D4633-10, “Standard Test Method for Energy Measurement for Dynamic Penetrometers.”

2.5.4-29. ASTM D1586-11, “Standard Test Method for Standard Penetration Test (SPT) and Split-Barrel Sampling of Soils.”

2.5.4-30. ASTM D4044-96, “Standard Test Method for (Field Procedure) for Instantaneous Change in Head (Slug) Tests for Determining Hydraulic Properties of Aquifers,” reapproved 2008.

2.5.4-31. ASTM D5607-08, “Standard Test Method for Performing Laboratory Direct Shear Strength Tests of Rock Specimens Under Constant Normal Force.”

2.5.4-32. ASTM D7128-05, “Standard Guide for Using the Seismic-Reflection Method for Shallow Subsurface Investigation.”

2.5.4-33. ASTM D5753-05, “Standard Guide for Planning and Conducting Borehole Geophysical Logging,” reapproved 2008.

2.5.4-34. ASTM D6274-10, “Standard Guide for Conducting Borehole Geophysical Logging – Gamma.”

2.5.4-35. ASTM D6726-01, “Standard Guide for Conducting Borehole Geophysical Logging-Electromagnetic Induction,” reapproved 2007.

2.5.4-36. ASTM D6167-11, “Standard Guide for Conducting Borehole Geophysical Logging: Mechanical Caliper.”

2.5.4-37. Tennessee Department of Transportation, “Standard Specification for Road and Bridge Construction,” Sections 303 and 903, March 2006.

2.5.4-38. NUREG/CR-5738, “Field Investigations for Foundations of Nuclear Power Facilities,” Rev. 2, November 1999.

2.5.4-39. Electric Power Research Institute, *Guidelines for Determining Design Basis Ground Motions*, EPRI TR-102293, 1993.

2.5.4-40. Youd, T.L. et al., *Liquefaction Resistance of Soils: Summary Report from the 1996 NCEER and 1998 NCEER/NSF Workshops on Evaluation of Liquefaction Resistance of Soils*, Journal of Geotechnical and Geoenvironmental Engineering, Vol. 127, No. 10, October 2001.

2.5.4-41. Polito, C.P., *The Effects of Non-Plastic and Plastic Fines on the Liquefaction of Sandy Soils*, Ph.D. Dissertation, Virginia Polytechnic Institute and State University, December 1999.

2.5.4-42. Seed, R.B., R.E.S. Moss, A.M. Kammerer, J. Wu, J.M. Pestana, M.F. Riemer, R.B. Sancio, J.D. Bray, R.E. Kayen, A. Faris, and K.O. Cetin, *Recent Advances in Soil Liquefaction Engineering: A Unified and Consistent Framework*, Earthquake Engineering Research Center Keynote Presentation, 26th Annual ASCE Geotechnical Spring Seminar, Long Beach, CA, April 30, 2003.

2.5.4-43. USACE, *Rock Foundations*, EM 1110-1-2908, 1994.

2.5.4-44. Serrano, A., and C. Olalla, *Ultimate Bearing Capacity of Rock Masses*, International Journal of Rock Mechanics and Mining Sciences, Vol. 31, No. 2, pp. 93–106, 1994.

2.5.4-45. Merifield, R.S. et al., *Limit Analysis Solutions for the Bearing Capacity of Rock Masses Using the Generalized Hoek-Brown Criterion*, International Journal of Rock Mechanics and Mining Sciences, Vol. 43, pp. 920–937, 2006.

2.5.4-46. Alemdag, S. et al., *Estimation of Bearing Capacity of Basalts at the Atasu Dam Site, Turkey*, Bulletin of Engineering Geology and the Environment, Vol. 67, pp. 79–85, 2007.

2.5.4-47. Kulhawy, F.H., and J.P. Carter, *Settlement and Bearing Capacity of Foundations on Rock Masses and Socketed Foundations in Rock Masses*, F.G. Bell (ed.), Engineering in Rock Masses, Butterworth-Heinemann, Oxford, pp. 231–245, 1992.

2.5.4-48. Bowles, J.E., *Foundation Analysis and Design*, 3rd ed., McGraw-Hill Inc., New York, 1982.

2.5.4-49. Wyllie, D.C., *Foundations on Rock*, 2nd ed., E&FN Spon, Abingdon, 1999.

2.5.4-50. Hoek, E., T.G. Carter, and M.S. Diederichs, *Quantification of the Geological Strength Index Chart*, 47th U.S. Rock Mechanics/Geomechanics Symposium, San Francisco, CA, 2013.

2.5.4-51. ACI 318-14 "Building Code Requirements for Structural Concrete (ACI 318-14) and Commentary," 2014.

2.5.4-52. Westinghouse Electric Company, *AP1000 Design Control Document*, Rev.19, Tier 1 Chap. 5 – Site Parameters, June 2011.

2.5.4-53. Christian, J.T., and W.D Carrier, *Janbu, Bjerrum and Kjaernsli's Chart Reinterpreted*, Canadian Geotechnical Journal, Vol. 15, pp. 123–128, 1978.

2.5.4-54. Hoek, E., *Dr. Evert Hoek's Practical Rock Engineering,* Chap.11 Rock Mass Properties, 2007 ed.

2.5.4-55. Rocscience, Equivalent Mohr-Coulomb Parameters. Available at http://www.rocscience.com/help/rocdata/webhelp/rocdata/Equivalent_Mohr-Coulomb_Parameters.htm, accessed July 10, 2014.

2.5.4-56. ASTM D4718-87, "Standard Practice for Correction of Unit Weight and Water Content for Soils Containing Oversize Particles," reapproved 2007.

2.5.4-57. Peck, R.B., W.E. Hanson, and T.H. Thornburn, *Foundation Engineering*, 2nd ed., John Wiley & Sons, Inc., New York, 1974.

2.5.4-58. Boore, D.M., and W.B. Joyner, *Site Amplifications for Generic Rock Sites*, Bulletin of the Seismological Society of America, Vol. 87, pp 327-341, 1997.

2.5.4-59. Rizzo Associates, "Non-Proprietary Report Foundation Assessment Clinch River Nuclear Site," Revision 0, June 16, 2017.

2.5.4-60. Rizzo Associates, "Addendum to Non-Proprietary Report Foundation Assessment Clinch River Nuclear Site," Revision 0, June 15, 2017.

2.5.4-61. U.S. Nuclear Regulatory Commission, *Safety Evaluation Report related to the construction of the Clinch River Breeder Reactor Plant*, Docket No. 50-537, NUREG-0968, Vol. 1, Main Report, 1983.

Table 2.5.4-1
Average Thickness and Variability of the Bedrock Stratigraphic Units

Strata	Average Thickness (ft)			Rock Coring		
	True[a]	Vertical (apparent)	Variability[b] (% of thickness)	No. of Boreholes	Length Cored (ft)	Percentage of Total
Rome	–	–	–	2	117	0.9%
Moccasin	–	–	–	2	79	0.6%
Witten	353	421	±10	–	–	–
Bowen	25	30	±10	2	41	0.3%
Benbolt	277	330	±10	25	3254	24%
Rockdell	241	287	±10	16	1794	13%
Fleanor	216	257	±10	29	2953	22%
Eidson	86	102	±15	17	1027	8%
Blackford	213	254	±50	15	1554	12%
Newala	–	–	–	16	2501	19%
			Total Footage		13,320	

(a) True thickness is calculated by multiplying the cosine of 33 degrees by the vertical thickness.
(b) Variability is given as the percent of average vertical thickness.

Notes:

"–" = not available.

Table 2.5.4-2 (Sheet 1 of 3)
Summary of Boring Locations and Ground Surface Elevations

Boring ID	GS Existing Elevation (NAVD88) (ft)	GS Historic Elevation (NGVD29) (ft)	Differential from Historic to Current GS El. (ft)[b]	Northing (ft)	Easting (ft)	Depth of Exploration (ft)
MP-101	800.5	794.0	-6.5	570249.6	2448355.2	540.6
MP-102	797.9	790.0	-7.9	570097.9	2448404.3	350.6
MP-103	800.6	790.0	-10.6	570287.2	2448367.5	174.5
MP-104	797.7	792.0	-5.7	570093.9	2448449.1	177.2
MP-105	800.2	796.0	-4.2	570210.2	2448343.5	195.2
MP-106	798.7	798.0	-0.7	570136.4	2448377.2	174.2
MP-107	801.6	784.0	-17.6	570291.6	2448284.8	174.6
MP-108	798.5	790.0	-8.5	570051.7	2448376.3	174.3
MP-109	799.9	801.0	1.1	570144.6	2448295.8	174.0
MP-110	798.7	792.0	-6.7	570190.7	2448403.3	174.0
MP-111	801.1	786.0	-15.1	570328.7	2448345.0	173.9
MP-112[a], 28	799.2	784.0	-15.2	570261.9	2448472.1	177.5
MP-113[a], 28	797.5	784.0	-13.5	570184.9	2448486.5	178.0
MP-114	797.2	791.0	-6.2	570052.5	2448464.6	175.2
MP-115	796.9	785.0	-11.9	570094.9	2448562.0	99.1
MP-116	797.6	778.0	-19.6	570202.4	2448560.2	100.4
MP-117	800.0	784.0	-16.0	570296.0	2448520.2	99.7
MP-118	799.8	792.0	-7.8	570370.9	2448445.5	99.1
MP-119	802.1	798.0	-4.1	570414.6	2448544.7	100.9
MP-120	800.1	786.0	-14.1	570319.1	2448584.2	350.0
MP-121	797.6	776.0	-21.6	570227.9	2448623.1	100.9
MP-122	796.7	779.0	-17.7	570130.4	2448654.4	99.3
MP-201	790.9	804.0	13.1	571083.7	2447980.8	420.6
MP-202	811.8	850.0	38.2	570922.1	2448050.0	461.0
MP-203	791.5	805.0	13.5	571118.2	2448014.3	225.6
MP-204	812.0	860.0	48.0	570921.7	2448097.0	176.9
MP-205	810.9	818.0	7.1	571025.3	2448006.8	225.5
MP-206	811.8	832.0	20.2	570964.0	2448025.6	176.4
MP-207	779.7	796.0	16.3	571101.6	2447930.3	225.7
MP-208	811.9	856.0	44.1	570880.5	2448024.1	174.6
MP-209	807.7	822.0	14.3	570972.7	2447945.1	225.7
MP-210	809.9	824.0	14.1	571019.3	2448051.2	174.4
MP-211	779.8	798.0	18.2	571162.0	2447986.6	176.0
MP-212[a], 27	810.7	828.0	17.3	571093.5	2448107.3	177.8
MP-213[a], 28	813.0	852.0	39.0	571009.3	2448148.5	177.3
MP-214	812.5	872.0	59.5	570881.2	2448110.8	175.8
MP-215	813.4	882.0	68.6	570924.5	2448210.7	100.6

Table 2.5.4-2 (Sheet 2 of 3)
Summary of Boring Locations and Ground Surface Elevations

Boring ID	GS Existing Elevation (NAVD88) (ft)	GS Historic Elevation (NGVD29) (ft)	Differential from Historic to Current GS El. (ft)[b]	Northing (ft)	Easting (ft)	Depth of Exploration (ft)
MP-216	813.4	860.0	46.6	571031.0	2448209.1	101.5
MP-217	811.6	832.0	20.4	571125.2	2448169.2	99.3
MP-218	810.9	820.0	9.1	571176.5	2448147.4	99.6
MP-219	812.9	818.0	5.1	571223.7	2448195.7	96.5
MP-219A	808.6	810.0	1.4	571254.2	2448184.6	269.1
MP-220	813.2	840.0	26.8	571146.9	2448232.2	101.3
MP-221	813.1	864.0	50.9	571056.6	2448270.6	101.2
MP-222	812.9	880.0	67.1	570965.5	2448308.6	101.0
MP-401	817.7	820.0	2.3	571954.2	2447605.1	419.6
MP-402	816.5	820.0	3.5	571941.4	2447479.8	199.3
MP-403	836.2	870.0	33.8	571646.0	2447607.5	199.2
MP-404	837.1	846.0	8.9	571709.4	2447758.1	199.8
MP-405	816.9	825.0	8.1	571979.1	2447644.2	20.4
MP-405A	817.1	ND	ND	571975.7	2447647.3	199.4
MP-406	855.1	856.0	0.9	571775.0	2447965.9	201.3
MP-407	761.5	756.0	-5.5	569888.8	2447094.2	200.2
MP-408	Borehole Deleted					
MP-409	807.0	830.0	23.0	570584.3	2448158.9	251.5
MP-410	809.4	840.0	30.6	570774.2	2448368.8	201.0
MP-411	836.8	883.0	46.2	571500.5	2447500.3	199.6
MP-412	823.7	840.0	16.3	571424.0	2447850.6	321.0
MP-413	809.0	792.0	-17.0	571645.7	2446938.7	199.2
MP-414	817.5	816.0	-1.5	572070.0	2447564.7	199.4
MP-415	784.3	780.0	-4.3	569577.1	2448164.8	320.1
MP-416	809.6	758.0	-51.6	569978.3	2447520.0	321.7
MP-417	772.7	750.0	-22.7	569915.4	2446630.3	320.1
MP-418	811.6	788.0	-23.6	570500.3	2447030.2	87.8
MP-418A	811.1	786.0	-25.1	570514.7	2447049.6	320.6
MP-419	799.6	784.0	-15.6	571269.8	2446700.6	321.1
MP-420	803.1	809.0	5.9	572033.0	2446918.3	319.4
MP-421	803.6	781.0	-22.6	570532.3	2446439.6	320.3
MP-422	799.9	799.0	-0.9	570423.7	2448732.0	320.0
MP-423	799.0	786.0	-13.0	571470.3	2448276.4	319.3
MP-424[a], 25	800.6	788.0	-12.6	570450.2	2448361.2	273.2
MP-425[a], 29	811.9	ND	ND	570814.6	2448199.5	272.9
MP-426[a], 28	842.2	841.0	-1.2	571764.5	2447811.0	272.3
MP-427	Borehole Deleted					
MP-428	803.8	800.0	-3.8	570755.5	2448681.6	250.7

Table 2.5.4-2 (Sheet 3 of 3)
Summary of Boring Locations and Ground Surface Elevations

Boring ID	GS Existing Elevation (NAVD88) (ft)	GS Historic Elevation (NGVD29) (ft)	Differential from Historic to Current GS El. (ft)[(b)]	Northing (ft)	Easting (ft)	Depth of Exploration (ft)
MP-429	796.0	776.0	-20.0	569975.5	2448591.1	199.2
CC-B1	800.3	ND	ND	569036.1	2449632.4	140.6
CC-B2	799.8	ND	ND	568891.0	2449759.9	206

(a) Angle boring with inclination angle indicated.
(b) Does not account for differences between NAVD88 and NGVD29.

Notes:

GS = ground surface.

ND = not determined.

Table 2.5.4-3 (Sheet 1 of 3)
Summary of Thicknesses of the Existing Fill/Residual Soil and Weathered Rock and Depth to the Top of Bedrock

Boring ID	Existing Elevation (NAVD88)	Bottom Elevation			Thickness (ft)			Depth to Top of Bedrock (ft)
		Fill	Residual	Weathered Rock	Fill	Residual	Weathered Rock	
MP-101	800.5	791.4	787.5	779.9	9.1	3.9	7.6	20.6
MP-102	797.9	793.4	–	776.3	4.5	0.0	17.1	21.6
MP-103	800.6	788.6	783.6	780.4	12.0	5.0	3.2	20.2
MP-104	797.7	790.7	786.5	784.9	7.0	4.2	1.6	12.8
MP-105	800.2	790.7	–	783.0	5.0	4.5	7.7	17.2
MP-106	798.7	793.7	–	774.5	5.0	0.0	19.2	24.2
MP-107	801.6	795.6	762.6	761.6	6.0	33.0	1.0	40.0
MP-108	798.5	796	790.4	790.4	2.5	5.6	0.0	8.1
MP-109	799.9	797.4	794.9	783.6	2.5	2.5	11.3	16.3
MP-110	798.7	795.7	784.4	774.7	3.0	11.3	9.7	24.0
MP-111	801.1	785.1	766.4	765.1	16.0	18.7	1.3	36.0
MP-114	797.2	795.2	785.3	785.3	2.0	9.9	0.0	11.9
MP-115	796.9	783.9	779.9	779.4	13.0	4.0	0.5	17.5
MP-116	797.6	769.8	764.9	763.6	21.0	7.0	6.0	34.0
MP-117	800.0	782	774	770.3	18.0	8.0	3.7	29.7
MP-118	799.8	786.8	781.2	780.7	13.0	5.6	0.5	19.1
MP-119	802.1	798.1	–	781.2	4.0	0.0	16.9	20.9
MP-120	800.1	793.1	775.1	770.2	7.0	18.0	4.9	29.9
MP-121	797.6	781.6	774.3	773.6	16.0	7.3	0.7	24.0
MP-122	796.7	780.7	769.7	765.8	16.0	11.0	3.9	30.9
				Minimum:	2.0	2.5	0.5	
				Maximum:	21.0	33.0	19.2	
MP-201	790.9	774.4	–	760.3	16.5	0.0	14.1	30.6
MP-202	811.8	806.8	–	802.8	5.0	0.0	4.0	9.0
MP-203	791.5	772.3	–	770.9	19.2	0.0	1.4	20.6
MP-204	812.0	809	–	808.6	3.0	0.0	0.4	3.4
MP-205	810.9	805.4	799.4	787.4	5.5	6.0	12.0	23.5
MP-206	811.8	809.3	806.8	798.0	2.5	2.5	8.8	13.8
MP-207	779.7	776.7	767.2	760.7	3.0	9.5	6.5	19.0
MP-208	811.9	808.8	–	805.9	3.1	0.0	2.9	6.0
MP-209	807.7	0	–	803.8	0.0	0.0	3.9	3.9
MP-210	809.9	789.4	–	786.2	20.5	0.0	3.2	23.7
MP-211	779.8	771.3	770.3	761.9	8.5	1.0	8.4	17.9
MP-214	812.5	808.5	–	807.7	4.0	0.0	0.8	4.8
MP-215	813.4	805.4	–	802.8	8.0	0.0	2.6	10.6
MP-216	813.4	0	–	806.9	0.0	0.0	6.5	6.5
MP-217	811.6	788.6	773.6	772.3	23.0	15.0	1.3	39.3

Table 2.5.4-3 (Sheet 2 of 3)
Summary of Thicknesses of the Existing Fill/Residual Soil and Weathered Rock and Depth to the Top of Bedrock

Boring ID	Existing Elevation (NAVD88)	Bottom Elevation			Thickness (ft)			Depth to Top of Bedrock (ft)
		Fill	Residual	Weathered Rock	Fill	Residual	Weathered Rock	
MP-218	810.9	775.9	772.5	769.6	35.0	3.4	2.9	41.3
MP-219	812.9	810.9	809	788.4	2.0	1.9	20.6	24.5
MP-219A	808.6	801.6	792.9	774.5	7.0	8.7	18.4	34.1
MP-220	813.2	810.2	805.2	784.5	3.0	5.0	20.7	28.7
MP-221	813.1	812.7	810.1	804.8	0.4	2.6	5.3	8.3
MP-222	812.9	809.9	–	806.9	3.0	0.0	3.0	6.0
				Minimum:	0.4	1.0	0.4	
				Maximum:	35.6	15.0	20.7	
MP-401	817.7	812.8	–	808.0	4.9	0.0	4.8	9.7
MP-402	816.5	809.5	799.7	799.7	2.0	14.8	0.0	16.8
MP-403	836.2	834.2	–	822.0	2.0	0.0	12.2	14.2
MP-404	837.1	833.1	790.1	788.1	4.0	43.0	2.0	49.0
MP-405	816.9	814.9	811.6	811.3	2.0	3.3	0.3	5.6
MP-405A	817.1	815.3	–	815.3	1.8	0.0	0.0	1.8
MP-406	855.1	853.1	847.1	827.8	2.0	6.0	19.3	27.3
MP-407	761.5	749.5	742.5	731.4	12.0	7.0	11.1	30.1
MP-409	807.0	804.5	761	755.9	2.5	43.5	5.1	51.1
MP-410	809.4	803.2	–	801.3	6.2	0.0	1.9	8.1
MP-411	836.8	834.3	–	828.8	2.5	0.0	5.5	8.0
MP-412	823.7	809.1	–	782.7	14.6	0.0	26.4	41.0
MP-413	809.0	787	756.8	756.8	22.0	30.2	0.0	52.2
MP-414	817.5	810.5	775.2	775.2	7.0	35.3	0.0	42.3
MP-415	784.3	781.8	773.3	734.2	2.5	8.5	39.1	50.1
MP-416	809.6	758.6	744.6	737.5	51.0	14.0	7.1	72.1
MP-417	772.7	756.2	735.7	720.0	16.5	20.5	15.7	52.7
MP-418	811.6	784.6	768.6	–	27.0	16.0	0.0	–
MP-418A	811.1	784.1	733.1	730.4	27.0	51.0	2.7	80.7
MP-419	799.6	785.6	748.2	740.4	14.0	37.4	7.8	59.2
MP-420	803.1	801.1	783.9	782.4	2.0	17.2	1.5	20.7
MP-421	803.6	781.6	754.7	745.6	22.0	26.9	9.1	58.0
MP-422	799.9	797.9	790.9	778.9	2.0	7.0	12.0	21.0
MP-423	799.0	797	765	753.6	2.0	32.0	11.4	45.4
MP-428	803.8	780.8	–	762.9	0.0	23.0	17.9	40.9
MP-429	796.0	791.5	769	758.4	4.5	22.5	10.6	37.6
				Minimum:	0.0	3.3	0.3	
				Maximum:	51.0	51.0	39.1	

Table 2.5.4-3 (Sheet 3 of 3)
Summary of Thicknesses of the Existing Fill/Residual Soil and Weathered Rock and Depth to the Top of Bedrock

Boring ID	Existing Elevation (NAVD88)	Bottom Elevation			Thickness (ft)			Depth to Top of Bedrock (ft)
		Fill	Residual	Weathered Rock	Fill	Residual	Weathered Rock	
CC-B1	800.3	–	755.3	751.6	–	45.0	3.8	48.7
CC-B2	799.8	–	765.5	684.1	–	34.8	81.4	115.7
							Minimum	1.8
							Maximum	80.7
							Average	26.2
							Median	22.6

Notes:

Angle borings and borings drilled specifically for intact sample retrieval and shear wave data are not included.

"–" = not encountered.

Table 2.5.4-4
Summary of Rock Core Recovery and Rock Quality Designation for the Bedrock Stratigraphic Units

Formation	Description of Value	Core Recovery (%)	RQD (%)
Benbolt	No. of Cores	677	
	Average	98	88
	Median	100	98
	Minimum	0	0
	Maximum	100	100
	Standard Deviation	10	23
Rockdell	No. of Cores	363	
	Average	98	88
	Median	100	96
	Minimum	22	0
	Maximum	100	100
	Standard Deviation	8	20
Fleanor	No. of Cores	619	
	Average	98	89
	Median	100	98
	Minimum	14	0
	Maximum	100	100
	Standard Deviation	7	20
Eidson	No. of Cores	220	
	Average	95	79
	Median	100	88
	Minimum	0	0
	Maximum	100	100
	Standard Deviation	14	28
Blackford	No. of Cores	332	
	Average	96	81
	Median	100	92
	Minimum	0	0
	Maximum	100	100
	Standard Deviation	11	25
Newala	No. of Cores	527	
	Average	99	93
	Median	100	98
	Minimum	28	0
	Maximum	100	100
	Standard Deviation	4	12

Notes:
RQD = Rock Quality Designation

Table 2.5.4-5
Summary of Previous Studies Performed for the Clinch River Breeder Reactor Project

Company	Subject	Date
Burns & Roe, Inc.	Interim Report, Site Investigation LMFBR Project	August 1973
Law Engineering Testing Company	Low Water and Groundwater Hydrology, Geology, and Seismology	May 1974
E. D'Appolonia Consulting Engineers, Inc.	Report of Subsurface Investigation, Proposed Railroad and Barge Unloading Facilities	May 1975
E. D'Appolonia Consulting Engineers, Inc.	Report of Subsurface Investigation, Proposed Cooling Water Pipeline System and Cooling Tower	May 1975
E. D'Appolonia Consulting Engineers, Inc.	Report of Subsurface Investigation, Proposed Balance of Plant Structures and Borrow Area	June 1975
E. D'Appolonia Consulting Engineers, Inc.	Subsurface Investigation & Foundation Recommendations, Barge Unloading Facility	March 1977

Table 2.5.4-6
Summary of the Clinch River Nuclear Site Subsurface Investigation Field Activities and Field Testing

Field Activity/Test	Number/Length/Duration
Boreholes, including soil borings and rock coring	82
Intact soil samples	3 boreholes, 14 tubes
Standard penetration test sampling	69 boreholes, 588 tests
Rock core sampling	76 boreholes, 13,320 linear ft
Test pits	3
Groundwater observation wells	44
Geochemical groundwater sampling	13 wells
Groundwater sampling for Kd adsorption testing	12 wells
Surface geophysical tests Refraction survey Reflection survey	 approximately 3,400 linear ft approximately 5,200 linear ft
Downhole geophysical tests • Temperature/conductivity • Suspension P-S velocity logging • Acoustic Televiewer logging • Three Arm Caliper • Natural-Gamma • Dual Induction • Borehole Deviation	30 boreholes
Field permeability (packer testing)	12 wells
Slug testing	30 wells
Pumping test	1
Water level measurements	Monthly and quarterly
Rock pressuremeter testing	2 boreholes, 17 tests

Table 2.5.4-7
Summary of Soil and Rock Laboratory Tests Performed for the Clinch River Nuclear Site Subsurface Investigation

Test	Fill	Residual Soil	Benbolt Fm.	Rockdell Fm.	Fleanor Mb.	Eidson Mb.	Blackford Fm.	Newala Fm.
Soil								
Index tests[(a)]	16	18	NA	NA	NA	NA	NA	NA
Unit weight	12	–	NA	NA	NA	NA	NA	NA
Specific gravity	7	–	NA	NA	NA	NA	NA	NA
Triaxial compression (UU)	4	–	NA	NA	NA	NA	NA	NA
Triaxial compression (CU)	3	–	NA	NA	NA	NA	NA	NA
Moisture density (modified Proctor)	3	–	NA	NA	NA	NA	NA	NA
Rock								
Unit weight and specific gravity	NA	NA	30	20	44	25	15	15
Unconfined compression	NA	NA	17	16	30	23	9	15
Direct shear	NA	NA	3	1	3	2	–	–
Slake durability	NA	NA	4	3	2	–	1	–
Calcium carbonate content	NA	NA	1	4	5	2	1	2

(a) Index tests include grain size, natural moisture content, and Atterberg Limits.

Notes:

"–" = Not tested.

NA = Not applicable

Fm. = Formation

Mb. = Member

Source: Reference 2.5.4-1

Table 2.5.4-8
Summary of Measured N-Values and Corrected N-Values

	Fill Soils		Residual Soils	
	N-Value	**N_{60}-Value**	**N-Value**	**N_{60}-Value**
Count	229		169	
Average	16	22	20	30
Median	10	14	14	19
Minimum	2	2	0	0
Maximum	100	191	100	191

Table 2.5.4-9 (Sheet 1 of 2)
Summary of Index Test Results

Boring Number	Material Type	Sample Number	Depth (ft)	Sample Type	Gravel (%)	Sand (%)	Fines (%)	Silt (%)	0.005mm Clay (%)	USCS Symbol	Natural Moisture (%)	LL (%)	PI (%)
Existing Fill													
MP-111UD	Fill	ST-3	9.9-11.9	UD	19.8	12.8	67.4	17.4	50.0	CH	26.2	57	32
MP-111UD	Fill	ST-5	17.4-19.4	UD	15.3	17.9	66.8	20.4	46.4	CH	31.0	56	32
MP-117	Fill	SS-4	8.8-10.0	SS	0.8	11.1	88.1	24.0	64.1	CH	32.0	72	46
MP-122	Fill	SS-5	11.1-12.6	SS	11.4	8.4	80.2	14.4	65.8	ND	ND	ND	ND
MP-122UDA	Fill	ST-2	7.1-9.3	UD	16.6	8.6	74.8	20.2	54.6	CH	27.8	63	33
MP-122UDA	Fill	ST-3	9.7-11.7	UD	15.5	7.4	77.1	16.0	61.1	CH	28.1	69	40
MP-122UDA	Fill	ST-4	12.2-14.2	UD	4.9	9.4	85.7	15.4	70.3	CH	32.7	70	42
MP-122UDB	Fill	ST-1	3.3-5.3	UD	2.7	4.3	93.0	20.2	72.8	CH	29.1	64	36
MP-122UDB	Fill	ST-3	9.2-11.2	UD	ND	ND	ND	ND	ND	ND	39.0	69	41
MP-122UDB	Fill	ST-5	14.6-16.6	UD	17.4	7.3	75.3	19.6	55.7	CH	27.7	59	32
MP-203	Fill	SS-3	5.1-6.6	SS	24.4	10.6	65.0	15.8	49.2	CH	34.3	56	35
MP-210	Fill	SS-4	8.4-9.9	SS	6.9	17.9	75.2	16.6	58.6	CH	20.3	51	31
MP-412	Fill	SS-2	3.6-5.1	SS	23.7	3.1	73.2	7.2	66.0	CH	58.1	109	78
MP-421	Fill	SS-7	15.0-16.5	SS	1.0	8.8	90.2	8.8	81.4	CH	37.3	75	48
MP-424	Fill	SS-8	21.5-23.0	SS	7.8	13.9	78.3	27.9	50.4	ND	ND	ND	ND
TP-2	Fill	S-1	1 -2.5	Bulk	21.1	19.8	59.1	26.2	32.9	CL	16.5	46	27
				Count	15	15	15	15	15		14	14	14
				Average	12.6	10.8	76.6	18.0	58.6		31.4	67	40
				Minimum	0.8	3.1	59.1	7.2	32.9		16.5	46	27
				Maximum	24.4	19.8	93.0	27.9	81.4		58.1	109	78

Table 2.5.4-9 (Sheet 2 of 2)
Summary of Index Test Results

Boring Number	Material Type	Sample Number	Depth (ft)	Sample Type	Gravel (%)	Sand (%)	Fines (%)	Silt (%)	0.005mm Clay (%)	USCS Symbol	Natural Moisture (%)	LL (%)	PI (%)
Residual Soil													
MP-114	Residual	SS-2	2.5-4.0	SS	8.8	11.0	80.2	10.7	69.5	CH	29.9	66	42
MP-116	Residual	SS-9	23.9-25.4	SS	0.0	2.5	97.5	31.7	65.8	CH	26.5	62	40
MP-117	Residual	SS-7	19.5-21.0	SS	0.0	13.2	86.8	27.3	59.5	CH	27.1	68	46
MP-207	Residual	SS-4	8.6-10.1	SS	0.1	15.3	84.6	50.3	34.3	CL	10.9	31	13
MP-217	Residual	SS-12	36-37.5	SS	42.4	28.9	28.7	13.7	15.0	ND	ND	ND	ND
MP-402	Residual	SS-4	7.4-8.9	SS	13.1	16.3	70.6	8.3	62.3	CH	31.9	74	48
MP-409	Residual	SS-2	3.2-4.7	SS	11.6	16.2	72.2	23.4	48.8	CH	24.1	51	30
MP-409	Residual	SS-9	23.4-24.9	SS	46.2	25.0	28.8	12.9	15.9	ND	ND	ND	ND
MP- 409	Residual	SS-12	38.4-39.9	SS	0.0	0.6	99.4	17.5	81.9	CH	45.7	62	42
MP-418A	Residual	SS-16	60.6-61.5	SS	4.0	6.5	89.5	23.8	65.7	ND	ND	ND	ND
MP-419	Residual	SS-13	44.6-46.6	SS	4.5	5.8	89.7	14.5	75.2	ND	ND	ND	ND
MP-421	Residual	SS-11	34.3-35.8	SS	0.0	1.1	98.9	8.8	90.1	CH	39.7	75	54
MP-421	Residual	SS-12	39.3-40.8	SS	0.0	2.9	97.1	6.6	90.5	ND	ND	ND	ND
MP-423	Residual	SS-6	12.4-13.9	SS	0.4	7.9	91.7	30.2	61.5	CH	21.9	67	42
MP-423	Residual	SS-9	25.1-26.6	SS	0.0	18.8	81.2	45.9	35.3	CL	19.0	45	24
MP-423	Residual	SS-10	30.1-31.6	SS	0.1	11.5	88.4	59.0	29.4	ND	ND	ND	ND
MP-424	Residual	SS-10	31.5-33.0	SS	14.8	15.8	69.4	23.9	45.5	ND	ND	ND	ND
TP-1	Residual	S-1	6.0-8.0	Bulk	16.1	6.2	77.7	14.2	63.5	CH	32.2	61	37
				Count	18	18	18	18	18		11	11	11
				Average	9.0	11.4	79.6	23.5	56.1		28.1	60	38
				Minimum	0.0	0.6	28.7	6.6	15.0		10.9	31	13
				Maximum	46.2	28.9	99.4	59.0	90.5		45.7	75	54

Notes:

UD = undisturbed; SS = split spoon; ND = not determined; CH = clay, high plasticity; CL = clay, low plasticity; LL = liquid limit; PI = plasticity index

Table 2.5.4-10
Summary of UU and CU Strength Tests

Unconsolidated Undrained

Source of Sample	Sample No.	Sample Depth (ft)	Material Type	Atterberg Limits		USCS Symbol	Estimated Specific Gravity	Dry Unit Weight (pcf)	Moisture Content (%)	Test Data (UU)		
				LL	PI					σ_c (psi)	ε_f (%)	Strength (psi)
MP-111UD	ST-4	15.5–17.5	FILL	ND	ND	ND	2.75	100.7	26.8	14	15.0	3.988
MP-122UDA	ST-4	12.2–14.2	FILL	70	42	CH	2.75	85.5	36.1	14	6.7	10.85
MP-122UDB	ST-1	3.3–5.3	FILL	64	36	CH	2.75	91.9	29.9	14	15.0	14.25
MP-122UDB	ST-3	9.2–11.2	FILL	69	41	CH	2.75	87.0	34.0	14	9.6	7.354
			Average	68	40			91.3	31.7			9.1
			Minimum	64	36			85.5	26.8			4.0
			Maximum	70	42			100.7	36.1			14.3

Consolidated Undrained

Source of Sample	Sample No.	Sample Depth (ft)	Material Type	Atterberg Limits		USCS Symbol	Estimated Specific Gravity	Dry Unit Weight (pcf)	Moisture Content (%)	Triaxial Test Data (CU)			
				LL	PI					c (psi)	ø (degree)	c' (psi)	ø' (degree)
MP-111UD	ST-3	9.9-11.9	FILL	57	32	CH	2.75	93.3	30.0	2.7	12.1	1.3	21.7
								94.8	28.9				
MP-122UDA	ST-3	9.7–11.7	FILL	69	40	CH	2.75	91.0	29.7	2.2	16.4	0.9	26.8
	ST-4	12.2–14.2		70	42			93.0	28.6				
	ST-3	9.7–11.7		69	40			94.4	28.3				
MP-122UDB	ST-5	14.6–16.6	FILL	59	32	CH	2.75	86.1	35.0	3	13.3	2	20.1
	ST-3	9.2–11.2		69	41			88.7	33.2				
	ST-5	14.6–16.6		59	32			97.1	27.5				
			Average	65	37			92.3	30.2	2.7	13.9	1.4	22.9
			Minimum	57	32			86.1	27.5	2.2	12.1	0.9	20.1
			Maximum	70	42			97.1	35.0	3.1	16.4	2.0	26.8

Notes:
ND = not determined.
CH = clay, high plasticity

Table 2.5.4-11
Summary of Shear and Compression Wave Velocities and Poisson's Ratio for the Existing Fill/Residual Soil and Weathered Rock

Strata Type	V_s (fps)		V_p (fps)		μ
	Mean	Standard Deviation	Mean	Standard Deviation	
Existing Fill/Residual Soil	600	130	3,020	1,170	0.40
Weathered Rock	1,870	600	5,740	1,080	0.40

Notes:

V_s = Shear wave velocity

V_p = Compression wave velocity

μ = Poisson's Ratio

Table 2.5.4-12
Summary of Soil Compaction Test Results

Source of Sample	Sample No.	Atterberg Limits		Natural Moisture [a] (%)	Percent Passing No. 200 Sieve (%)	USCS Classification	Moisture-Density Relationship Data [b]		
		Liquid Limit (LL)	Plasticity Index (PI)				Maximum Dry Density (pcf)	Optimum Moisture (%)	
Test Pit TP-1, 6 - 8 ft	S-1	61	37	32.2	77.7	CH	109	16.7	A
Test Pit TP-2, 1 - 2.5 ft	S-1	46	27	16.5	59.1	CL	120.6	10.9	B
							122.7	10.3	C
Test Pit TP-3, 3 - 6 ft	S-1	58	31	20.9	41.0	SC	105.4	17.4	A
	Average	55	32	23.2	59.3		114.4	13.8	
	Minimum	46	27	16.5	41.0		105.4	10.3	
	Maximum	61	37	32.2	77.7		122.7	17.4	

(a) Natural moisture content tests performed on jar samples obtained at same time as bulk samples

(b) Proctor compaction tests performed as indicated by letter - A, B, C.

A. ASTM D 1557-12 Modified Method C (Reference 2.5.4-15)

B. ASTM D 1557-12 Modified Method C with no oversize correction applied (Reference 2.5.4-15)

C. ASTM D 1557-12 Modified Method C with oversize correction (Reference 2.5.4-15); [ASTM D 4718-87 (Reference 2.5.4-56) applied].

Notes:

CH = clay, high plasticity

CL = clay, low plasticity

SC = clayey sand

Table 2.5.4-13
Summary of Unit Weight Test Results for the Bedrock Stratigraphic Units

Formation	Description of Value	Unit Weight (pcf)	Specific Gravity (G_s)
Benbolt	No. of Tests	30	30
	Average	167.9	2.70
	Median	168	2.70
	Minimum	163	2.62
	Maximum	170	2.72
	Standard Deviation	1.3	0.02
Rockdell	No. of Tests	20	20
	Average	167.4	2.69
	Median	168	2.69
	Minimum	160	2.57
	Maximum	169	2.71
	Standard Deviation	2.0	0.03
Fleanor	No. of Tests	44	44
	Average	168.2	2.70
	Median	168	2.70
	Minimum	166	2.67
	Maximum	176	2.83
	Standard Deviation	1.5	0.02
Eidson	No. of Tests	25	25
	Average	167.2	2.69
	Median	167	2.69
	Minimum	164	2.64
	Maximum	169	2.71
	Standard Deviation	1.4	0.02
Blackford	No. of Tests	15	15
	Average	166.8	2.68
	Median	167	2.68
	Minimum	164	2.64
	Maximum	169	2.71
	Standard Deviation	1.4	0.02
Newala	No. of Tests	15	15
	Average	174.0	2.79
	Median	176	2.82
	Minimum	161	2.59
	Maximum	177	2.84
	Standard Deviation	4.1	0.07

Table 2.5.4-14
Summary of Moisture Contents for the Fleanor Member

Boring Number	Sample ID	Sample Depth (ft)	Unit Weight (pcf)	Moisture Content (%)	Specific Gravity	Comments
MP-218	CL9-1	66.7-67.7	168.7	0.6	2.71	Special care
MP-218	CL9-6	67.8-68.8	167.1	1	2.68	Routine care
MP-218	CL9-2	71.3-72.3	166.4	1.6	2.67	Special care
MP-218	CL9-7	72.3-73.3	168.8	1.1	2.71	Routine care
MP-218	CL9-3	79.5-80.5	168.1	1.7	2.7	Special care
MP-218	CL9-8	80.5-81.5	167.5	1.4	2.69	Routine care
MP-218	CL9-4	85.3-86.3	169.2	1.1	2.72	Special care
MP-218	CL9-9	86.3-87.3	168.9	1	2.71	Routine care
MP-218	CL9-5	90.3-91.3	167.6	1.4	2.69	Special care
MP-218	CL9-10	91.3-92.3	167.2	1.4	2.69	Routine care
			Minimum	0.6		
			Maximum	1.7		
			Average	1.23		
			Median	1.25		

Notes:

Routine or Special care indicates whether the sample was prepared in accordance with ASTM D5079 Sections 7.5.1 or 7.5.2, respectively (Reference 2.5.4-17).

Table 2.5.4-15
Summary of Unconfined Compression Test Results

Formation	Description of Value	Unconfined Compressive Strength (psi)	Modulus of Elasticity (psi)	Poisson's Ratio
Benbolt	No. of Tests	17	6	
	Average	6,173	6,720,000	0.23
	Median	6,300	6,890,000	0.21
	Minimum	2,300	2,490,000	0.18
	Maximum	12,430	10,510,000	0.32
	σ	3,060	2,842,921	0.05
Rockdell	No. of Tests	16	7	
	Average	8,714	7,462,857	0.23
	Median	7,550	8,410,000	0.25
	Minimum	3,830	1,920,000	0.11
	Maximum	15,990	13,660,000	0.43
	σ	4,199	4,386,862	0.11
Fleanor	No. of Tests	30	9	
	Average	5,423	2,854,444	0.18
	Median	5,315	2,370,000	0.18
	Minimum	1,130	930,000	0.03
	Maximum	9,910	5,950,000	0.30
	σ	2,266	1,554,374	0.08
Eidson	No. of Tests	23	9	
	Average	8,032	6,000,000	0.21
	Median	7,390	4,980,000	0.20
	Minimum	3,500	1,620,000	0.14
	Maximum	18,310	11,080,000	0.29
	σ	3,499	3,473,860	0.05
Blackford	No. of Tests	9	4	
	Average	6,236	4,952,500	0.19
	Median	4,770	4,700,000	0.22
	Minimum	1,340	3,150,000	0.10
	Maximum	10,250	7,260,000	0.23
	σ	3,063	1,888,657	0.06
Newala	No. of Tests	15	10	
	Average	21,421	10,438,000	0.27
	Median	21,790	11,415,000	0.29
	Minimum	5,810	2,360,000	0.05
	Maximum	33,110	13,980,000	0.45
	σ	7,658	3,395,483	0.11

Notes:
σ = Standard Deviation

Table 2.5.4-16
Summary of Shear (V_s) and Compression (V_p) Wave Velocities for the Bedrock Stratigraphic Units Obtained for the Clinch River Nuclear Site and from the Clinch River Breeder Reactor Project

Rock Unit	Shear Wave Velocity (V_s) (fps)						Compression Wave Velocity (V_p) (fps)					
	Average		Maximum		Minimum		Average		Maximum		Minimum	
	CRN Site	CRBRP	CRN Site	CRBRP	CRN Site	CRBRP	CRN Site	CRBRP	CRN Site	CRBRP	CRN Site	CRBRP
Bowen	4,700	–	6,730	–	2,460	–	9,200	–	12,350	–	5,010	–
Benbolt	8,000	–	10,500	–	5,070	–	15,400	–	21,510	–	10,100	–
Rockdell	9,000	–	11,490	–	6,260	–	17,100	–	21,510	–	12,120	–
Fleanor	7,200	7,200	10,180	7,800	4,650	4,400	14,500	13,800	19,610	17,000	10,420	9,200
Eidson	9,000	9,400	11,490	10,000	5,380	8,200	17,000	17,600	20,200	20,200	10,580	16,400
Upper Blackford	8,200	9,200	11,400	10,400	4,880	7,000	15,700	17,000	22,220	19,400	9,390	14,200
Lower Blackford												
Newala	10,800	–	12,820	–	6,500	–	19,900	–	23,810	–	12,820	–

Notes:
"–" = not determined/not available.
CRN = Clinch River Nuclear
CRBRP = Clinch River Breeder Reactor Project

Table 2.5.4-17
Summary of Rock Pressuremeter Test Results for the Bedrock Stratigraphic Units

Formation	Test	Depth at Center of Test (ft)	Elevation of Center of Test (ft)	Pressuremeter Shear Modulus at 500 psi	Pressuremeter Shear Modulus at 1000 psi	Pressuremeter Shear Modulus at 1500 psi	Average Pressuremeter Shear Modulus	RQD at Test Interval (%)
Benbolt	PM105-1A	84	716.2	175.3	272.0	667.4	371.6	98
	PM105-1B	82.5	717.7	201.5	646.6	1,118.4	655.5	98
	PM105-2B	138.6	661.6	370.0	957.0	1,372.0	899.7	100
	Average Values (G_{avg})			248.9	625.2	1,052.6	–	–
Rockdell	PM105-2A	141.3	658.9	91.0	466.0	973.3	510.1	98
	PM105-3A	188.9	611.3	208.0	575.0	715.0	499.3	74
	PM105-3B	187.4	612.8	220.0	530.0	713.0	487.7	74
	PM105-3F	193.7	606.5	253.0	423.0	823.0	499.7	26
	PM105-3G	191.3	608.9	136.0	339.0	589.0	354.7	26
	Average Values (G_{avg})			181.6	466.6	762.7	–	–
Fleanor	PM205-1A	74	736.9	254.0	434.0	564.0	417.3	90
	PM205-1B	72.5	738.4	466.0	866.0	1,176.0	836.0	90
	Average Values (G_{avg})			360.0	650.0	870.0	–	–
Eidson	PM205-2A	163.8	647.1	336.0	578.0	796.0	570.0	100
	PM205-2B	162.3	648.6	276.0	506.0	725.0	502.3	100
	PM205-3A	209.2	601.7	252.0	366.0	404.0	340.7	52
	PM205-3B	207.7	603.2	268.0	538.0	710.0	505.3	52
	Average Values (G_{avg})			283.0	497.0	658.8	–	–

Notes:
Dash (–) = Not applicable
RQD = Rock Quality Designation

Table 2.5.4-18
Summary of Rock Pressuremeter Analysis

Formation	Description of Value	G_{500} (ksi)	Calculated E[(a)] from G_{500} (ksi)	G_{avg} (ksi)	Calculated E[(a)] from G_{avg} (ksi)	Reported PSAR[(b)] E value (ksi)
Benbolt	minimum	175.3	462.8	371.6	980.9	NA
	maximum	370.0	976.8	899.7	2,375.1	NA
	average	248.9	657.1	642.2	1,695.5	NA
Rockdell	minimum	91.0	238.4	354.7	929.2	NA
	maximum	253.0	662.9	510.1	1,336.5	NA
	average	181.6	475.8	470.3	1,232.2	NA
Fleanor	minimum	254.0	680.7	417.3	1,118.5	890
	maximum	466.0	1,248.9	836.0	2,240.5	3,340
	average	360.0	964.8	626.7	1,679.5	1,740
Eidson	minimum	252.0	660.2	340.7	892.5	500
	maximum	336.0	880.3	570.0	1,493.4	4,340
	average	283.0	741.5	479.6	1,256.5	2,380

(a) For each formation above, E is calculated with Equation 2.5.4-4 using the Poisson's ratio given in Table 2.5.4-21.
(b) Reference 2.5.4-2, different formation names are used in Reference 2.5.4-2, see Table 2.5.1-1.

Notes:
NA = Not applicable

Table 2.5.4-19
Summary of Slake Durability Test Results

Formation	Description of Value	Slake Durability Index (%)
Benbolt	No. of Tests	4
	Average	97
	Median	98
	Minimum	93
	Maximum	99
	Standard Deviation	3.0
Rockdell	No. of Tests	3
	Average	99
	Median	99
	Minimum	98
	Maximum	99
	Standard Deviation	0.8
Fleanor	No. of Tests	2
	Average	98
	Median	98
	Minimum	97
	Maximum	98
	Standard Deviation	1.1
Eidson	No. of Tests	NA
	Average	NA
	Median	NA
	Minimum	NA
	Maximum	NA
	Standard Deviation	NA
Blackford	No. of Tests	1
	Value	94
	Median	NA
	Minimum	NA
	Maximum	NA
	Standard Deviation	NA

Notes:
NA = Not applicable

Table 2.5.4-20
Summary of Calcium Carbonate Test Results

Formation	Description of Value	Calcite Equivalent (%)
Benbolt	No. of Tests	1
	Value	27
	Median	NA
	Minimum	NA
	Maximum	NA
	Standard Deviation	NA
Rockdell	No. of Tests	4
	Average	58
	Median	55
	Minimum	45
	Maximum	75
	Standard Deviation	13.8
Fleanor	No. of Tests	5
	Average	34
	Median	28
	Minimum	28
	Maximum	45
	Standard Deviation	8.1
Eidson	No. of Tests	2
	Average	53
	Median	53
	Minimum	51
	Maximum	54
	Standard Deviation	2.1
Blackford	No. of Tests	1
	Value	39
	Median	NA
	Minimum	NA
	Maximum	NA
	Standard Deviation	NA
Newala	No. of Tests	2
	Average	84
	Median	84
	Minimum	77
	Maximum	90
	Standard Deviation	9.2

Notes:
NA = Not applicable

Table 2.5.4-21 (Sheet 1 of 2)
Summary of Best-Estimate Engineering Property Values for the Subsurface Materials in the Power Block Area

Unit	Existing Fill/ Residual Soil	Granular Backfill	Weathered Rock	Benbolt	Rockdell	Fleanor	Eidson	Blackford	Newala
Material/USCS symbol	ML, MH, CH	SW	Limestone/ Siltstone[b]	Limestone/ Siltstone	Limestone	Siltstone	Limestone	Limestone/ Siltstone	Dolomite
Total unit weight, γ (pcf)	120	135	140	168	168	168	168	168	175
Specific gravity	2.75	2.70	–	2.70	2.69	2.70	2.69	2.68	2.80
Natural water content, w (%)	30	–	–	1	1	1	1	1	1
Fines content (%)	80	5[a]	–	–	–	–	–	–	–
Atterberg limits									
Liquid limit, LL (%)	67	–	–	–	–	–	–	–	–
Plastic limit, PL (%)	27	–	–	–	–	–	–	–	–
Plasticity index, PI (%)	40	–	–	–	–	–	–	–	–
SPT N_{60}-value (blows/ft)	15	50	Refusal[c]	–	–	–	–	–	–
Undrained properties									
Undrained shear strength, s_u (psf)	1,300	–	–	–	–	–	–	–	–
Drained properties									
Effective cohesion, c' (psf)	150	–	–	–	–	–	–	–	–
Effective friction angle, Φ' (deg)	20	36	–	–	–	–	–	–	–
Rock core recovery (%)	–	–	–	98	98	98	95	96	99
RQD (%)	–	–	<25	88	88	89	80	81	93
Unconfined compressive strength, U (psi)	–	–	–	6,200	7,500	5,000	7,000	4,500	20,000
Shear wave velocity, V_s (fps)	600	1,200	1,870	8,000	9,000	7,200	9,000	8,200	10,800
Compression wave velocity, V_p (fps)	3,020	2,500	5,740	15,400	17,100	14,500	17,000	15,700	19,900
Poisson's ratio, μ	0.40	0.35	0.40	0.32	0.31	0.34	0.31	0.31	0.29
Low strain shear modulus (G_L)	1,350 ksf	6,000 ksf	–	2,300 ksi	2,900 ksi	1,900 ksi	2,900 ksi	2,400 ksi	4,400 ksi
High strain shear modulus (G_H)	280 ksf	670 ksf	–						
Low Strain elastic modulus (E_L)	3,750 ksf	16,000 ksf	–	6,100 ksi	7,700 ksi	5,000 ksi	7,700 ksi	6,400 ksi	11,400 ksi
High strain elastic modulus (E_H)	780 ksf	1,800 ksf	–						

Table 2.5.4-21 (Sheet 2 of 2)
Summary of Best-Estimate Engineering Property Values for the Subsurface Materials in the Power Block Area

Unit	Existing Fill/ Residual Soil	Granular Backfill	Weathered Rock	Benbolt	Rockdell	Fleanor	Eidson	Blackford	Newala
Maximum dry density (ASTM D1557) (pcf)	116	125	–	–	–	–	–	–	–
Optimum moisture content (%)	12	8	–	–	–	–	–	–	–
Coefficient of sliding (tanδ)	–	0.5	–	0.7	0.7	0.7	0.7	0.7	0.7
Calcium carbonate content - calcite equivalent (%)	–	–	–	27	58	34	53	39	84
Slake durability index	–	–	–	97	99	98	NA	94	NA

Notes:
(a) Material classification: Tennessee Department of Transportation Type A has 5% fines (% passing the No. 200 sieve)
(b) Generally weathered rock from the parent rock, either limestone or siltstone
(c) Refusal = 50 blows/6 inches of penetration or less

NA = Not applicable

"–" = not determined/not available

Table 2.5.4-22 (Sheet 1 of 6)
RocData Input and Output Results (D = 0)

Benbolt Formation

Input Parameters	Hoek-Brown Classification		
	σ_{ci}[a]	6200	psi
	GSI[b]	70	
	m_i[c]	7	
	D[d]	0	
	Ei[a]	6.10E+06	psi
	Hoek-Brown Criterion		
	m_b	2.398	
	s	0.036	
	a	0.501	
	Failure Envelope Range		
	Application	General	
	σ_{3MAX}[e]	1550	psi
Output Parameters	Mohr-Coulomb Fit		
	c	415	psi
	Φ	33	degrees
	Rock Mass Parameters		
	σt	-92	psi
	σc	1166	psi
	σcm	1533	psi
	Erm[f]	4.470E+06	psi
	Erm[g]	5.632E+06	psi
	Erm[h]	2.999E+06	psi

Input Parameters	Hoek-Brown Classification		
	σ_{ci}	6200	psi
	GSI	80	
	m_i	7	
	D	0	
	Ei	6.10E+06	psi
	Hoek-Brown Criterion		
	m_b	3.427	
	s	0.108	
	a	0.501	
	Failure Envelope Range		
	Application	General	
	σ_{3MAX}	1550	psi
Output Parameters	Mohr-Coulomb Fit		
	c	557	psi
	Φ	36	degrees
	Rock Mass Parameters		
	σt	-196	psi
	σc	2038	psi
	σcm	2169	psi
	Erm	5.370E+06	psi
	Erm	8.872E+06	psi
	Erm	5.333E+06	psi

Table 2.5.4-22 (Sheet 2 of 6)
RocData Input and Output Results (D = 0)

Rockdell Formation

Input Parameters	Hoek-Brown Classification		
	σ_{ci}[a]	7500	psi
	GSI[b]	55	
	m_i[c]	9	
	D[d]	0	
	Ei[a]	7.70E+06	psi
	Hoek-Brown Criterion		
	m_b	1.804	
	s	0.0067	
	a	0.504	
	Failure Envelope Range		
	Application	General	
	σ_{3MAX}[e]	1875	psi
Output Parameters	Mohr-Coulomb Fit		
	c	393	psi
	Φ	31	degrees
	Rock Mass Parameters		
	σt	-28	psi
	σc	603	psi
	σcm	1392	psi
	Erm[f]	3.144E+06	psi
	Erm[g]	2.025E+06	psi
	Erm[h]	1.391E+06	psi

Input Parameters	Hoek-Brown Classification		
	σ_{ci}	7500	psi
	GSI	80	
	m_i	9	
	D	0	
	Ei	7.70E+06	psi
	Hoek-Brown Criterion		
	m_b	4.406	
	s	0.1084	
	a	0.501	
	Failure Envelope Range		
	Application	General	
	σ_{3MAX}	1875	psi
Output Parameters	Mohr-Coulomb Fit		
	c	680	psi
	Φ	38	degrees
	Rock Mass Parameters		
	σt	-184	psi
	σc	2466	psi
	σcm	2788	psi
	Erm	6.779E+06	psi
	Erm	8.872E+06	psi
	Erm	5.865E+06	psi

Table 2.5.4-22 (Sheet 3 of 6)
RocData Input and Output Results (D = 0)

Fleanor Member

Input Parameters	Hoek-Brown Classification		
	σ_{ci}[a]	5000	psi
	GSI[b]	65	
	m_i[c]	7	
	D[d]	0	
	Ei[a]	5.00E+06	psi
	Hoek-Brown Criterion		
	m_b	2.006	
	s	0.0205	
	a	0.502	
	Failure Envelope Range		
	Application	General	
	σ_{3MAX}[e]	1250	psi
Output Parameters	Mohr-Coulomb Fit		
	c	298	psi
	Φ	32	degrees
	Rock Mass Parameters		
	σt	-51	psi
	σc	710	psi
	σcm	1070	psi
	Erm[f]	3.159E+06	psi
	Erm[g]	4.165E+06	psi
	Erm[h]	2.019E+06	psi

Input Parameters	Hoek-Brown Classification		
	σ_{ci}	5000	psi
	GSI	85	
	m_i	7	
	D	0	
	Ei	5.00E+06	psi
	Hoek-Brown Criterion		
	m_b	4.097	
	s	0.1889	
	a	0.500	
	Failure Envelope Range		
	Application	General	
	σ_{3MAX}	1250	psi
Output Parameters	Mohr-Coulomb Fit		
	c	540	psi
	Φ	37	degrees
	Rock Mass Parameters		
	σt	-231	psi
	σc	2172	psi
	σcm	2153	psi
	Erm[1]	4.633E+06	psi
	Erm[2]	1.034E+07	psi
	Erm[3]	6.386E+06	psi

Table 2.5.4-22 (Sheet 4 of 6)
RocData Input and Output Results (D = 0)

Eidson Member

Input Parameters	Hoek-Brown Classification		
	σ_{ci}[a]	7000	psi
	GSI[b]	50	
	m_i[c]	9	
	D[d]	0	
	Ei[a]	7.70E+06	psi
	Hoek-Brown Criterion		
	m_b	1.509	
	s	0.004	
	a	0.506	
	Failure Envelope Range		
	Application	General	
	σ_{3MAX}[e]	1750	psi
Output Parameters	Mohr-Coulomb Fit		
	c	338	psi
	Φ	30	degrees
	Rock Mass Parameters		
	σt	-18	psi
	σc	422	psi
	σcm	1161	psi
	Erm[f]	2.365E+06	psi
	Erm[g]	1.355E+06	psi
	Erm[h]	1.008E+06	psi

Input Parameters	Hoek-Brown Classification		
	σ_{ci}	7000	psi
	GSI	80	
	m_i	9	
	D	0	
	Ei	7.70E+06	psi
	Hoek-Brown Criterion		
	m_b	4.406	
	s	0.108	
	a	0.501	
	Failure Envelope Range		
	Application	General	
	σ_{3MAX}	1750	psi
Output Parameters	Mohr-Coulomb Fit		
	c	634	psi
	Φ	38	degrees
	Rock Mass Parameters		
	σt	-172	psi
	σc	2301	psi
	σcm	2602	psi
	Erm[a]	6.779E+06	psi
	Erm[b]	8.872E+06	psi
	Erm[c]	5.666E+06	psi

Table 2.5.4-22 (Sheet 5 of 6)
RocData Input and Output Results (D = 0)

Blackford Formation

Input Parameters	Hoek-Brown Classification		
	σ_{ci}[a]	4500	psi
	GSI[b]	60	
	m_i[c]	7	
	D[d]	0	
	Ei[a]	6.40E+06	psi
	Hoek-Brown Criterion		
	m_b	1.678	
	s	0.0117	
	a	0.503	
	Failure Envelope Range		
	Application	General	
	σ_{3MAX}[e]	1125	psi
Output Parameters	Mohr-Coulomb Fit		
	c	242	psi
	Φ	30	degrees
	Rock Mass Parameters		
	σt	-32	psi
	σc	482	psi
	σcm	844	psi
	Erm[f]	3.328E+06	psi
	Erm[g]	2.954E+06	psi
	Erm[h]	1.437E+06	psi

Input Parameters	Hoek-Brown Classification		
	σ_{ci}	4500	psi
	GSI	80	
	m_i	7	
	D	0	
	Ei	6.40E+06	psi
	Hoek-Brown Criterion		
	m_b	3.427	
	s	0.1084	
	a	0.501	
	Failure Envelope Range		
	Application	General	
	σ_{3MAX}	1125	psi
Output Parameters	Mohr-Coulomb Fit		
	c	404	psi
	Φ	36	degrees
	Rock Mass Parameters		
	σt	-142	psi
	σc	1479	psi
	σcm	1574	psi
	Erm[a]	5.634E+06	psi
	Erm[b]	8.872E+06	psi
	Erm[c]	4.543E+06	psi

Table 2.5.4-22 (Sheet 6 of 6)
RocData Input and Output Results (D = 0)

Newala Formation

Input Parameters	Hoek-Brown Classification		
	σ_{ci}[(a)]	20,000	psi
	GSI[(b)]	70	
	m_i[(c)]	9	
	D[(d)]	0	
	Ei[(a)]	1.14E+07	psi
	Hoek-Brown Criterion		
	m_b	3.083	
	s	0.0357	
	a	0.501	
	Failure Envelope Range		
	Application	General	
	σ_{3MAX}[(e)]	5000	psi
Output Parameters	Mohr-Coulomb Fit		
	c	1396	psi
	Φ	35	degrees
	Rock Mass Parameters		
	σt	-231	psi
	σc	3760	psi
	σcm	5404	psi
	Erm[(f)]	8.354E+06	psi
	Erm[(g)]	5.632E+06	psi
	Erm[(h)]	4.586E+06	psi

Input Parameters	Hoek-Brown Classification		
	σ_{ci}	20,000	psi
	GSI	80	
	m_i	9	
	D	0	
	Ei	1.140E+07	psi
	Hoek-Brown Criterion		
	m_b	4.406	
	s	0.1084	
	a	0.501	
	Failure Envelope Range		
	Application	General	
	σ_{3MAX}	5000	psi
Output Parameters	Mohr-Coulomb Fit		
	c	1812	psi
	Φ	38	degrees
	Rock Mass Parameters		
	σt	-492	psi
	σc	6575	psi
	σcm	7434	psi
	Erm[(a)]	1.004E+07	psi
	Erm[(b)]	8.872E+06	psi
	Erm[(c)]	8.156E+06	psi

(a) See Table 2.5.4-21 (Unconfined compressive strength, U).
(b) See Table 2.5.1-15.
(c) The material constant, m_i, values used are 9 ± 3 for dolomite, 9 ± 2 for micritic limestone and 7 ± 2 for siltstone from Reference 2.5.4-54.
(d) The disturbance factor, D, values used are D = 0 for the bedrock units below the foundations and D = 0.7 for the bedrock units at the excavation face from Reference 2.5.4-19.
(e) The maximum principal stress at failure, σ_{3MAX}, was selected whereby σ_{3MAX} is equal to $\sigma_{ci}/4$ (Reference 2.5.4-55).
(f) General Hoek and Diederichs (Reference 2.5.4-22)
(g) Simplified Hoek and Diederichs (Reference 2.5.4-22)
(h) Reference 2.5.4-19.

Table 2.5.4-23 (Sheet 1 of 6)
RocData Input and Output Results (D = 0.7)

Benbolt Formation

Input Parameters	Hoek-Brown Classification		
	σ_{ci}[a]	6200	psi
	GSI[b]	70	
	m_i[c]	7	
	D[d]	0.7	
	Ei[a]	6.10E+06	psi
	Hoek-Brown Criterion		
	m_b	1.347	
	s	0.013	
	a	0.501	
	Failure Envelope Range		
	Application	General	
	σ_{3MAX}[e]	1550	psi
Output Parameters	Mohr-Coulomb Fit		
	c	322	psi
	Φ	28	degrees
	Rock Mass Parameters		
	σt	-60	psi
	σc	701	psi
	σcm	1081	psi
	Erm[f]	2.059E+06	psi
	Erm[g]	1.080E+06	psi
	Erm[h]	1.949E+06	psi

Input Parameters	Hoek-Brown Classification		
	σ_{ci}	6200	psi
	GSI	80	
	m_i	7	
	D	0.7	
	Ei	6.10E+06	psi
	Hoek-Brown Criterion		
	m_b	2.333	
	s	0.055	
	a	0.501	
	Failure Envelope Range		
	Application	General	
	σ_{3MAX}	1550	psi
Output Parameters	Mohr-Coulomb Fit		
	c	454	psi
	Φ	33	degrees
	Rock Mass Parameters		
	σt	-146	psi
	σc	1453	psi
	σcm	1660	psi
	Erm[a]	2.911E+06	psi
	Erm[b]	2.291E+06	psi
	Erm[c]	3.466E+06	psi

Table 2.5.4-23 (Sheet 2 of 6)
RocData Input and Output Results (D = 0.7)

Rockdell Formation

Input Parameters	Hoek-Brown Classification		
	σ_{ci}[a]	7500	psi
	GSI[b]	55	
	m_i[c]	9	
	D[d]	0.7	
	Ei[a]	7.70E+06	psi
	Hoek-Brown Criterion		
	m_b	0.759	
	s	0.0015	
	a	0.504	
	Failure Envelope Range		
	Application	General	
	σ_{3MAX}[e]	1875	psi
Output Parameters	Mohr-Coulomb Fit		
	c	284	psi
	Φ	24	degrees
	Rock Mass Parameters		
	σt	-15	psi
	σc	280	psi
	σcm	878	psi
	Erm[f]	1.137E+06	psi
	Erm[g]	3.018E+05	psi
	Erm[h]	9.040E+05	psi

Input Parameters	Hoek-Brown Classification		
	σ_{ci}	7500	psi
	GSI	80	
	m_i	9	
	D	0.7	
	Ei	7.70E+06	psi
	Hoek-Brown Criterion		
	m_b	2.999	
	s	0.0551	
	a	0.501	
	Failure Envelope Range		
	Application	General	
	σ_{3MAX}	1875	psi
Output Parameters	Mohr-Coulomb Fit		
	c	563	psi
	Φ	35	degrees
	Rock Mass Parameters		
	σt	-138	psi
	σc	1758	psi
	σcm	2160	psi
	Erm[a]	3.675E+06	psi
	Erm[b]	2.291E+06	psi
	Erm[c]	3.812E+06	psi

Table 2.5.4-23 (Sheet 3 of 6)
RocData Input and Output Results (D = 0.7)

Fleanor Member

Input Parameters	Hoek-Brown Classification		
	σ_{ci}[a]	5000	psi
	GSI[b]	65	
	m_i[c]	7	
	D[d]	0.7	
	Ei[a]	5.00E+06	psi
	Hoek-Brown Criterion		
	m_b	1.023	
	s	0.0063	
	a	0.502	
	Failure Envelope Range		
	Application	General	
	σ_{3MAX}[e]	1250	psi
Output Parameters	Mohr-Coulomb Fit		
	c	225	psi
	Φ	26	degrees
	Rock Mass Parameters		
	σt	-31	psi
	σc	392	psi
	σcm	726	psi
	Erm[f]	1.327E+06	psi
	Erm[g]	7.151E+05	psi
	Erm[h]	1.313E+06	psi

Input Parameters	Hoek-Brown Classification		
	σ_{ci}	5000	psi
	GSI	85	
	m_i	7	
	D	0.7	
	Ei	5.00E+06	psi
	Hoek-Brown Criterion		
	m_b	3.070	
	s	0.1137	
	a	0.500	
	Failure Envelope Range		
	Application	General	
	σ_{3MAX}	1250	psi
Output Parameters	Mohr-Coulomb Fit		
	c	456	psi
	Φ	35	degrees
	Rock Mass Parameters		
	σt	-185	psi
	σc	1685	psi
	σcm	1735	psi
	Erm[a]	2.664E+06	psi
	Erm[b]	3.166E+06	psi
	Erm[c]	4.151E+06	psi

Table 2.5.4-23 (Sheet 4 of 6)
RocData Input and Output Results (D = 0.7)

Eidson Member

Input Parameters	Hoek-Brown Classification		
	σ_{ci}[a]	7000	psi
	GSI[b]	50	
	m_i[c]	9	
	D[d]	0.7	
	Ei[a]	7.70E+06	psi
	Hoek-Brown Criterion		
	m_b	0.577	
	s	0.0007	
	a	0.506	
	Failure Envelope Range		
	Application	General	
	σ_{3MAX}[e]	1750	psi
Output Parameters	Mohr-Coulomb Fit		
	c	236	psi
	Φ	22	degrees
	Rock Mass Parameters		
	σt	-9	psi
	σc	179	psi
	σcm	701	psi
	Erm[f]	8.261E+05	psi
	Erm[g]	1.938E+05	psi
	Erm[h]	6.549E+05	psi

Input Parameters	Hoek-Brown Classification		
	σ_{ci}	7000	psi
	GSI	80	
	m_i	9	
	D	0.7	
	Ei	7.70E+06	psi
	Hoek-Brown Criterion		
	m_b	2.999	
	s	0.055	
	a	0.501	
	Failure Envelope Range		
	Application	General	
	σ_{3MAX}	1750	psi
Output Parameters	Mohr-Coulomb Fit		
	c	526	psi
	Φ	35	degrees
	Rock Mass Parameters		
	σt	-129	psi
	σc	1640	psi
	σcm	2016	psi
	Erm[a]	3.675E+06	psi
	Erm[b]	2.291E+06	psi
	Erm[c]	3.683E+06	psi

Table 2.5.4-23 (Sheet 5 of 6)
RocData Input and Output Results (D = 0.7)

Blackford Formation

Input Parameters	Hoek-Brown Classification		
	σ_{ci}[a]	4500	psi
	GSI[b]	60	
	m_i[c]	7	
	D[d]	0.7	
	Ei[a]	6.40E+06	psi
	Hoek-Brown Criterion		
	m_b	0.777	
	s	0.0030	
	a	0.503	
	Failure Envelope Range		
	Application	General	
	σ_{3MAX}[e]	1125	psi
Output Parameters	Mohr-Coulomb Fit		
	c	178	psi
	Φ	24	degrees
	Rock Mass Parameters		
	σt	-18	psi
	σc	244	psi
	σcm	551	psi
	Erm[f]	1.284E+06	psi
	Erm[g]	4.669E+05	psi
	Erm[h]	9.338E+05	psi

Input Parameters	Hoek-Brown Classification		
	σ_{ci}	4500	psi
	GSI	80	
	m_i	7	
	D	0.7	
	Ei	6.40E+06	psi
	Hoek-Brown Criterion		
	m_b	2.333	
	s	0.0551	
	a	0.501	
	Failure Envelope Range		
	Application	General	
	σ_{3MAX}	1125	psi
Output Parameters	Mohr-Coulomb Fit		
	c	330	psi
	Φ	33	degrees
	Rock Mass Parameters		
	σt	-106	psi
	σc	1055	psi
	σcm	1205	psi
	Erm[a]	3.054E+06	psi
	Erm[b]	2.291E+06	psi
	Erm[c]	2.953E+06	psi

Table 2.5.4-23 (Sheet 6 of 6)
RocData Input and Output Results (D = 0.7)

Newala Formation

Input Parameters	Hoek-Brown Classification		
	σ_{ci}[(a)]	20,000	psi
	GSI[(b)]	70	
	m_i[(c)]	9	
	D[(d)]	0.7	
	Ei[(a)]	1.14E+07	psi
	Hoek-Brown Criterion		
	m_b	1.731	
	s	0.0129	
	a	0.501	
	Failure Envelope Range		
	Application	General	
	σ_{3MAX}[(e)]	5000	psi
Output Parameters	Mohr-Coulomb Fit		
	c	1098	psi
	Φ	31	degrees
	Rock Mass Parameters		
	σt	-149	psi
	σc	2261	psi
	σcm	3852	psi
	Erm[(f)]	3.849E+06	psi
	Erm[(g)]	1.080E+06	psi
	Erm[(h)]	2.981E+06	psi

Input Parameters	Hoek-Brown Classification		
	σ_{ci}	20,000	psi
	GSI	80	
	m_i	9	
	D	0.7	
	Ei	1.14E+07	psi
	Hoek-Brown Criterion		
	m_b	2.999	
	s	0.0551	
	a	0.501	
	Failure Envelope Range		
	Application	General	
	σ_{3MAX}	5000	psi
Output Parameters	Mohr-Coulomb Fit		
	c	1502	psi
	Φ	35	degrees
	Rock Mass Parameters		
	σt	-367	psi
	σc	4687	psi
	σcm	5759	psi
	Erm[(a)]	5.440E+06	psi
	Erm[(b)]	2.291E+06	psi
	Erm[(c)]	5.301E+06	psi

(a) See Table 2.5.4-21 (Unconfined compressive strength, U).
(b) See Table 2.5.1-15.
(c) The material constant, mi, values used are 9 ± 3 for dolomite, 9 ± 2 for micritic limestone and 7 ± 2 for siltstone from Reference 2.5.4-54.
(d) The disturbance factor, D, values used are D = 0 for the bedrock units below the foundations and D = 0.7 for the bedrock units at the excavation face from Reference 2.5.4-19.
(e) The maximum principal stress at failure, σ_{3MAX}, was selected whereby σ_{3MAX} is equal to $\sigma_{ci}/4$ (Reference 2.5.4-55).
(f) General Hoek and Diederichs (Reference 2.5.4-22)
(g) Simplified Hoek and Diederichs (Reference 2.5.4-22)
(h) Reference 2.5.4-19.

Table 2.5.4-24
Summary of Rock Mass Strength for the Bedrock Stratigraphic Units

Rock Mass Properties (psi)	Formations											
					Lincolnshire							
	Benbolt		Rockdell		Fleanor Member		Eidson Member		Blackford		Newala	
GSI	70	80	55	80	65	85	50	80	60	80	70	80
D = 0 (rock below disturbed zone)												
Tensile Strength	-92	-196	-28	-184	-51	-231	-18	-172	-32	-142	-231	-492
Uniaxial Compressive Strength	1166	2038	603	2466	710	2172	422	2301	482	1479	3760	6575
Global Strength	1533	2169	1392	2788	1070	2153	1161	2602	844	1574	5404	7434
Cohesion	415	557	393	680	298	540	338	634	242	404	1396	1812
Friction Angle (degrees)	33	36	31	38	32	37	30	38	30	36	35	38
D = 0.7 (disturbed zone adjacent to foundation)												
Tensile Strength	-60	-146	-15	-138	-31	-185	-9	-129	-18	-106	-149	-367
Uniaxial Compressive Strength	701	1453	280	1758	392	1685	179	1640	244	1055	2261	4687
Global Strength	1081	1660	878	2159	726	1735	701	2016	551	1205	3852	5759
Cohesion	322	454	284	563	225	456	236	526	178	330	1098	1502
Friction Angle (degrees)	28	33	24	35	26	35	22	35	24	33	31	35

Notes:

Disturbed zone is from blasting damage and stress unloading.

Cohesion and friction angle approximate the nonlinear Hoek-Brown failure envelope for $\sigma_t < \sigma'_3 < \sigma_{ci}/4$.

GSI = Geological Strength Index

Table 2.5.4-25
Summary of Rock Mass Deformation Moduli for the Bedrock Stratigraphic Units

Author/Method (ksi)	Formations											
	Benbolt		Rockdell		Lincolnshire				Blackford		Newala	
					Fleanor Member		Eidson Member					
GSI	70	80	55	80	65	85	50	80	60	80	70	80
D = 0 (rock below disturbed zone)												
Generalized Hoek and Diederichs (2006) (RocData v4.0)[a]	4,470	5,370	3,144	6,779	3,159	4,633	2,365	6,779	3,328	5,634	8,354	10,036
Simplified Hoek and Diederichs (2006) (RocData v4.0)[a]	5,632	8,872	2,025	8,872	4,165	10,338	1,355	8,872	2,954	8,872	5,632	8,872
Hoek et al. (2002) (RocData v4.0)[a]	2,999	5,333	1,391	5,865	2,019	6,386	1,008	5,666	1,437	4,543	4,586	8,156
D = 0.7 (disturbed zone adjacent to foundation)												
Generalized Hoek and Diederichs (2006) (RocData v4.0)[a]	2,059	2,911	1,137	3,675	1,327	2,664	826	3,675	1,284	3,054	3,849	5,440
Simplified Hoek and Diederichs (2006) (RocData v4.0)[a]	1,080	2,291	302	2,291	715	3,166	194	2,291	467	2291	1,080	2,291
Hoek et al. (2002) (RocData v4.0)[a]	1,949	3,466	904	3,812	1,313	4,151	655	3,683	934	2,953	2,981	5,301
No explicit disturbance factor												
Gokceoglu et al. (2003) (Excel)[b]	2,048	3,939	768	3,939	1,477	5,463	554	3,939	1,065	3,939	2,048	3,939
Pressuremeter Test Typical Range (from G_{avg})[c]	981 to 2,375		929 to 1,336		1,118 to 2,240		893 to 1,493		NA		NA	
Elastic modulus estimated from seismic velocity (low strain)[d]	6,100		7,700		5,000		7,700		6,400		11,400	

(a) RocData results tabulated in Tables 2.5.4-22 and 2.5.4-23.
(b) $E_{rm} = 0.1451 \exp^{0.0654GSI}$
(c) Table 2.5.4-18
(d) Table 2.5.4-21.

Notes:

The deformation moduli considered to be the most reliable are the values estimated using the empirical relationships provided by the Generalized Hoek-Diederichs method in Hoek and Diederichs (Reference 2.5.4-22) and Gokceoglu et al. (Reference 2.5.4-23).

GSI = Geological Strength Index

NA = Not available.

Table 2.5.4-26
Strata Thicknesses

Strata	Depth to Top (ft)	Elevation (ft)		Thickness (ft)	Variability[a] (%)
		Begin	End		
Location A					
New Granular Fill	0	821	800	21	±20
Existing Cohesive Fill / Residual Soil	21	800	790	10	±50
Weathered Rock	31	790	780	10	±80
Benbolt Formation[b]	41	780	633	147	±10
Rockdell Formation	188	633	346	287	±10
Fleanor Member	475	346	89	257	±10
Eidson Member	732	89	-13	102	±15
Blackford Formation	834	-13	-267	254	±50
Newala Formation	1088	-267	–	–	–
Location B					
New Granular Fill	0	821	810	11	±20
Existing Cohesive Fill / Residual Soil	11	810	789	21	±50
Weathered Rock	32	789	780	9	±80
Fleanor Member[b]	41	780	652	128	±10
Eidson Member	169	652	550	102	±15
Blackford Formation	271	550	296	254	±50
Newala Formation	525	296	–	–	–

(a) Variability is given as percent of average vertical thickness.
(b) Top of sound rock, for truncated profile.
(c) Thickness of Weathered Rock was determined from boring log data, suspension data, and natural gamma data.

Table 2.5.4-27
Summary of Allowable Bearing Capacity Values at Locations A, B, and A&B

Calculation Method	Location A				Both Locations		Location B					
	Benbolt		Rockdell		Fleanor		Eidson		Blackford		Newala	
	[(a)]Min.	Max.	Min.	Max.	Min.	Max.	Min.	Max.	Min.	Max.	Min.	Max.
Wyllie (ksf)	174	480	86	636	101	494	58	594	65	349	614	1697
Kulhawy and Carter (ksf)	154	428	75	567	89	441	49	530	57	311	546	1513
U.S. Army (ksf)	74	274	48	350	58	315	40	350	48	284	98	365
Bowles (ksf)	149		180		120		168		[(b)]108		480	

(a) Minimum (min.) and maximum (max.) refer to the range of estimated bearing capacities considering embedment depths of 138 ft and 80 ft, upper and lower geological strength index, and disturbed and undisturbed (D = 0.7 and D = 0) rock mass properties.

(b) 108 ksf (approximately 110 ksf) is the recommended value for the plant parameter envelope.

Table 2.5.4-28
Total Estimated Settlement at Locations A, B, and A&B

E_{rm} Method	Total Estimated Settlement (in.), Upper-bound GSI					
	Location A		Both Locations	Location B		
	Benbolt	Rockdell	Fleanor Member	Eidson Member	Blackford	Newala
Generalized Hoek and Diederichs 2006[a], D=0	0.03	0.02	0.03	0.02	0.03	0.02
Generalized Hoek and Diederichs 2006[a], D=0.7	0.05	0.04	0.06	0.04	0.05	0.03
Gokceoglu et al. 2003[b]	0.04	0.04	0.03	0.04	0.04	0.04
E_{rm} Method	Total Estimated Settlement (in.), Lower-bound GSI					
	Location A		Both Locations	Location B		
	Benbolt	Rockdell	Fleanor Member	Eidson Member	Blackford	Newala
Generalized Hoek and Diederichs 2006[a], D= 0	0.03	0.05	0.05	0.06	0.05	0.02
Generalized Hoek and Diederichs 2006[a], D=0.7	0.07	0.14	0.11	0.19	0.12	0.04
Gokceoglu et al. 2003[b]	0.07	0.20	0.10	0.28	0.14	0.08

(a) Reference 2.5.4-22
(b) Reference 2.5.4-23

Notes:
GSI = Geological Strength Index

Table 2.5.4-29
Total Estimated Heave at Locations A, B, and A&B

E_{rm} Method	Total Estimated Heave (in.), Upper-bound GSI					
	Location A		Both Locations	Location B		
	Benbolt	Rockdell	Fleanor Member	Eidson Member	Blackford	Newala
Generalized Hoek and Diederichs 2006[(a)], D= 0	0.04	0.03	0.04	0.03	0.04	0.02
Generalized Hoek and Diederichs 2006[(a)], D=0.7	0.07	0.05	0.07	0.05	0.06	0.04
Gokceoglu et al. 2003[(b)]	0.05	0.05	0.04	0.05	0.05	0.05
E_{rm} Method	Total Estimated Heave (in.), Lower-bound GSI					
	Location A		Both Locations	Location B		
	Benbolt	Rockdell	Fleanor Member	Eidson Member	Blackford	Newala
Generalized Hoek and Diederichs 2006[(a)], D= 0	0.04	0.06	0.06	0.08	0.06	0.02
Generalized Hoek and Diederichs 2006[(a)], D=0.7	0.10	0.17	0.15	0.24	0.15	0.05
Gokceoglu et al. 2003[(b)]	0.10	0.26	0.13	0.36	0.19	0.10

(a) Reference 2.5.4-22
(b) Reference 2.5.4-23

Notes:
GSI = Geological Strength Index

Table 2.5.4-30 (Sheet 1 of 2)
Smoothed Basecase Shear Wave Velocity Profiles, Damping and Densities For Location A

Thickness (m)	Depth (m)	Best Estimate Profile (P1)			Lower-Range Profile (P2)			Upper-Range Profile (P3)			Density (g/cm^3)
		Vs (m/s)	Damping (% critical)		Vs (m/s)	Damping (% critical)		Vs (m/s)	Damping (% critical)		
			M1	M2		M1	M2		M1	M2	
3.00	3.00	2321.50	2.00	1.25	1857.20	2.00	1.25	2901.88	2.00	1.25	2.69
3.00	6.00	2321.50	2.00	1.25	1857.20	2.00	1.25	2901.88	2.00	1.25	2.69
2.25	8.25	2196.20	2.00	1.25	1756.96	2.00	1.25	2745.25	2.00	1.25	2.69
2.26	10.52	2196.20	2.00	1.25	1756.96	2.00	1.25	2745.25	2.00	1.25	2.69
2.50	13.01	2398.10	2.00	1.25	1918.48	2.00	1.25	2997.63	2.00	1.25	2.69
2.50	15.51	2398.10	2.00	1.25	1918.48	2.00	1.25	2997.63	2.00	1.25	2.69
2.99	18.50	2398.10	2.00	1.25	1918.48	2.00	1.25	2997.63	2.00	1.25	2.69
3.00	21.51	2398.10	2.00	1.25	1918.48	2.00	1.25	2997.63	2.00	1.25	2.69
3.00	24.51	2398.10	2.00	1.25	1918.48	2.00	1.25	2997.63	2.00	1.25	2.69
3.00	27.51	2398.10	2.00	1.25	1918.48	2.00	1.25	2997.63	2.00	1.25	2.69
3.00	30.51	2398.10	2.00	1.25	1918.48	2.00	1.25	2997.63	2.00	1.25	2.69
3.00	33.51	2398.10	2.00	1.25	1918.48	2.00	1.25	2997.63	2.00	1.25	2.69
3.00	36.51	2398.10	2.00	1.25	1918.48	2.00	1.25	2997.63	2.00	1.25	2.69
2.75	39.26	2398.10	2.00	1.25	1918.48	2.00	1.25	2997.63	2.00	1.25	2.69
2.75	42.02	2398.10	2.00	1.25	1918.48	2.00	1.25	2997.63	2.00	1.25	2.69
2.75	44.77	2398.10	2.00	1.25	1918.48	2.00	1.25	2997.63	2.00	1.25	2.69
2.75	47.52	2398.10	2.00	1.25	1918.48	2.00	1.25	2997.63	2.00	1.25	2.69
3.10	50.61	2615.30	2.00	1.25	2092.24	2.00	1.25	3269.13	2.00	1.25	2.69
3.10	53.71	2615.30	2.00	1.25	2092.24	2.00	1.25	3269.13	2.00	1.25	2.69
3.10	56.81	2615.30	2.00	1.25	2092.24	2.00	1.25	3269.13	2.00	1.25	2.69
3.10	59.90	2615.30	2.00	1.25	2092.24	2.00	1.25	3269.13	2.00	1.25	2.69
3.10	63.00	2615.30	2.00	1.25	2092.24	2.00	1.25	3269.13	2.00	1.25	2.69
3.25	66.25	2894.30	2.00	1.25	2315.44	2.00	1.25	3520.00	2.00	1.25	2.69
3.25	69.51	2894.30	2.00	1.25	2315.44	2.00	1.25	3520.00	2.00	1.25	2.69
3.25	72.76	2894.30	2.00	1.25	2315.44	2.00	1.25	3520.00	2.00	1.25	2.69
3.25	76.01	2894.30	2.00	1.25	2315.44	2.00	1.25	3520.00	2.00	1.25	2.69
3.10	79.11	2894.30	2.00	1.25	2315.44	2.00	1.25	3520.00	2.00	1.25	2.69
3.10	82.21	2894.30	2.00	1.25	2315.44	2.00	1.25	3520.00	2.00	1.25	2.69
3.10	85.31	2894.30	2.00	1.25	2315.44	2.00	1.25	3520.00	2.00	1.25	2.69
3.10	88.40	2894.30	2.00	1.25	2315.44	2.00	1.25	3520.00	2.00	1.25	2.69
3.10	91.50	2894.30	2.00	1.25	2315.44	2.00	1.25	3520.00	2.00	1.25	2.69
3.47	94.97	2743.07	2.00	1.25	2194.45	2.00	1.25	3428.83	2.00	1.25	2.69
3.47	98.45	2743.07	2.00	1.25	2194.45	2.00	1.25	3428.83	2.00	1.25	2.69
3.47	101.92	2743.07	2.00	1.25	2194.45	2.00	1.25	3428.83	2.00	1.25	2.69
3.47	105.40	2743.07	2.00	1.25	2194.45	2.00	1.25	3428.83	2.00	1.25	2.69

Table 2.5.4-30 (Sheet 2 of 2)
Smoothed Basecase Shear Wave Velocity Profiles, Damping and Densities For Location A

Thickness (m)	Depth (m)	Best Estimate Profile (P1)			Lower-Range Profile (P2)			Upper-Range Profile (P3)			Density (g/cm^3)
		Vs (m/s)	Damping (% critical)		Vs (m/s)	Damping (% critical)		Vs (m/s)	Damping (% critical)		
			M1	M2		M1	M2		M1	M2	
3.47	108.87	2743.07	2.00	1.25	2194.45	2.00	1.25	3428.83	2.00	1.25	2.69
3.47	112.35	2743.07	2.00	1.25	2194.45	2.00	1.25	3428.83	2.00	1.25	2.69
3.47	115.82	2743.07	2.00	1.25	2194.45	2.00	1.25	3428.83	2.00	1.25	2.69
3.47	119.30	2743.07	2.00	1.25	2194.45	2.00	1.25	3428.83	2.00	1.25	2.69
3.47	122.77	2743.07	2.00	1.25	2194.45	2.00	1.25	3428.83	2.00	1.25	2.69
3.47	126.25	2743.07	2.00	1.25	2194.45	2.00	1.25	3428.83	2.00	1.25	2.69
3.47	129.72	2743.07	2.00	1.25	2194.45	2.00	1.25	3428.83	2.00	1.25	2.69
3.47	133.19	2743.07	2.00	1.25	2194.45	2.00	1.25	3428.83	2.00	1.25	2.69
3.13	136.33	2194.45	2.00	1.25	1755.56	2.00	1.25	2743.07	2.00	1.25	2.69
3.13	139.46	2194.45	2.00	1.25	1755.56	2.00	1.25	2743.07	2.00	1.25	2.69
3.13	142.60	2194.45	2.00	1.25	1755.56	2.00	1.25	2743.07	2.00	1.25	2.69
3.13	145.73	2194.45	2.00	1.25	1755.56	2.00	1.25	2743.07	2.00	1.25	2.69
3.13	148.87	2194.45	2.00	1.25	1755.56	2.00	1.25	2743.07	2.00	1.25	2.69
3.13	152.00	2194.45	2.00	1.25	1755.56	2.00	1.25	2743.07	2.00	1.25	2.69
59.53	211.53	2194.45	0.37	0.39	1755.56	0.49	0.54	2743.07	0.21	0.23	2.69
31.09	242.62	2743.07	0.30	0.31	2194.45	0.39	0.43	3428.83	0.17	0.18	2.69
77.42	320.04	2499.24	0.33	0.34	1999.39	0.43	0.47	3124.05	0.19	0.20	2.69
1218.23	1538.26	3352.64	0.24	0.25	2682.11	0.32	0.35	3520.00	0.17	0.18	2.69
640.05	2178.31	2194.45	0.37	0.39	1755.56	0.49	0.54	2743.07	0.21	0.23	2.72
701.01	2879.32	3093.87	0.27	0.27	2475.10	0.35	0.38	3520.00	0.17	0.18	2.80
213.35	3092.67	2234.99	0.37	0.38	1787.99	0.48	0.53	2793.74	0.21	0.24	2.72
213.35	3306.02	2234.99	0.37	0.38	1787.99	0.48	0.53	2793.74	0.21	0.24	2.72
548.13	3854.15	3117.34	0.26	0.27	2493.87	0.35	0.38	3520.00	0.17	0.18	2.80
–	3854.15	3520.00	–	–	3520.00	–	–	3520.00	–	–	2.71

Notes:

Dash (–) is representative of the half-space with an infinite thickness and no damping.

Vs = shear wave velocity

Table 2.5.4-31 (Sheet 1 of 2)
Smoothed Basecase Shear Wave Velocity Profiles, Damping and Densities For Location B

Thickness (m)	Depth	Best Estimate Profile (P1)			Lower-Range Profile (P2)			Upper-Range Profile (P3)			Density (g/cm^3)
		Vs (m/s)	Damping (% critical)		Vs (m/s)	Damping (% critical)		Vs (m/s)	Damping (% critical)		
			M1	M2		M1	M2		M1	M2	
2.01	2.01	1917.70	2.00	1.25	1534.16	2.00	1.25	2397.13	2.00	1.25	2.69
2.00	4.01	2237.30	2.00	1.25	1789.84	2.00	1.25	2796.63	2.00	1.25	2.69
2.00	6.00	2237.30	2.00	1.25	1789.84	2.00	1.25	2796.63	2.00	1.25	2.69
3.51	9.51	2237.30	2.00	1.25	1789.84	2.00	1.25	2796.63	2.00	1.25	2.69
3.51	13.01	2237.30	2.00	1.25	1789.84	2.00	1.25	2796.63	2.00	1.25	2.69
2.50	15.51	2465.80	2.00	1.25	1972.64	2.00	1.25	3082.25	2.00	1.25	2.69
3.50	19.01	2465.80	2.00	1.25	1972.64	2.00	1.25	3082.25	2.00	1.25	2.69
3.50	22.51	2465.80	2.00	1.25	1972.64	2.00	1.25	3082.25	2.00	1.25	2.69
3.50	26.01	2465.80	2.00	1.25	1972.64	2.00	1.25	3082.25	2.00	1.25	2.69
3.50	29.51	2465.80	2.00	1.25	1972.64	2.00	1.25	3082.25	2.00	1.25	2.69
3.50	33.01	2465.80	2.00	1.25	1972.64	2.00	1.25	3082.25	2.00	1.25	2.69
3.50	36.51	2465.80	2.00	1.25	1972.64	2.00	1.25	3082.25	2.00	1.25	2.69
3.50	40.02	2465.80	2.00	1.25	1972.64	2.00	1.25	3082.25	2.00	1.25	2.69
3.50	43.52	2465.80	2.00	1.25	1972.64	2.00	1.25	3082.25	2.00	1.25	2.69
3.50	47.03	2465.80	2.00	1.25	1972.64	2.00	1.25	3082.25	2.00	1.25	2.69
3.50	50.53	2465.80	2.00	1.25	1972.64	2.00	1.25	3082.25	2.00	1.25	2.69
2.82	53.35	2477.00	2.00	1.25	1981.60	2.00	1.25	3096.25	2.00	1.25	2.69
2.82	56.18	2477.00	2.00	1.25	1981.60	2.00	1.25	3096.25	2.00	1.25	2.69
2.82	59.00	2477.00	2.00	1.25	1981.60	2.00	1.25	3096.25	2.00	1.25	2.69
3.30	62.31	2838.20	2.00	1.25	2270.56	2.00	1.25	3520.00	2.00	1.25	2.69
3.30	65.61	2838.20	2.00	1.25	2270.56	2.00	1.25	3520.00	2.00	1.25	2.69
3.30	68.91	2838.20	2.00	1.25	2270.56	2.00	1.25	3520.00	2.00	1.25	2.69
3.30	72.22	2838.20	2.00	1.25	2270.56	2.00	1.25	3520.00	2.00	1.25	2.69
3.30	75.52	2838.20	2.00	1.25	2270.56	2.00	1.25	3520.00	2.00	1.25	2.69
3.16	78.68	2838.20	2.00	1.25	2270.56	2.00	1.25	3520.00	2.00	1.25	2.69
3.16	81.84	2838.20	2.00	1.25	2270.56	2.00	1.25	3520.00	2.00	1.25	2.69
3.16	85.00	2838.20	2.00	1.25	2270.56	2.00	1.25	3520.00	2.00	1.25	2.69
3.16	88.15	2838.20	2.00	1.25	2270.56	2.00	1.25	3520.00	2.00	1.25	2.69
3.16	91.31	2838.20	2.00	1.25	2270.56	2.00	1.25	3520.00	2.00	1.25	2.69
3.26	94.57	2838.20	2.00	1.25	2270.56	2.00	1.25	3520.00	2.00	1.25	2.69
3.26	97.83	2838.20	2.00	1.25	2270.56	2.00	1.25	3520.00	2.00	1.25	2.69
3.26	101.08	2838.20	2.00	1.25	2270.56	2.00	1.25	3520.00	2.00	1.25	2.69
3.26	104.34	2838.20	2.00	1.25	2270.56	2.00	1.25	3520.00	2.00	1.25	2.69
3.66	108.00	2838.20	2.00	1.25	2270.56	2.00	1.25	3520.00	2.00	1.25	2.69
3.70	111.70	3352.64	2.00	1.25	2682.11	2.00	1.25	3520.00	2.00	1.25	2.80

Table 2.5.4-31 (Sheet 2 of 2)
Smoothed Basecase Shear Wave Velocity Profiles, Damping and Densities For Location B

Thickness (m)	Depth	Best Estimate Profile (P1)			Lower-Range Profile (P2)			Upper-Range Profile (P3)			Density (g/cm^3)
		Vs (m/s)	Damping (% critical)		Vs (m/s)	Damping (% critical)		Vs (m/s)	Damping (% critical)		
			M1	M2		M1	M2		M1	M2	
3.70	115.40	3352.64	2.00	1.25	2682.11	2.00	1.25	3520.00	2.00	1.25	2.80
3.70	119.10	3352.64	2.00	1.25	2682.11	2.00	1.25	3520.00	2.00	1.25	2.80
3.70	122.80	3352.64	2.00	1.25	2682.11	2.00	1.25	3520.00	2.00	1.25	2.80
3.70	126.50	3352.64	2.00	1.25	2682.11	2.00	1.25	3520.00	2.00	1.25	2.80
3.70	130.20	3352.64	2.00	1.25	2682.11	2.00	1.25	3520.00	2.00	1.25	2.80
3.70	133.90	3352.64	2.00	1.25	2682.11	2.00	1.25	3520.00	2.00	1.25	2.80
3.70	137.59	3352.64	2.00	1.25	2682.11	2.00	1.25	3520.00	2.00	1.25	2.80
3.70	141.29	3352.64	2.00	1.25	2682.11	2.00	1.25	3520.00	2.00	1.25	2.80
3.70	144.99	3352.64	2.00	1.25	2682.11	2.00	1.25	3520.00	2.00	1.25	2.80
3.70	148.69	3352.64	2.00	1.25	2682.11	2.00	1.25	3520.00	2.00	1.25	2.80
3.70	152.39	3352.64	2.00	1.25	2682.11	2.00	1.25	3520.00	2.00	1.25	2.80
1175.25	1327.64	3352.64	0.24	0.25	2682.11	0.32	0.35	3520.00	0.17	0.18	2.80
640.05	1967.69	2173.12	0.38	0.39	1738.49	0.50	0.54	2716.40	0.22	0.23	2.72
426.70	2394.39	3080.77	0.27	0.28	2464.61	0.35	0.38	3520.00	0.17	0.18	2.80
76.20	2470.59	2224.32	0.37	0.38	1779.46	0.48	0.53	2780.40	0.21	0.22	2.72
365.74	2836.33	3097.84	0.26	0.27	2478.27	0.35	0.38	3520.00	0.17	0.18	2.80
228.59	3064.92	2234.99	0.37	0.38	1787.99	0.48	0.53	2793.74	0.21	0.22	2.72
228.59	3293.51	2234.99	0.37	0.38	1787.99	0.48	0.53	2793.74	0.21	0.22	2.72
548.13	3841.64	3116.43	0.26	0.27	2493.14	0.35	0.38	3520.00	0.17	0.18	2.80
–	3841.64	3520.00	–	–	3520.00	–	–	3520.00	–	–	2.71

Notes:

Dash (–) is representative of the half-space with an infinite thickness and no damping.

Vs = shear wave velocity

Table 2.5.4-32 (Sheet 1 of 2)
Kappa Estimates Using the Method of Anderson and Hough

Earthquake Date (YrMoDy)	Kappa bandwidth (Hz-Hz)	Kappa (s) $Qo= 630f^{0.5}$ crustal amplification of unity	Kappa (s) $Qo= 630f^{0.5}$ crustal amplification	Kappa (s) $Qo= 410f^{0.5}$ crustal amplification of unity	Kappa (s) $Qo= 410f^{0.5}$ crustal amplification	Kappa (s) No Q correction crustal amplification of unity	Kappa (s) No Qo correction crustal amplification
041223[a]	75.2-80	0.0570	0.0511	0.0565	0.0506	0.0579	0.0521
060317[b]	64-69.5	0.0097	0.0058	0.0094	0.0055	0.0102	0.0063
060411[b]	71-76	0.0311	0.0249	0.0304	0.0242	0.0323	0.0262
060413	70-79	0.0163	0.0102	0.0160	0.0099	0.0169	0.0108
060510[b]	71-76	0.0210	0.0148	0.0205	0.0143	0.0220	0.0158
061218	67-80	0.0122	0.0064	0.0116	0.0057	0.0135	0.0076
061226	65-71	0.0120	0.0076	0.0118	0.0074	0.0124	0.0080
070103	71-79	0.0130	0.0069	0.0125	0.0064	0.0138	0.0078
070210[c]	70.5-80	0.0253	0.0157	0.0244	0.0190	0.0257	0.0196
070221[b]	74-79	0.0217	0.0157	0.0215	0.0155	0.0221	0.0161
070412	67-80	0.0127	0.0069	0.0123	0.0064	0.0137	0.0078
070608[b]	75-80	0.0043	-0.0016	0.0040	-0.0019	0.0049	-0.0010
070614[b]	77-80	0.0048	-0.0010	0.0044	-0.0014	0.0055	-0.0003
070811[b]	75.5-80	0.0283	0.0225	0.0281	0.0223	0.0287	0.0229
070910[c]	68-80	0.0148	0.0089	0.0145	0.0085	0.0155	0.0095
070916[c]	65.5-80	0.0195	0.0138	0.0193	0.0136	0.0199	0.0142
071023	64.5-74	0.0400	0.0350	0.0396	0.0346	0.0409	0.0358
071123	64-76	0.0236	0.0176	0.0223	0.0172	0.0236	0.0184
071209	64-79	0.0100	0.0046	0.0093	0.0038	0.0115	0.0060
080111[c]	64-73	0.0110	0.0064	0.0107	0.0006	0.0116	0.0070
N=12 earthquakes	Kappa Median (s)	0.0160	0.0098	0.0156	0.0101	0.0169	0.0109

Table 2.5.4-32 (Sheet 2 of 2)
Kappa Estimates Using the Method of Anderson and Hough

Earthquake Date (YrMoDy)	Kappa bandwidth (Hz-Hz)	Kappa (s) $Qo= 630f^{0.5}$ crustal amplification of unity	Kappa (s) $Qo= 630f^{0.5}$ crustal amplification	Kappa (s) $Qo= 410f^{0.5}$ crustal amplification of unity	Kappa (s) $Qo= 410f^{0.5}$ crustal amplification	Kappa (s) No Q correction crustal amplification of unity	Kappa (s) No Qo correction crustal amplification
N=8 earthquakes, **M** $\geq$ 1.8	Kappa Median (s)	0.0157	0.0095	0.0151	0.0098	0.0167	0.0106

(a) Recording rejected due to only recording on a single horizontal component with an earlier instrument, not included in the median.
(b) Recording rejected due to too narrow of a bandwidth, not included in the median.
(c) Recording rejected due to small magnitude and possible source corner frequency above the bandwidth to estimate kappa. These estimates were not included in the median estimated from 8 larger earthquakes.

Table 2.5.4-33
Analyzed Cases for Location A and B

Location[a]	Section[b]	Foundation Depth[c] (ft)	Cavity Size[d] (ft)	Cavity Location[e]	Remarks[f]
A	A-A'	40	5,10,15	Center of common basemat	5 ft below basemat
				Center of common basemat	30 ft below basemat
				Bedding (Benbolt-Rockdell)	1 Interface
				Bedding (Benbolt-Rockdell)	2 Interfaces
				Edge of common basemat	5 ft below basemat
		90	5,10,15	Center of common basemat	5 ft below basemat
				Bedding (Benbolt-Rockdell)	1 Interface
		140	5,10,15	Bedding (Benbolt-Rockdell)	1 Interface
	E-E'	40	5,10,15	Center of common basemat	5 ft below basemat
				Center of common basemat	30 ft below basemat
		90	5,10,15	Center of common basemat	5 ft below basemat
				Bedding (Benbolt-Rockdell)	1 Interface
		140	5,10,15	Bedding (Benbolt-Rockdell)	1 Interface
B	B-B'	40	5,10,15	Center of common basemat	5 ft below basemat
				Center of common basemat	30 ft below basemat
				Bedding (Fleanor-Eidson)	1 Interface
				Edge of common basemat	5 ft below basemat
		90	5,10,15	Center of common basemat	5 ft below basemat
				Bedding (Fleanor-Eidson)	1 Interface
		140	5,10,15	Bedding (Fleanor-Eidson)	1 Interface
	F-F'	40	5,10,15	Center of common basemat	5 ft below basemat
				Center of common basemat	30 ft below basemat
		90	5,10,15	Center of common basemat	5 ft below basemat
				Bedding (Fleanor-Eidson)	1 Interface
		140	5,10,15	Bedding (Fleanor-Eidson)	1 Interface

Reference 2.5.4-59 Table 2-1

Notes:
(a) The CRN Site contains two potential locations for safety related structures.
(b) Typical Modeled Location A and B cross sections, shear values and vertical deformations (see Figure 2.5.4-27 through Figure 2.5.4-30).
(c) Modeled foundation embedment depth (ft below ground surface).
(d) Modeled cavity diameters.
(e) Modeled cavity locations.
(f) Additional detail related to cavity location. For Location A, “1 interface” indicates a single interface element introduced on both sides of the contact between the Benbolt and Rockdell formations. In turn, “2 interfaces” indicates simulation of an interface element on both sides of the Benbolt Formation and Rockdell Formation contact, and simulation of a second interface element located approximately 15 ft above the contact between the Benbolt and Rockdell formations. For Location B, “1 interface” indicates a single interface element introduced on both sides of the contact between the Fleanor and Eidson members of the Lincolnshire Formation.

Table 2.5.4-34
Model Results in Loading Phases for Location A and B

Location[a]	Section[b]	Foundation Depth[c] (ft)	Cavity Size[d] (ft)	Critical Cavity Location[e]	Remarks[f]	Relative Shear[g]	Deformation[h] (ft)
Location A	**A-A'**	40	15	Center of common basemat	5 ft below basemat	0.60	0.008
				Bedding (Benbolt-Rockdell)	1 Interface	0.90	0.006
		90	15	Center of common basemat	5 ft below basemat	0.70	0.008
				Bedding (Benbolt-Rockdell)	1 Interface	0.90	0.006
		140	15	Bedding (Benbolt-Rockdell)	1 Interface	0.90	0.007
Location A	**E-E'**	40	15	Center of common basemat	5 ft below basemat	0.60	0.008
		90	15	Center of common basemat	5 ft below basemat	0.60	0.008
				Bedding (Benbolt-Rockdell)	1 Interface	0.90	0.005
		140	15	Bedding (Benbolt-Rockdell)	1 Interface	0.90	0.006
Location B	**B-B'**	40	15	Center of common basemat	5 ft below basemat	0.80	0.008
				Bedding (Benbolt-Rockdell)	1 Interface	0.95	0.009
		90	15	Center of common basemat	5 ft below basemat	0.75	0.011
				Bedding (Benbolt-Rockdell)	1 Interface	0.90	0.007
		140	15	Bedding (Benbolt-Rockdell)	1 Interface	0.92	0.011
Location B	**F-F'**	40	15	Center of common basemat	5 ft below basemat	0.75	0.007
		90	15	Center of common basemat	5 ft below basemat	0.70	0.010
				Bedding (Benbolt-Rockdell)	1 Interface	0.90	0.006

Reference 2.5.4-59 Table 3-1

Notes:
(a) The CRN Site contains two locations for safety related structures.
(b) Typical Modeled Location A and B cross sections, relative shear values and vertical deformations (see Figure 2.5.4-27 through Figure 2.5.4-30).
(c) Modeled foundation embedment depth (ft below ground surface).
(d) Critical cavity diameter.
(e) Critical cavity locations.
(f) Additional detail related to cavity location. For Location A, “1 interface” indicates a single interface element introduced on both sides of the contact between the Benbolt and Rockdell formations. For Location B, “1 interface” indicates a single interface element introduced on both sides of the contact between the Fleanor and Eidson members of the Lincolnshire Formation.
(g) Calculated relative shear.
(h) Calculated vertical deformation.

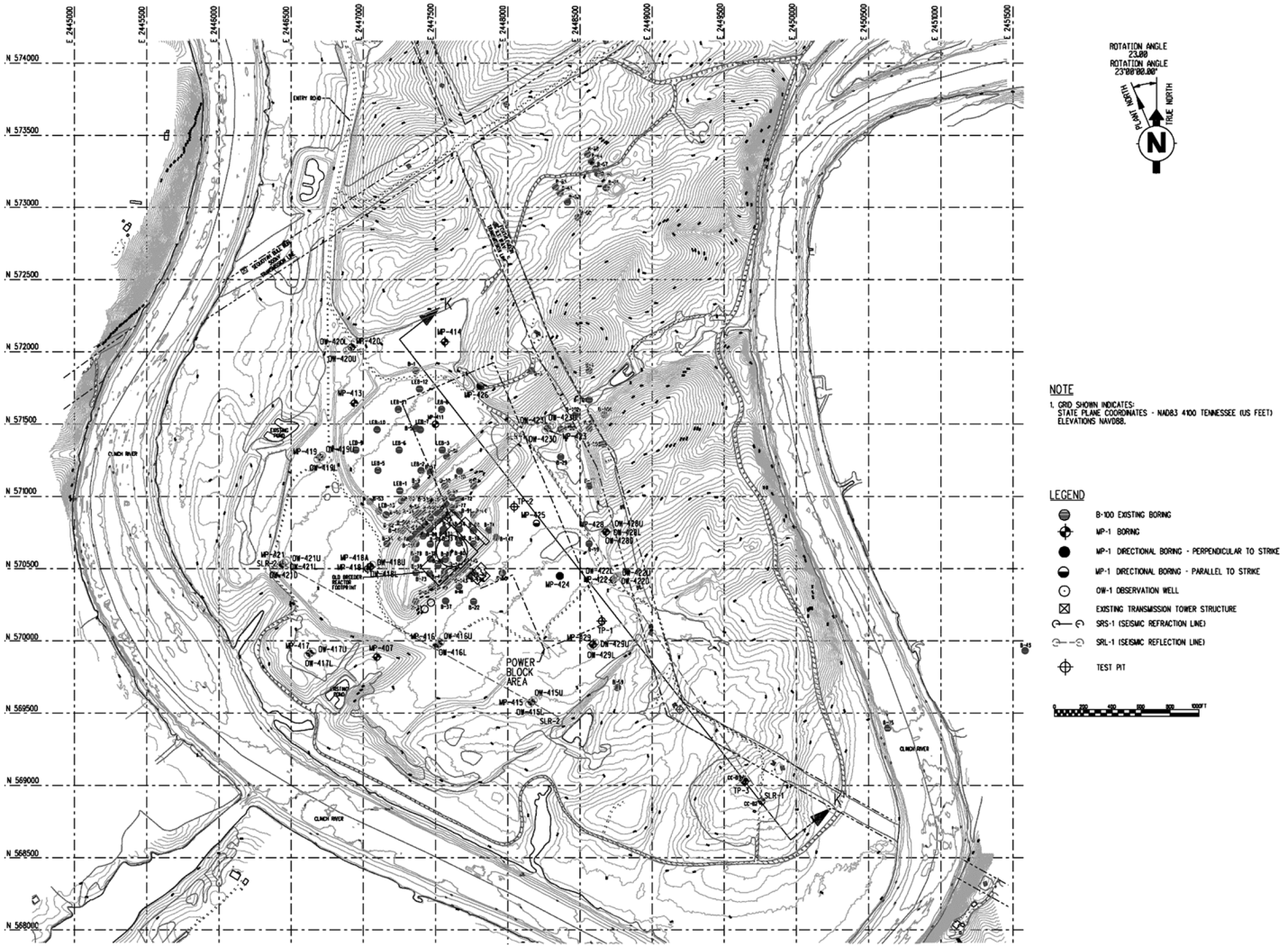

Figure 2.5.4-1. (Sheet 1 of 2) Site Layout and Boring Location Plan

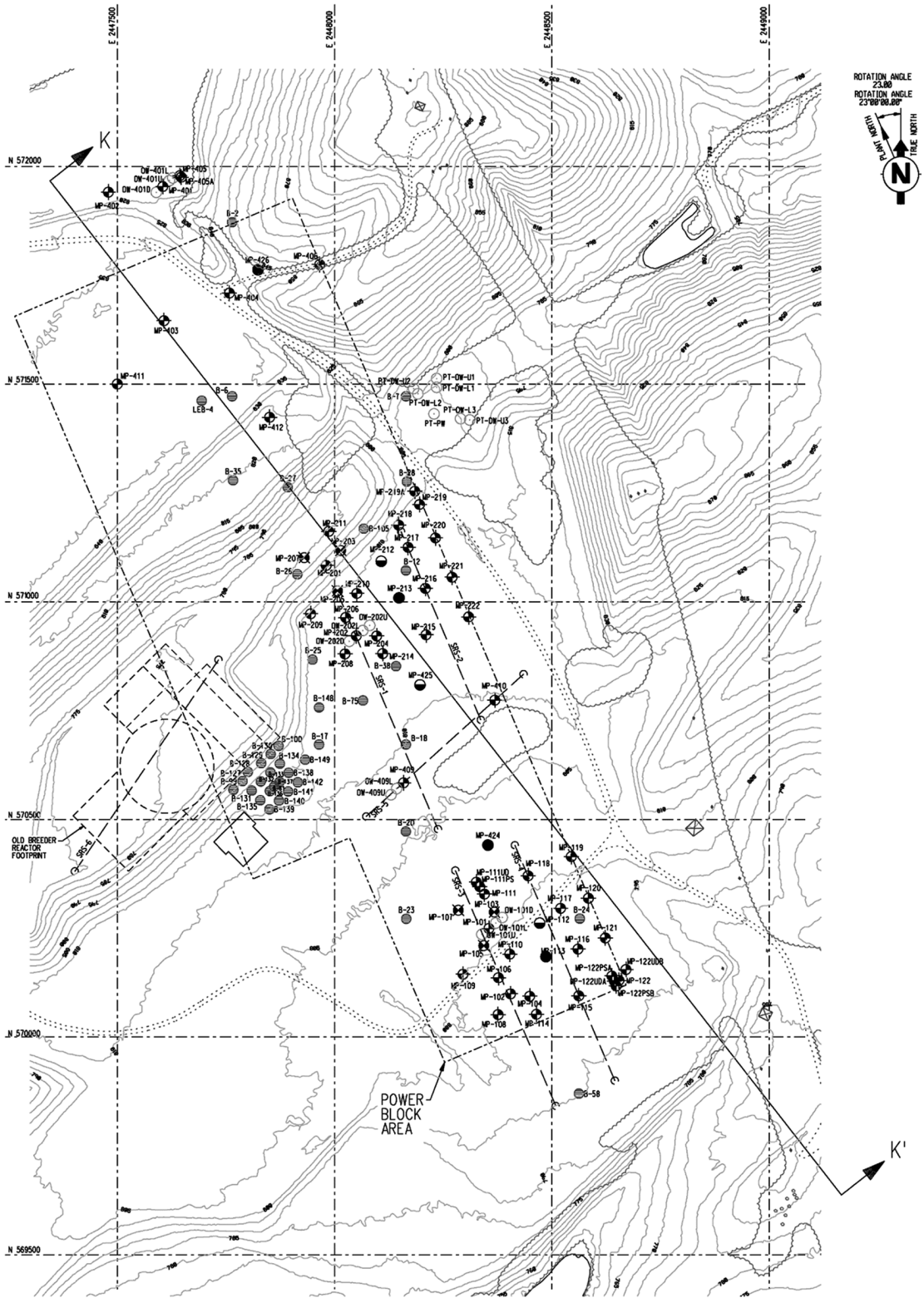

Figure 2.5.4-1. (Sheet 2 of 2) Site Layout and Boring Location Plan

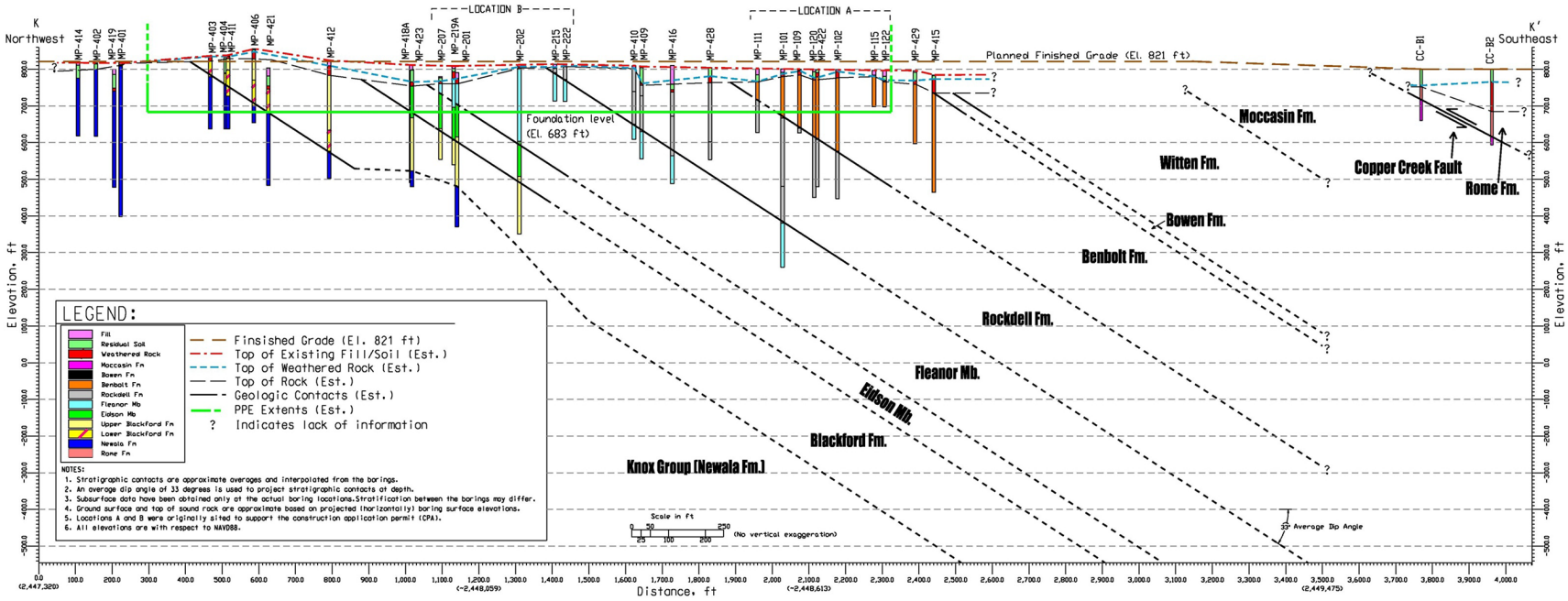

Figure 2.5.4-2. Geotechnical Cross-Section K-K' Through Power Block Area

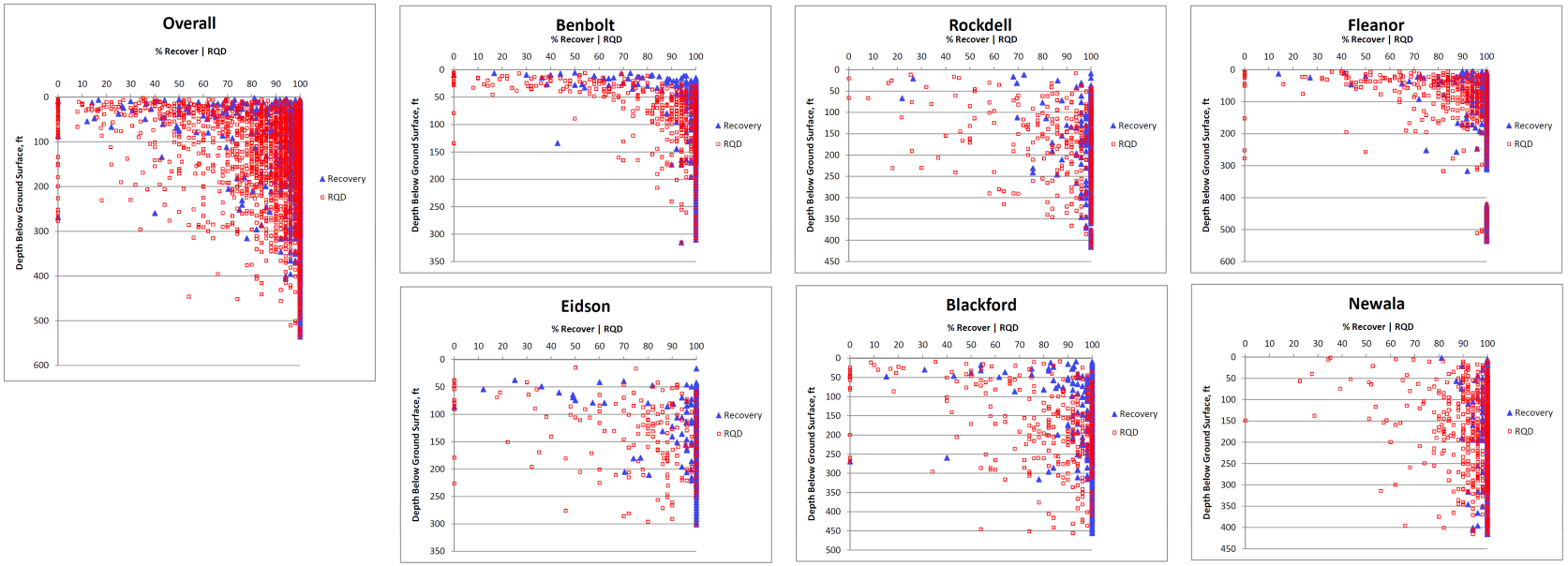

Figure 2.5.4-3. Summary of Rock Core Recovery and Rock Quality Designation

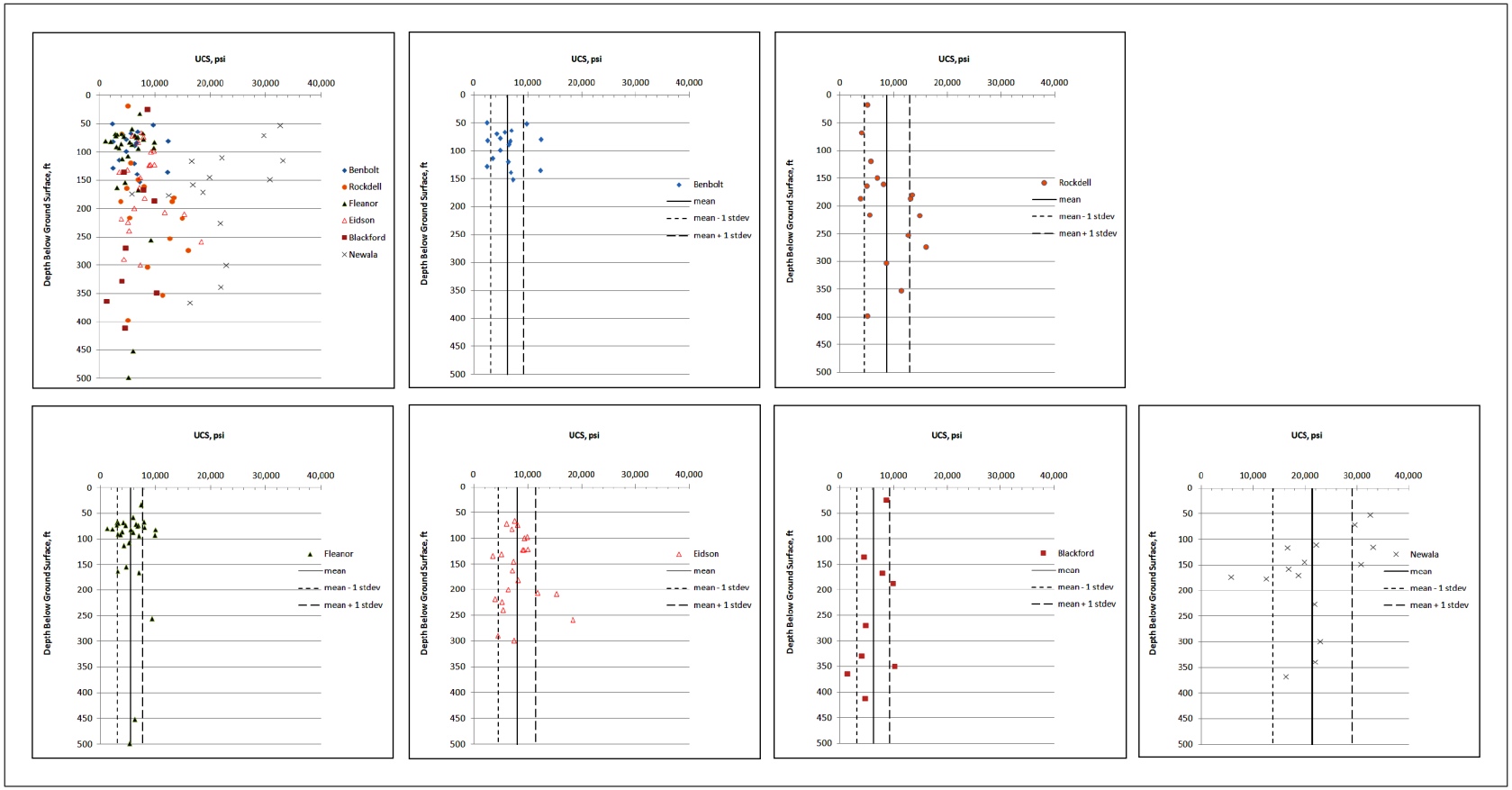

Figure 2.5.4-4. Summary of Unconfined Compression Test Results

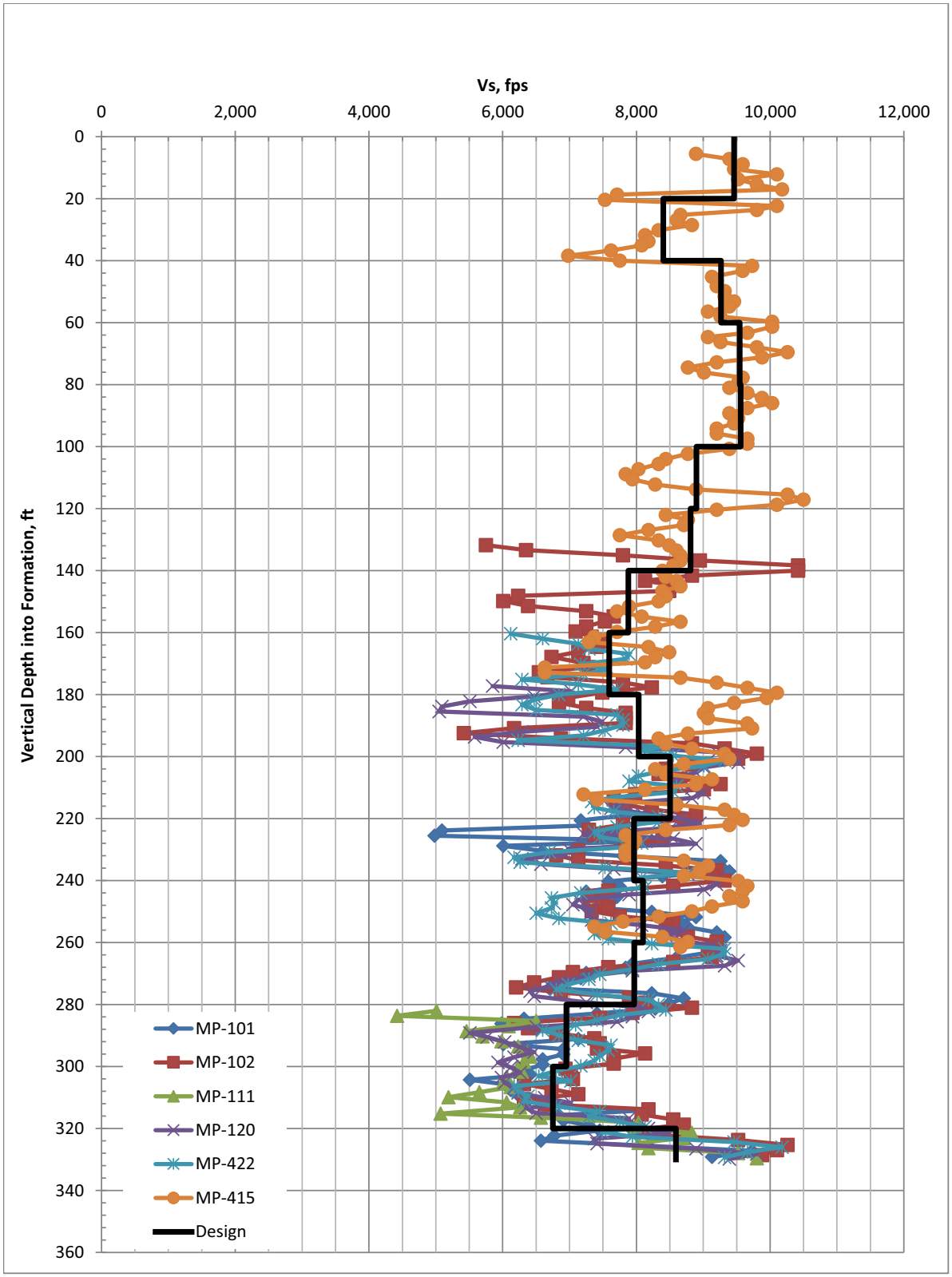

Figure 2.5.4-5. (Sheet 1 of 6) Shear Wave Velocity Data – Benbolt Formation

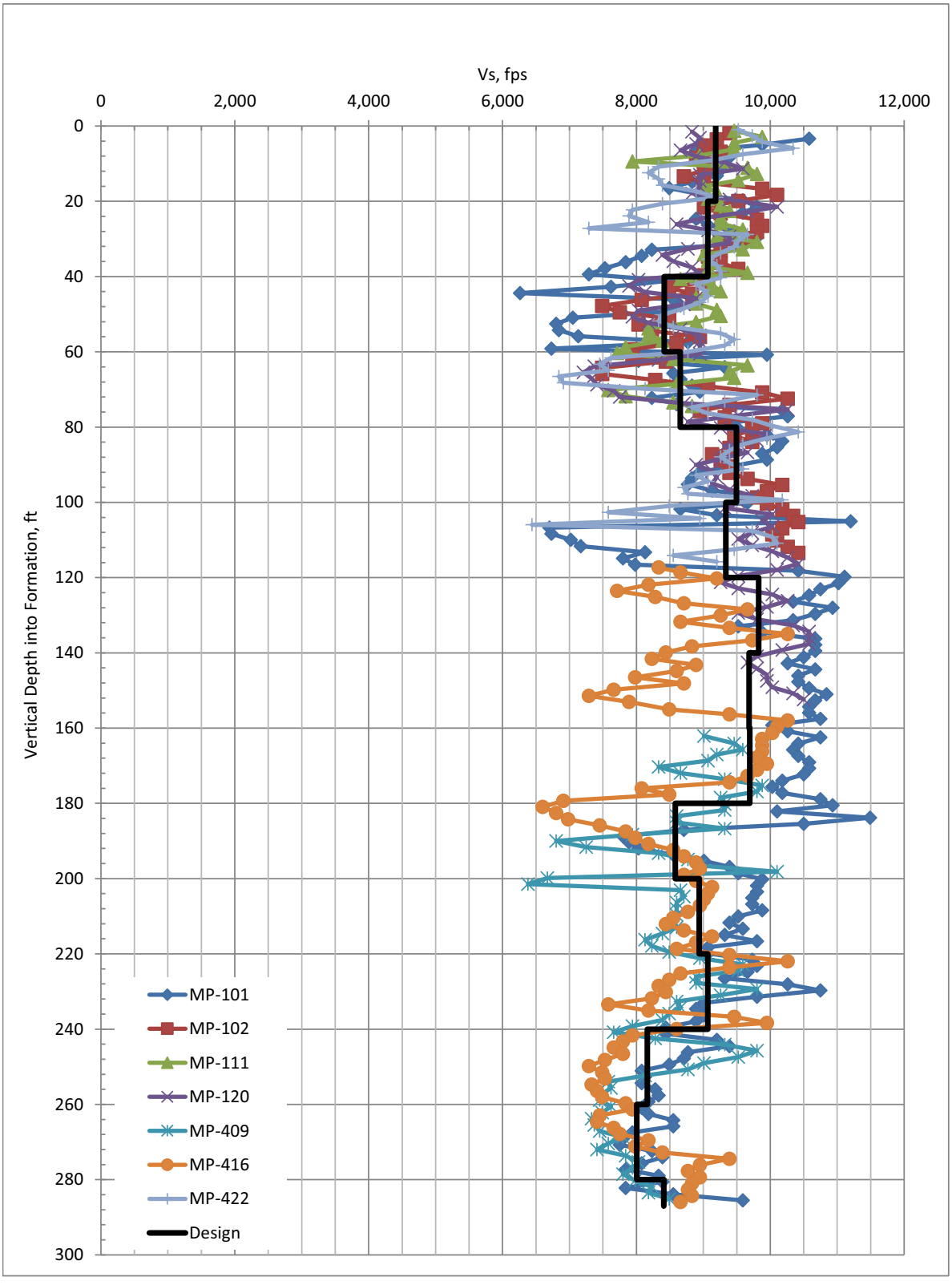

Figure 2.5.4-5. (Sheet 2 of 6) Shear Wave Velocity Data – Rockdell Formation

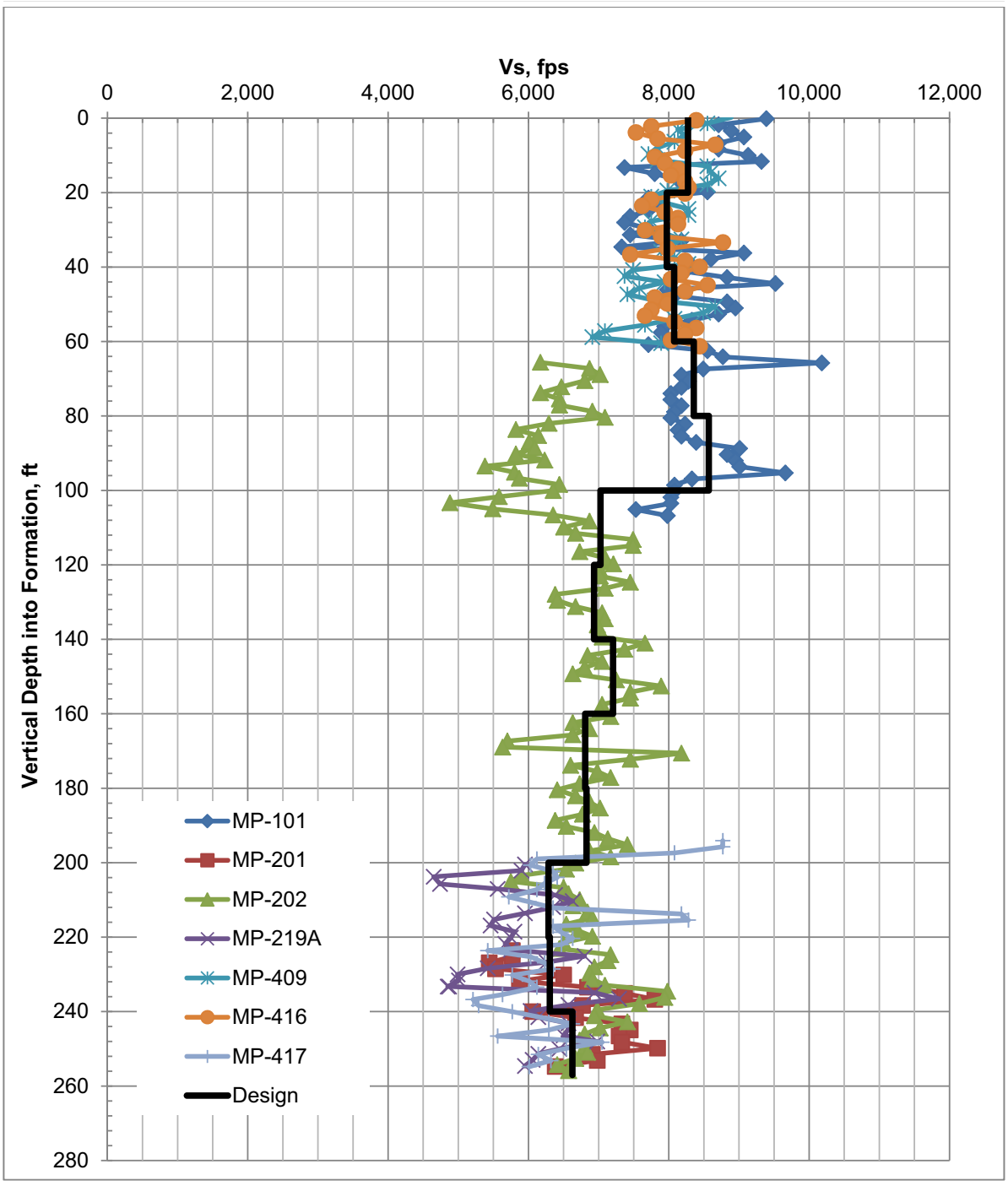

Figure 2.5.4-5. (Sheet 3 of 6) Shear Wave Velocity Data – Fleanor Formation

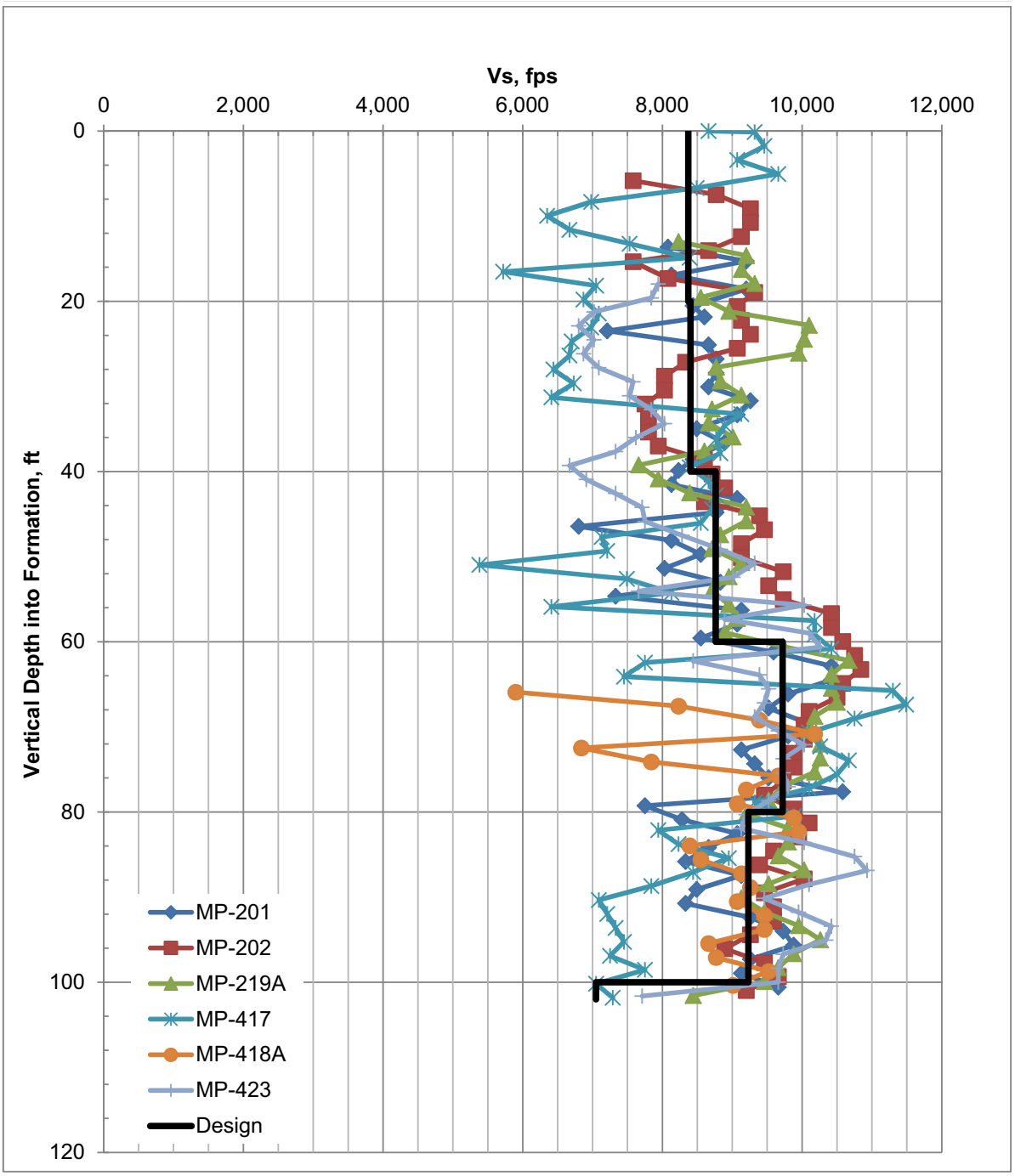

Figure 2.5.4-5. (Sheet 4 of 6) Shear Wave Velocity Data – Eidson Formation

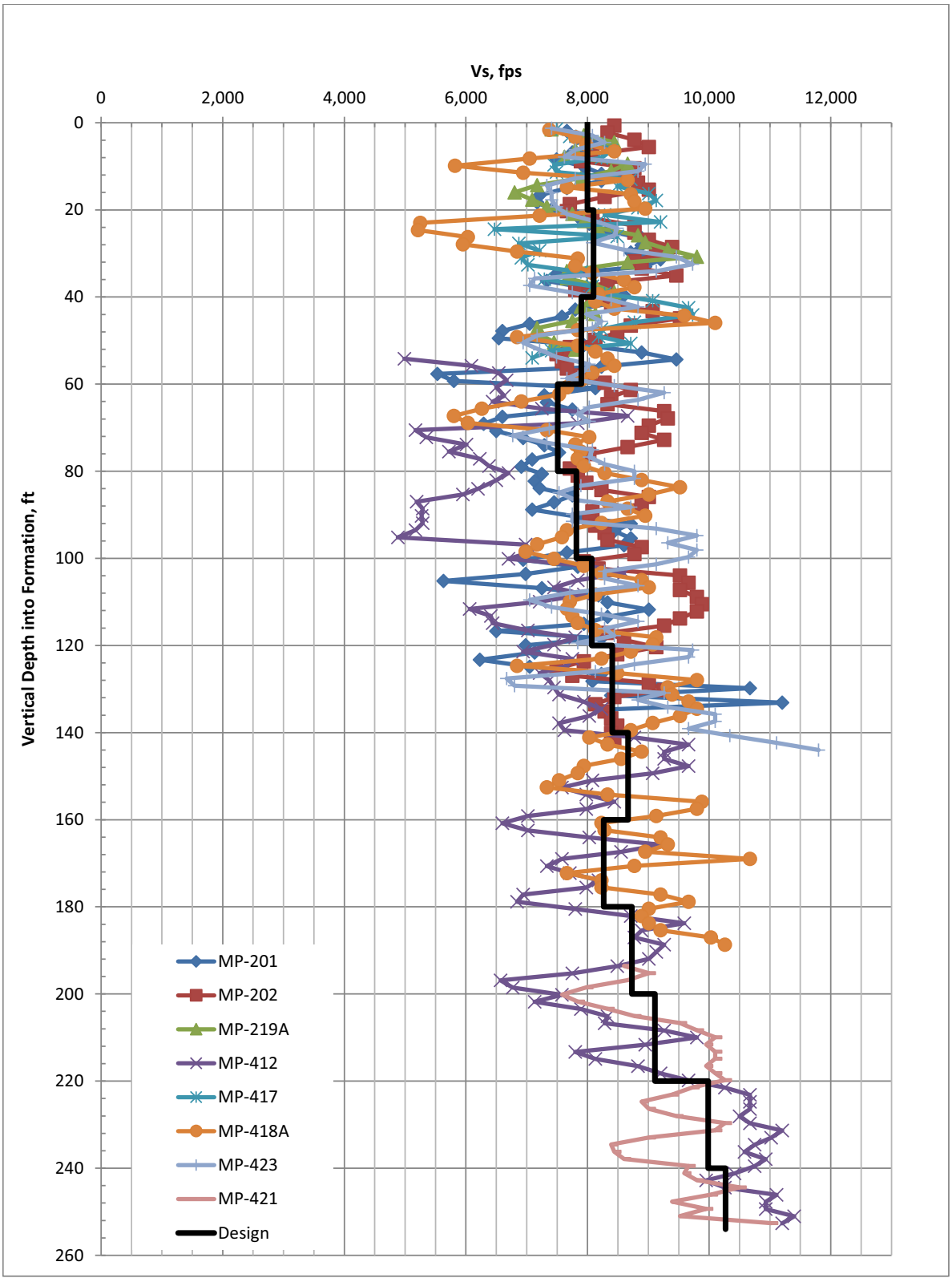

Figure 2.5.4-5. (Sheet 5 of 6) Shear Wave Velocity Data – Blackford Formation

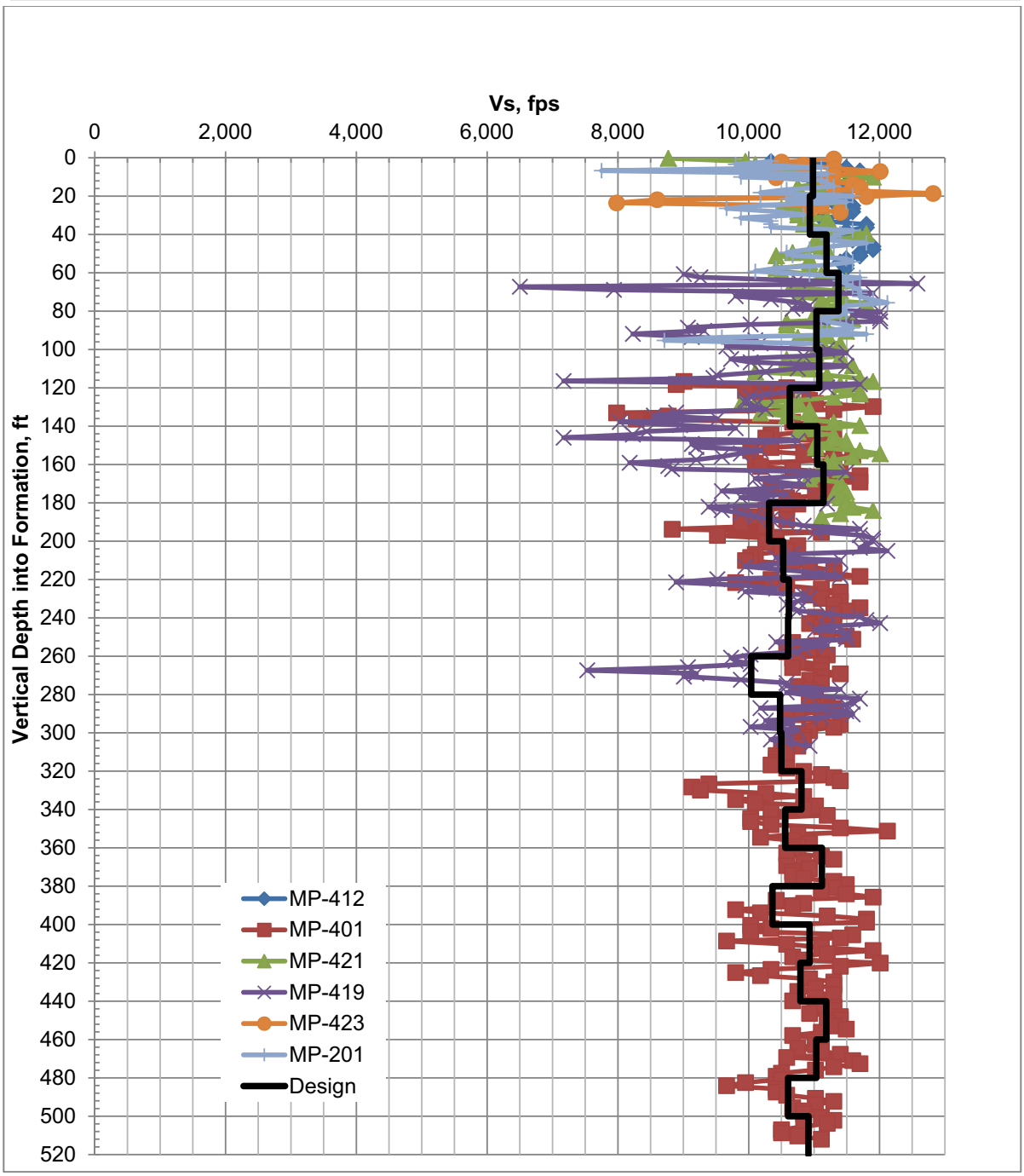

Figure 2.5.4-5. (Sheet 6 of 6) Shear Wave Velocity Data – Newala Formation

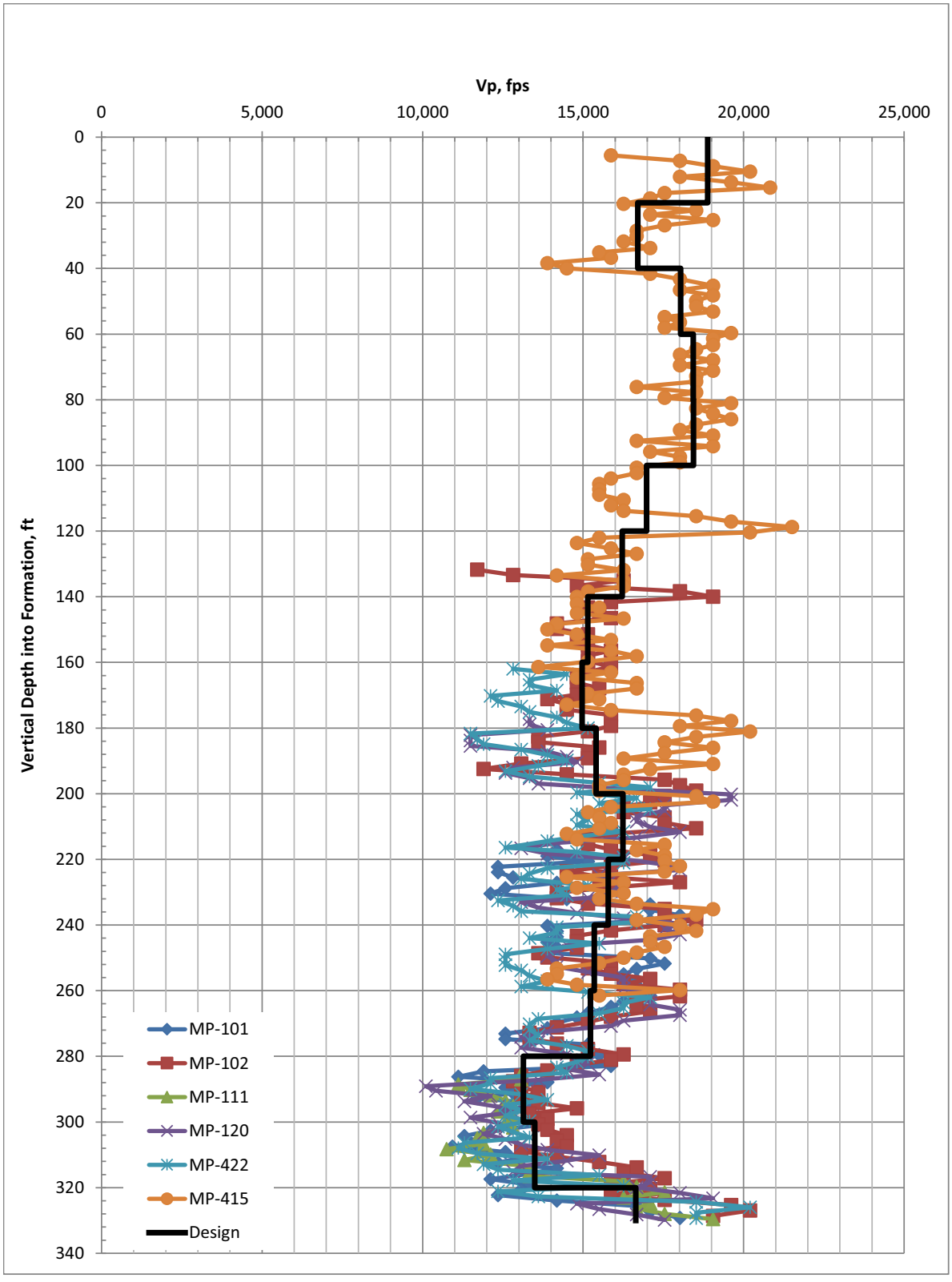

Figure 2.5.4-6. (Sheet 1 of 6) Compression Wave Velocity Data – Benbolt Formation

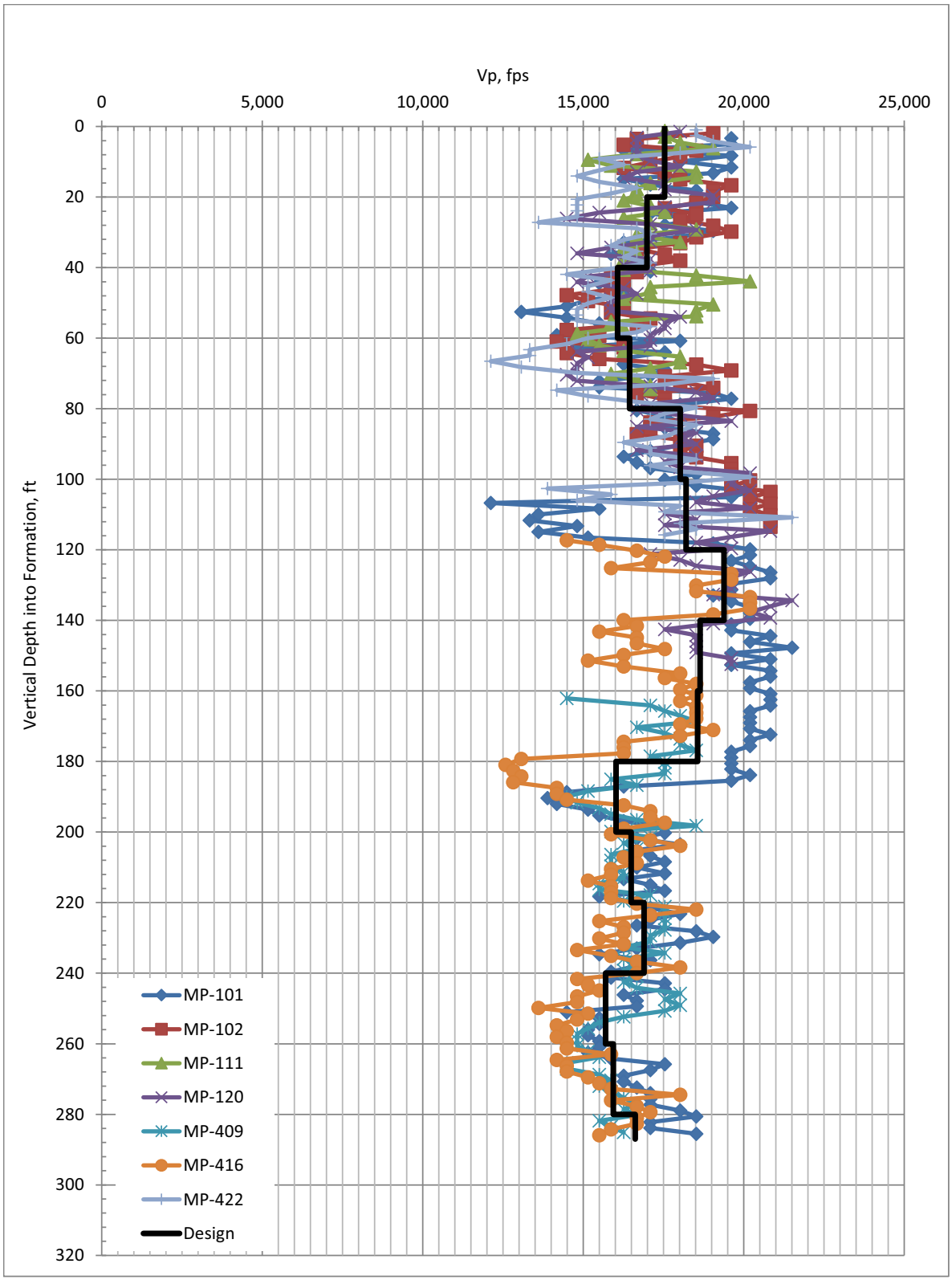

Figure 2.5.4-6. (Sheet 2 of 6) Compression Wave Velocity Data – Rockdell Formation

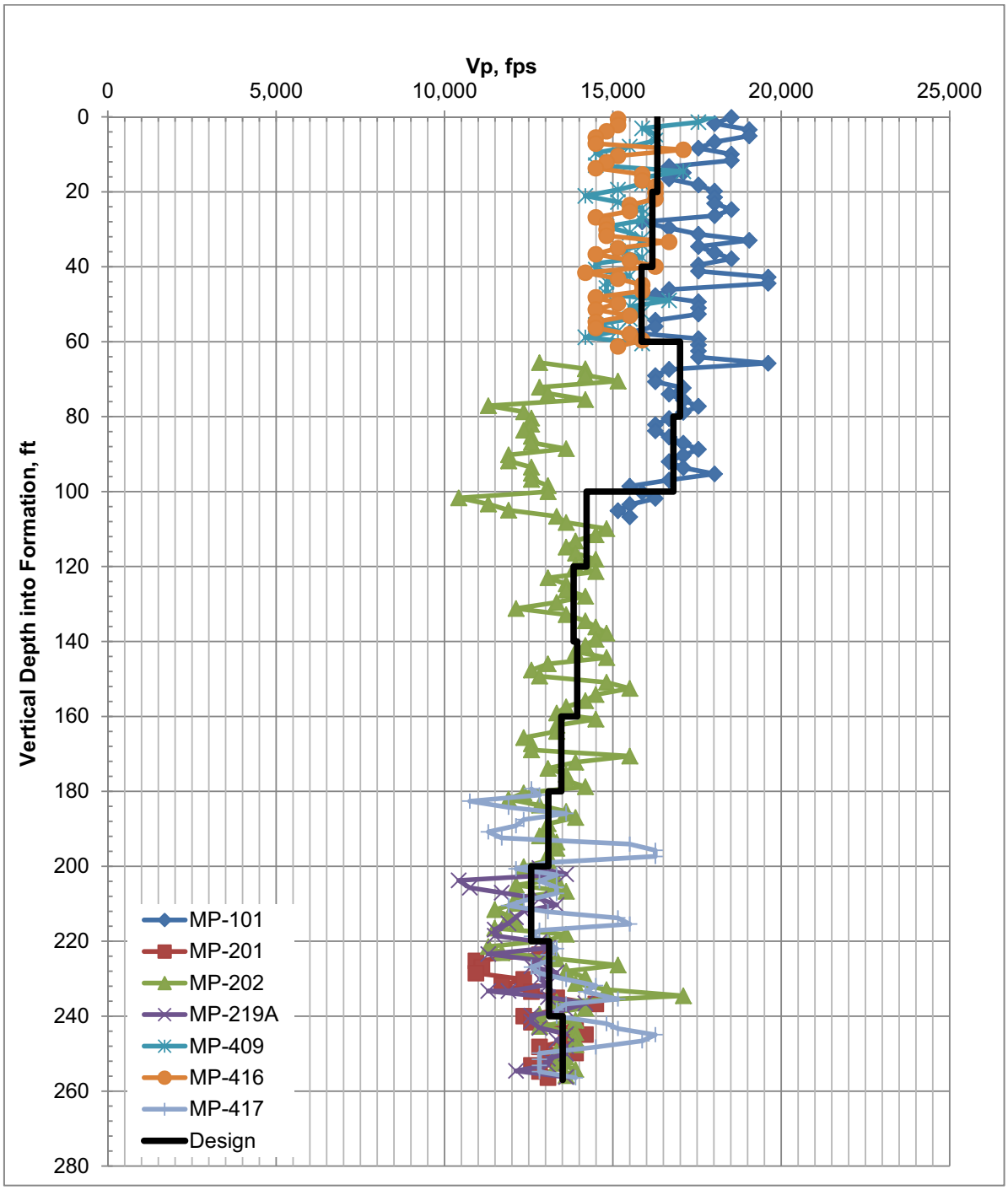

Figure 2.5.4-6. (Sheet 3 of 6) Compression Wave Velocity Data – Fleanor Formation

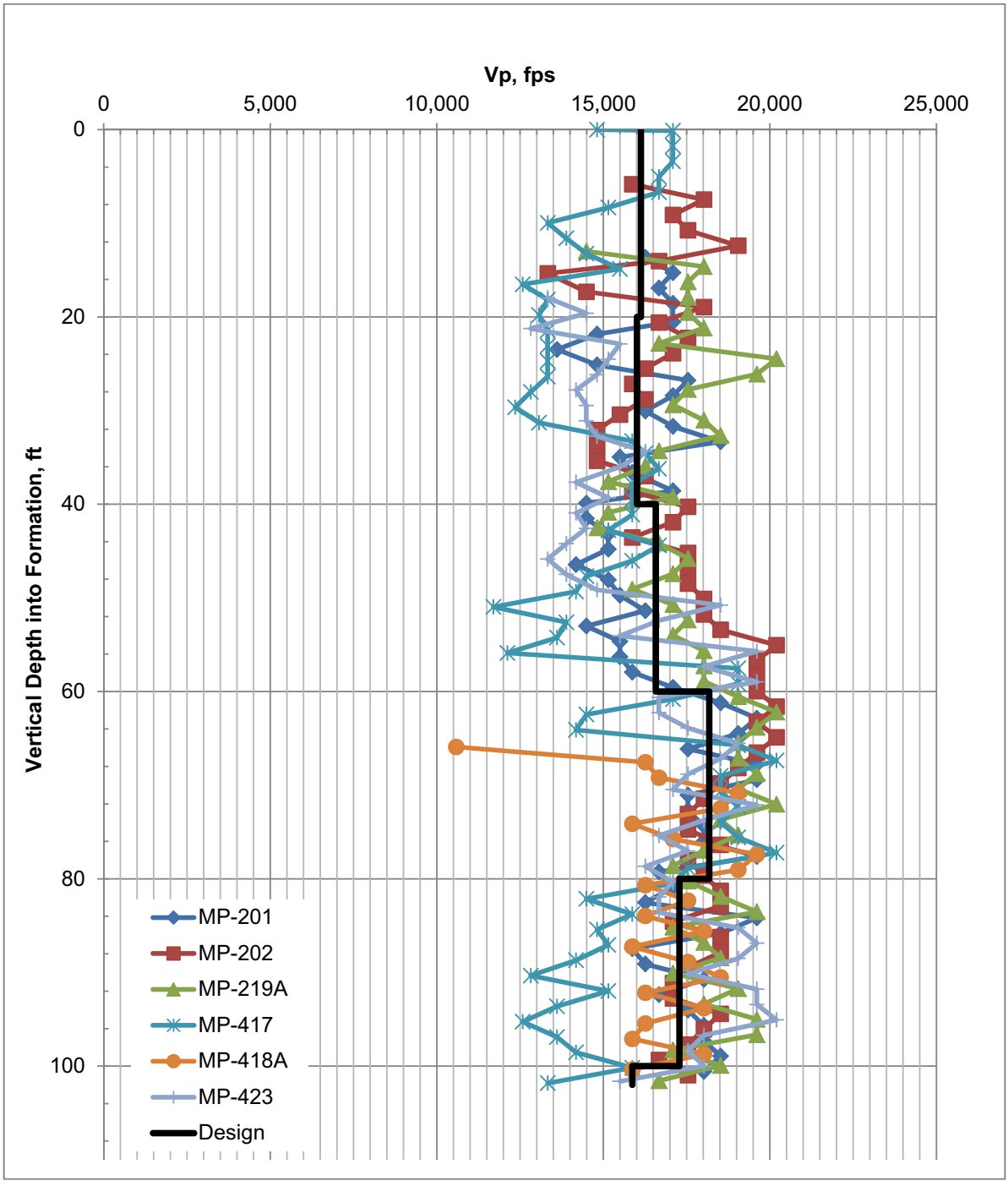

Figure 2.5.4-6. (Sheet 4 of 6) Compression Wave Velocity Data – Eidson Formation

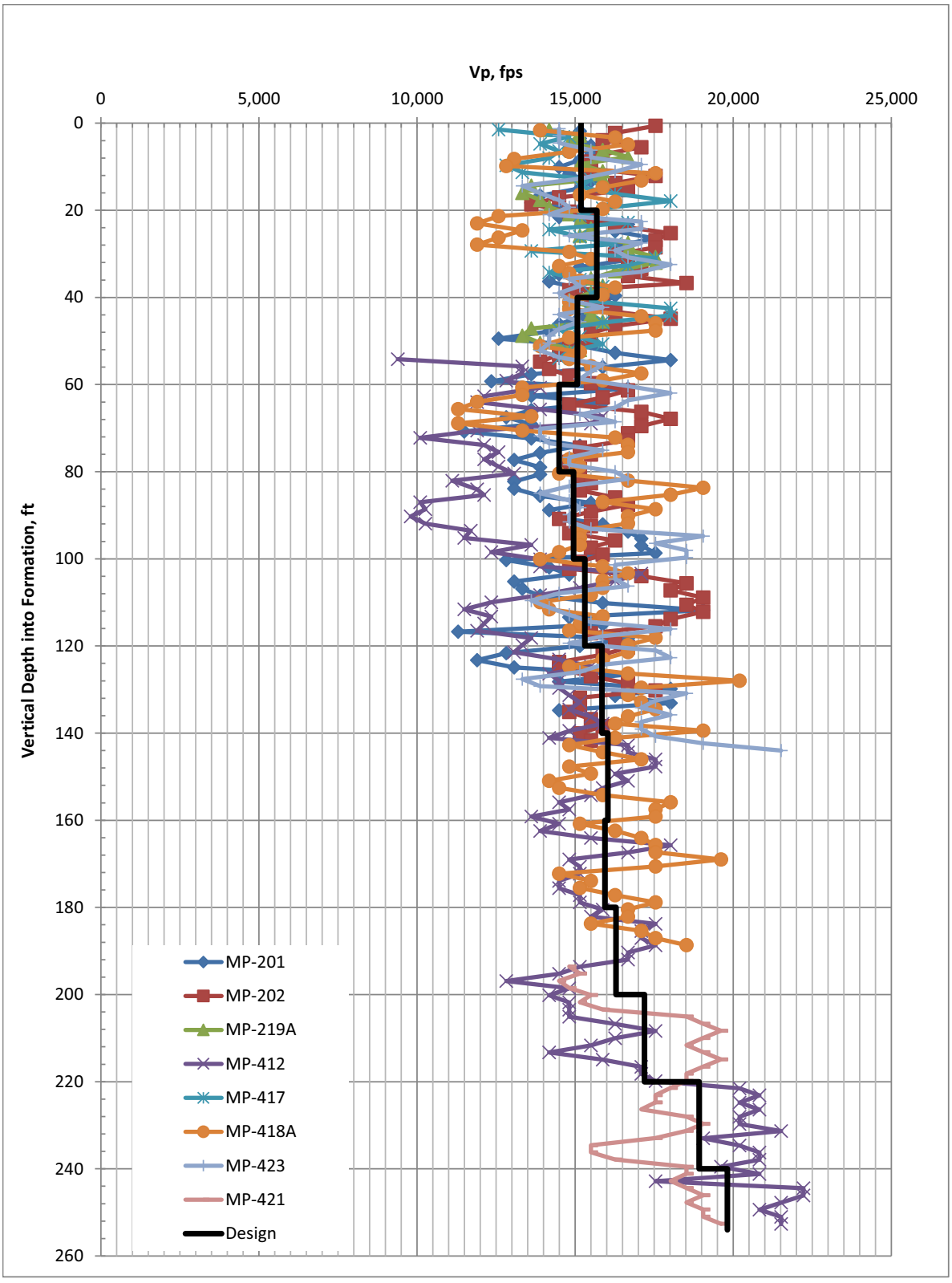

Figure 2.5.4-6. (Sheet 5 of 6) Compression Wave Velocity Data – Blackford Formation

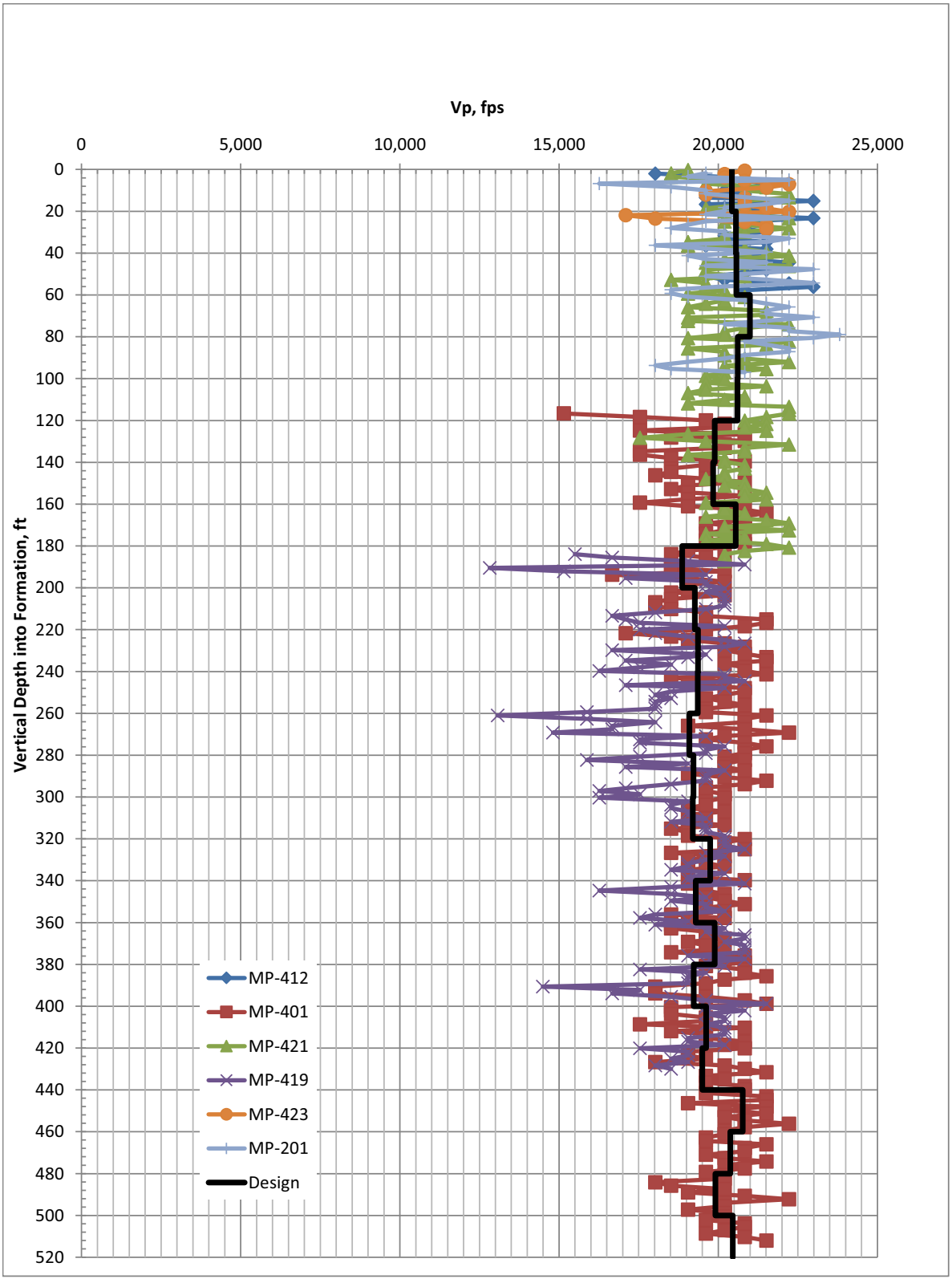

Figure 2.5.4-6. (Sheet 6 of 6) Compression Wave Velocity Data – Newala Formation

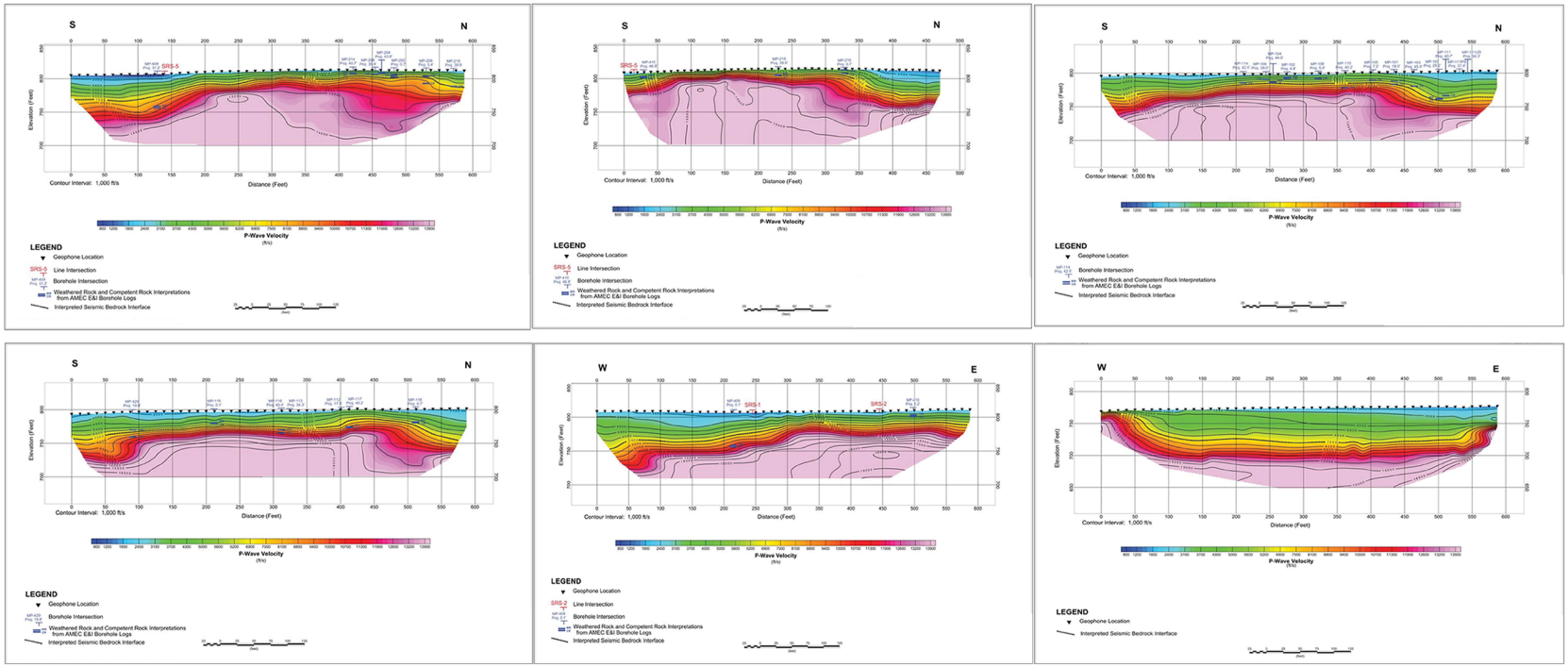

Source: Reference 2.5.4-1, Appendix C.

Figure 2.5.4-7. Seismic Tomography Models SRS-1 to SRS-6

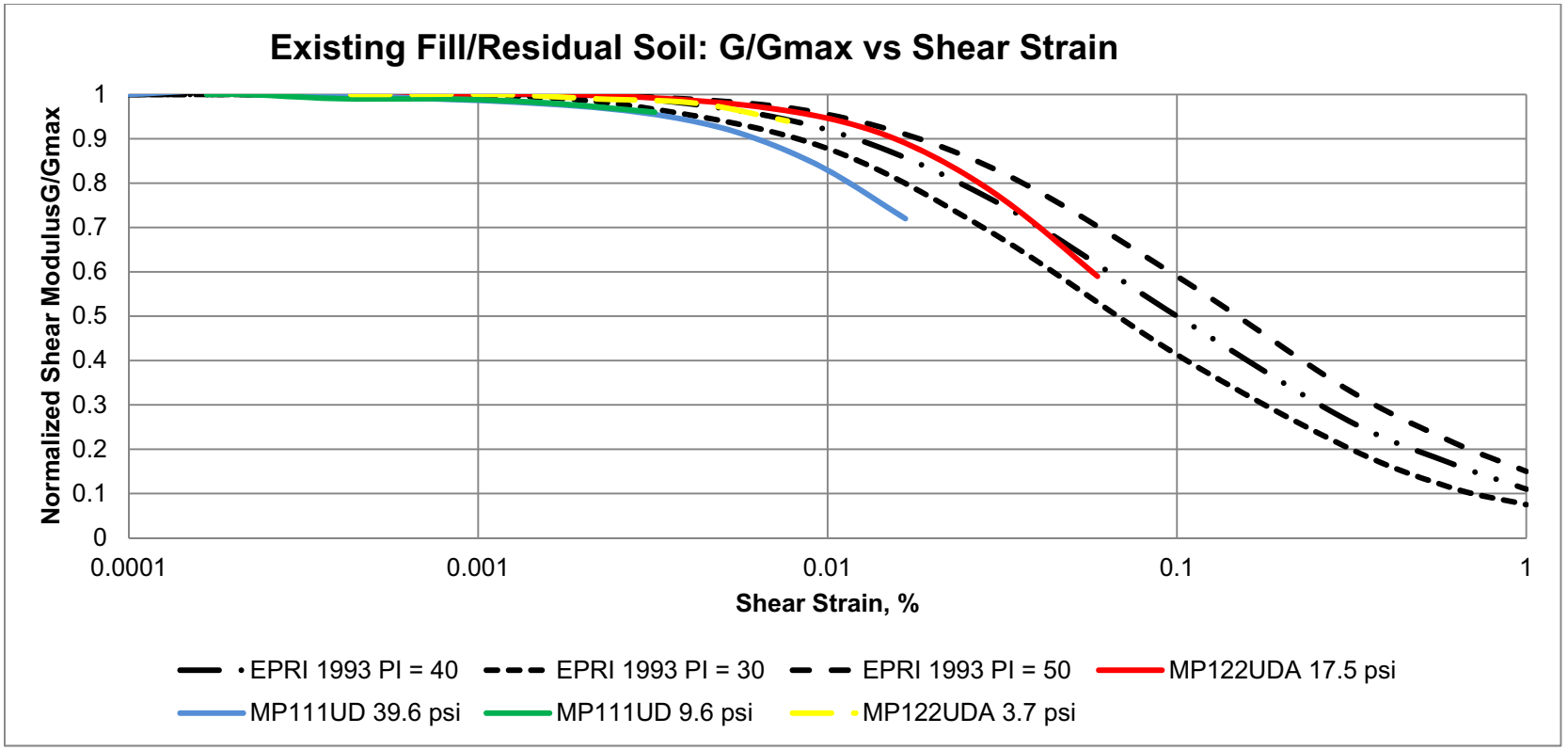

Figure 2.5.4-8. Normalized Shear Modulus Comparison for Existing Fill/Residual Soil

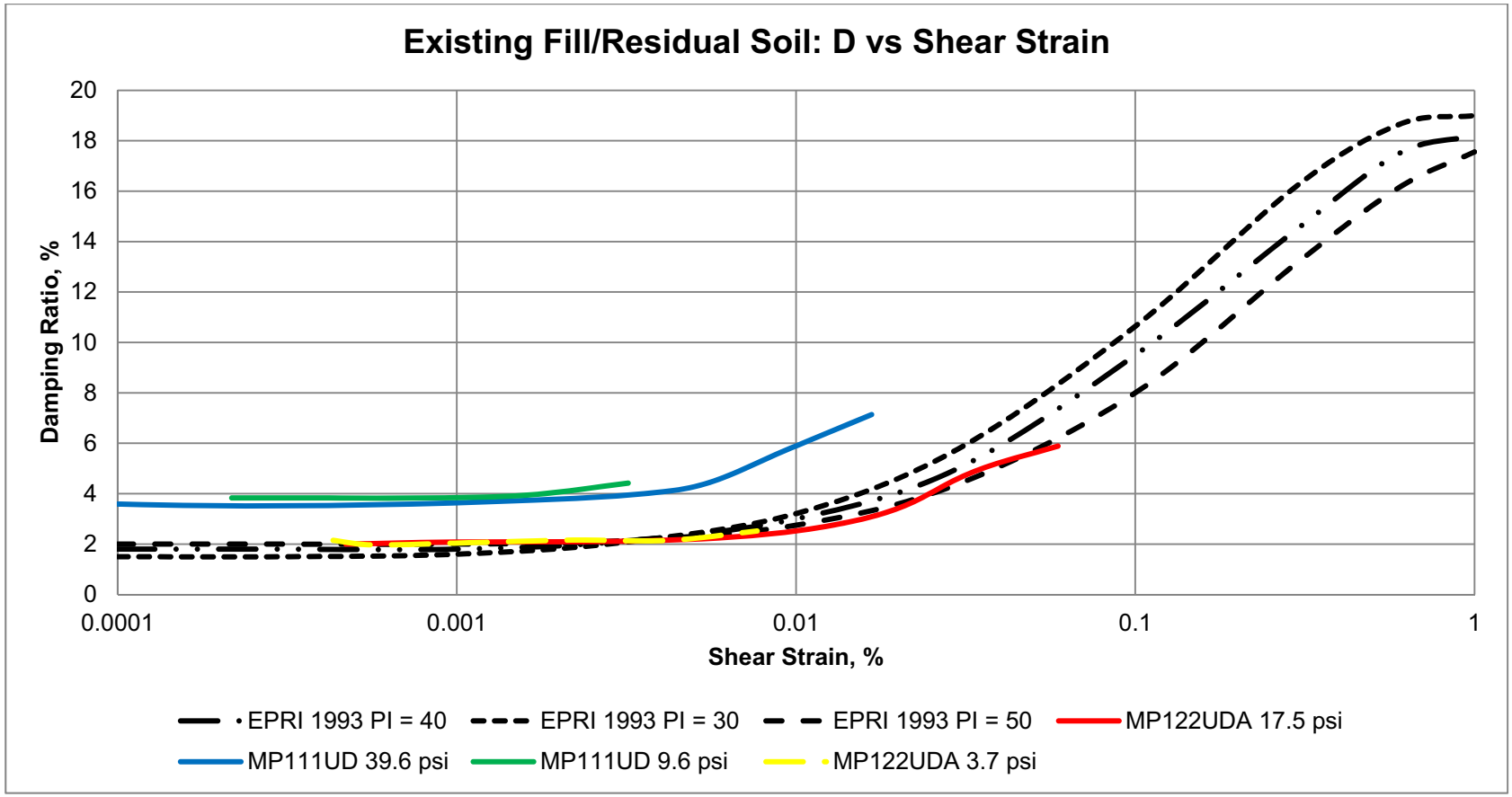

Figure 2.5.4-9. Damping Ratio Comparison for Existing Fill/Residual Soil

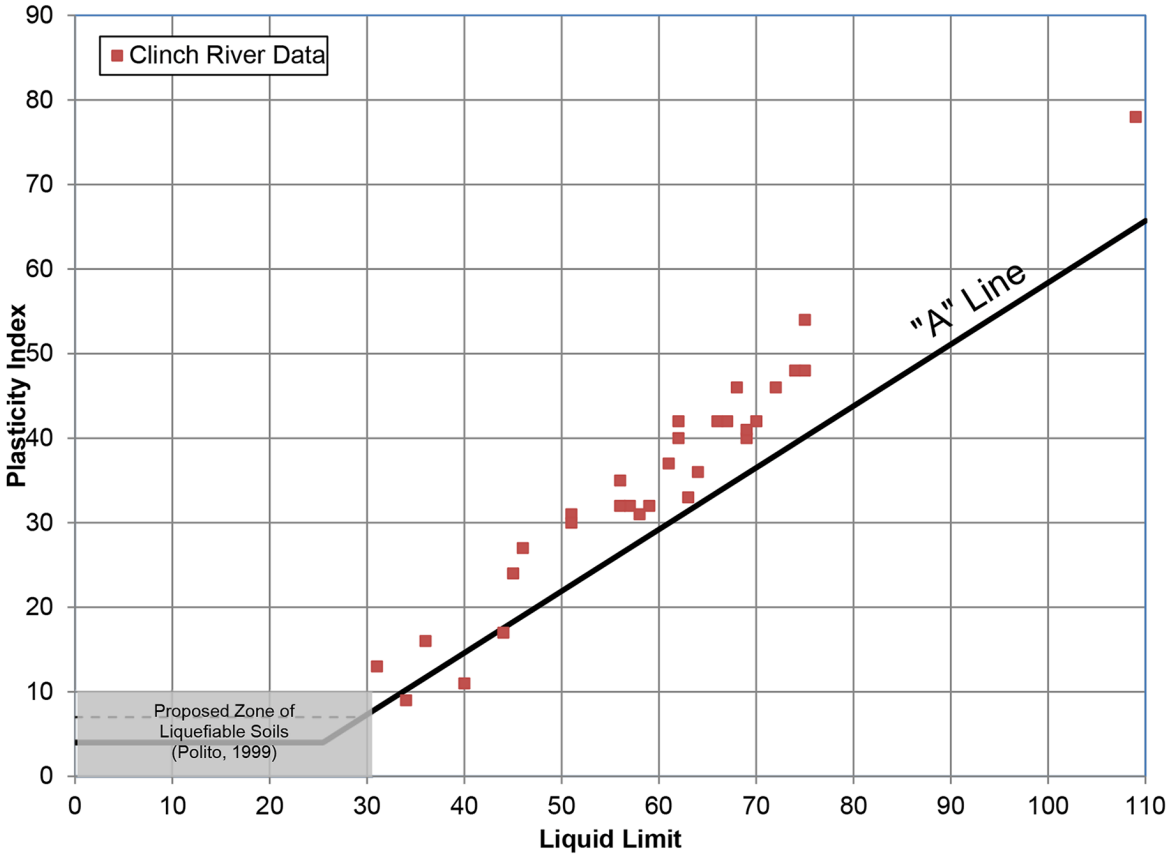

Figure 2.5.4-10. Atterberg Limits and Zone of Liquefiable Soils

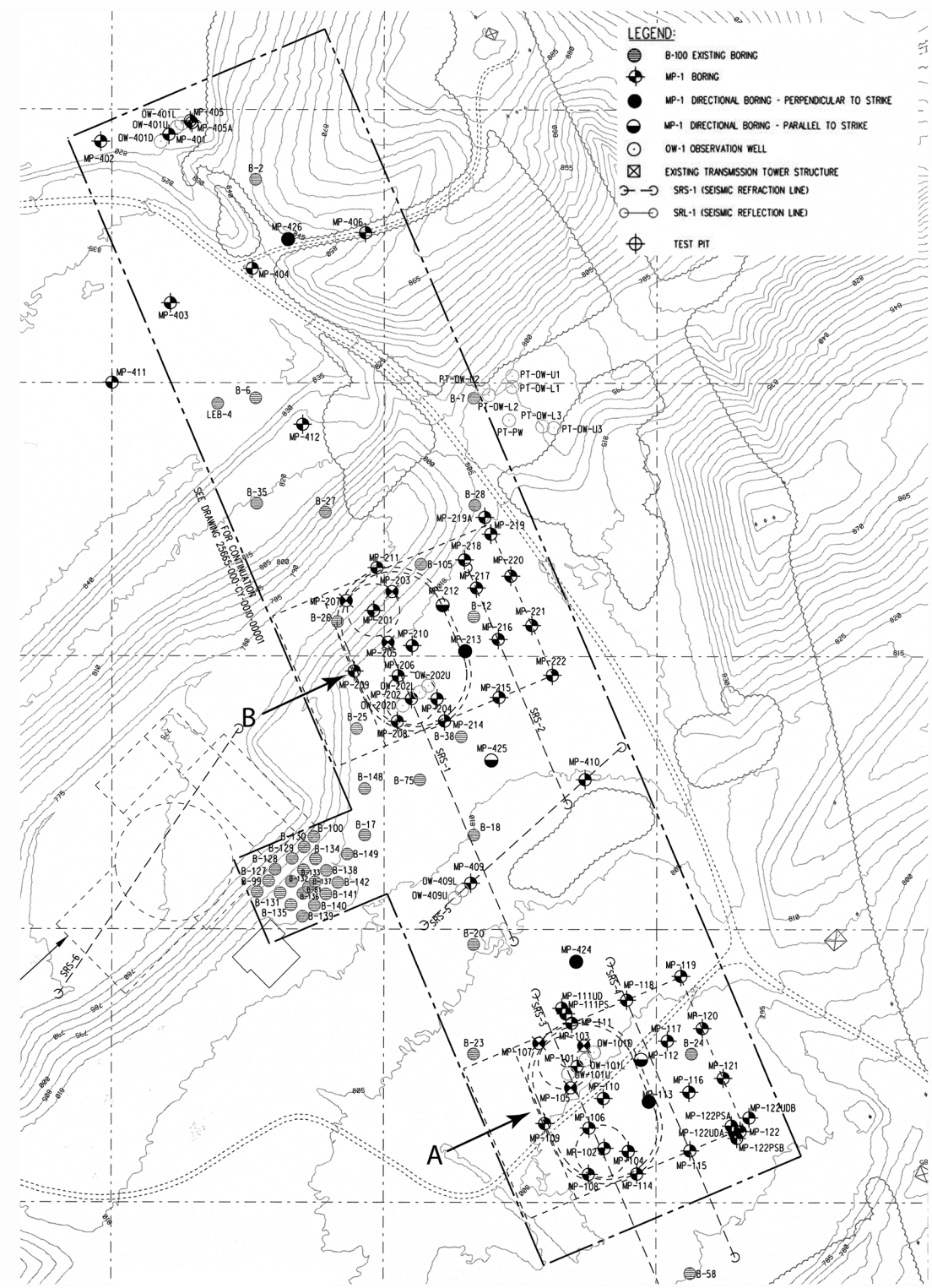

Figure 2.5.4-11. Boreholes at Locations A and B

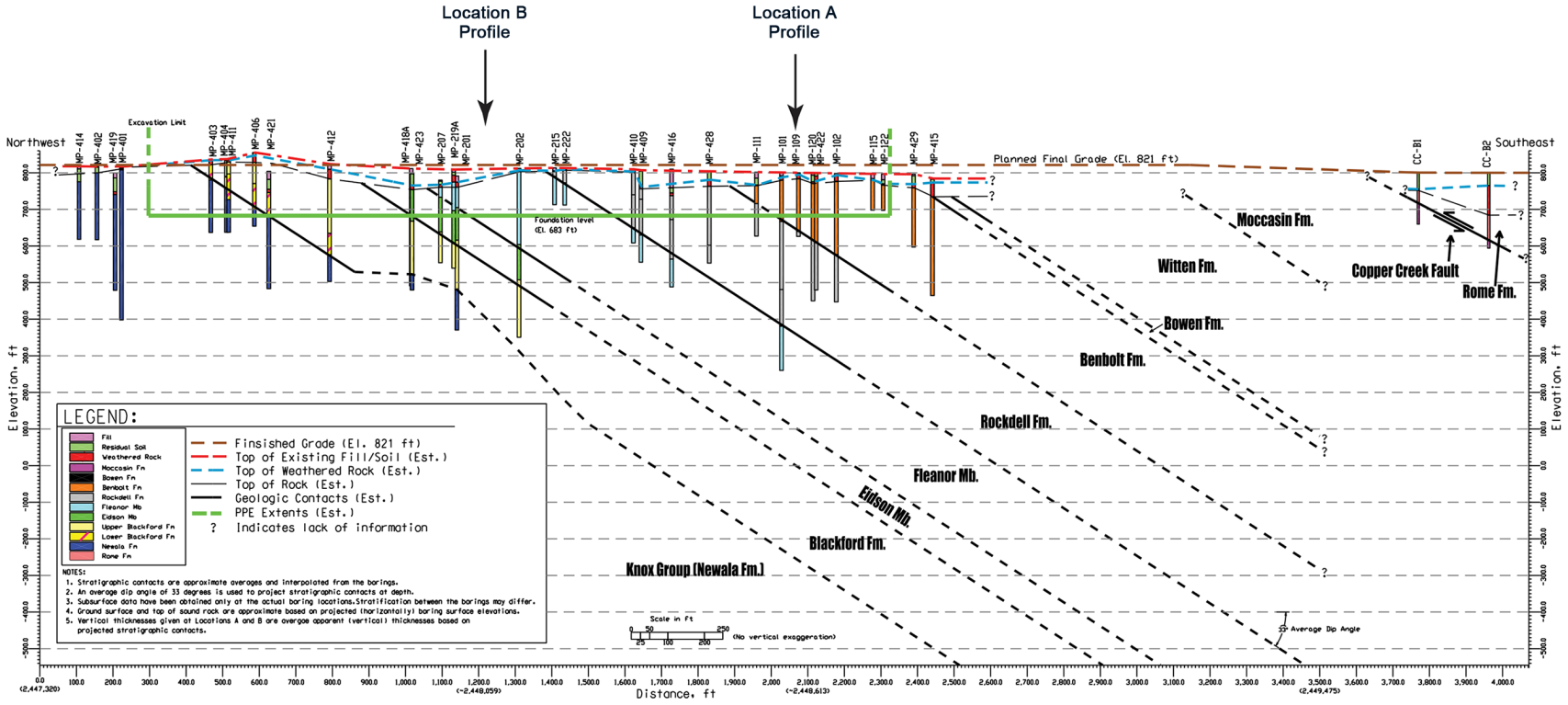

Figure 2.5.4-12. Cross-Section Showing Borehole Locations and Location of Profiles

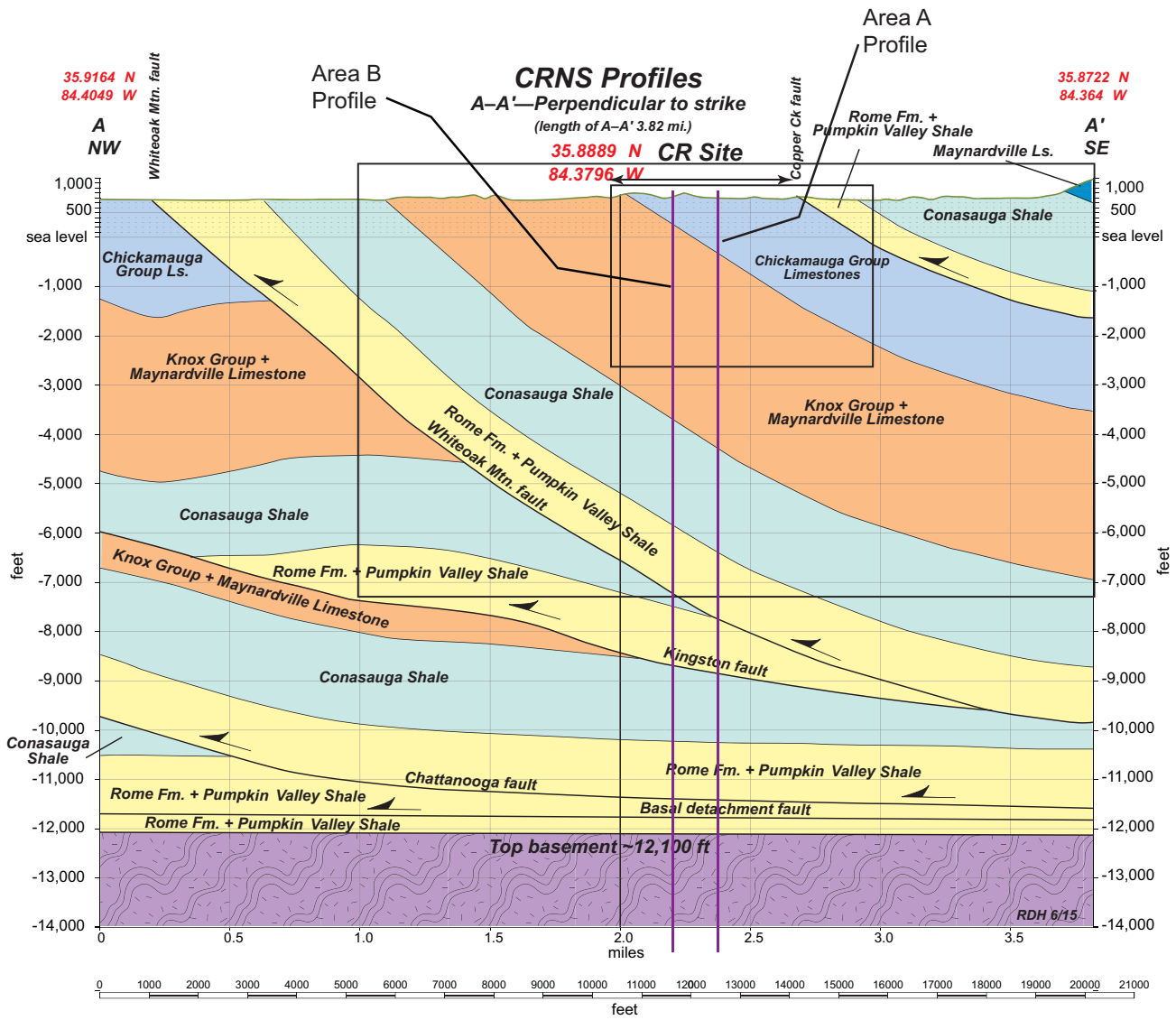

Figure 2.5.4-13. Geologic Cross-Section and Location of Profiles

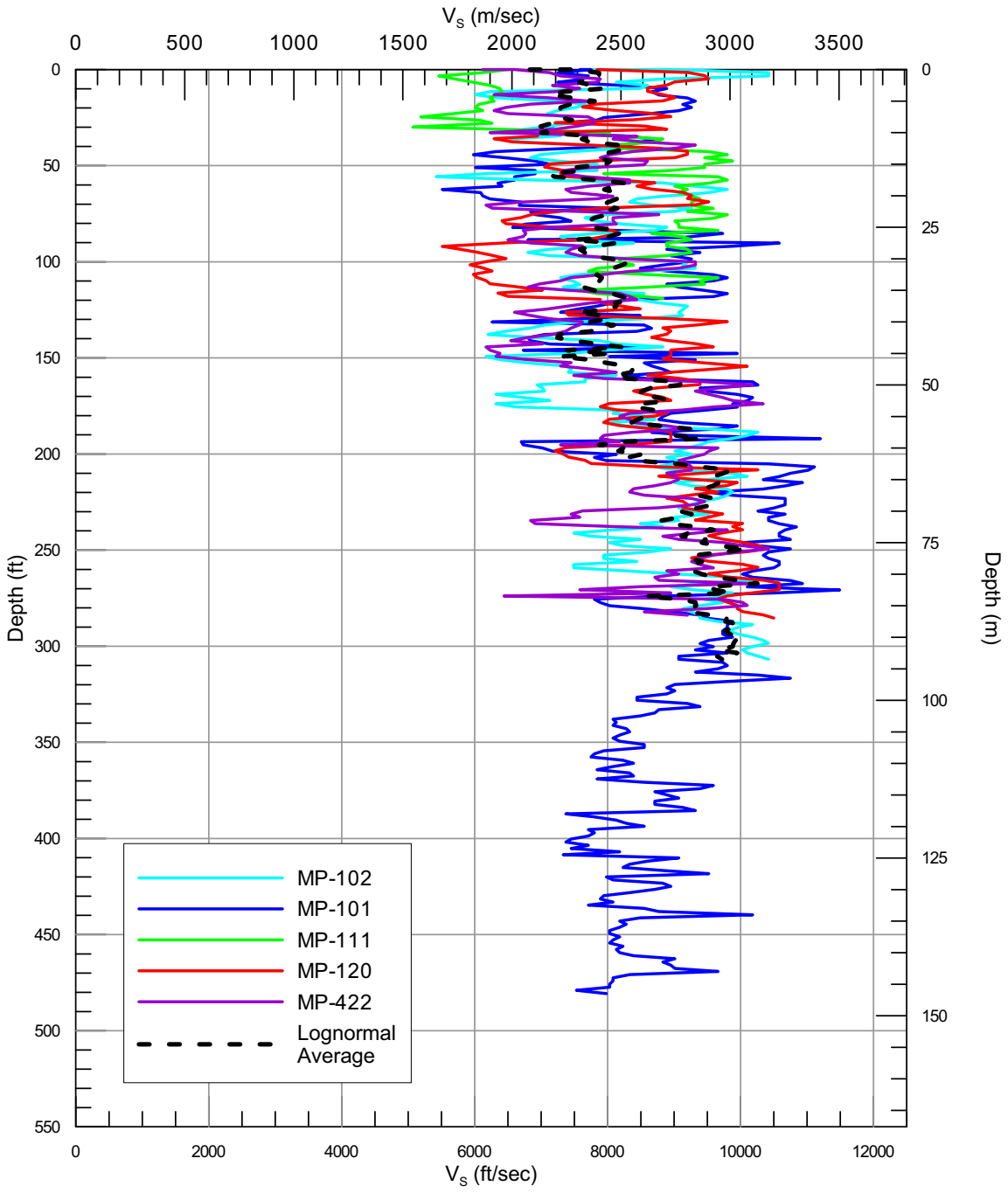

Notes: Data from P-S borehole logging
V_S based on receiver-to-receiver travel time

Figure 2.5.4-14. Shear Wave Velocity Profiles for Location A

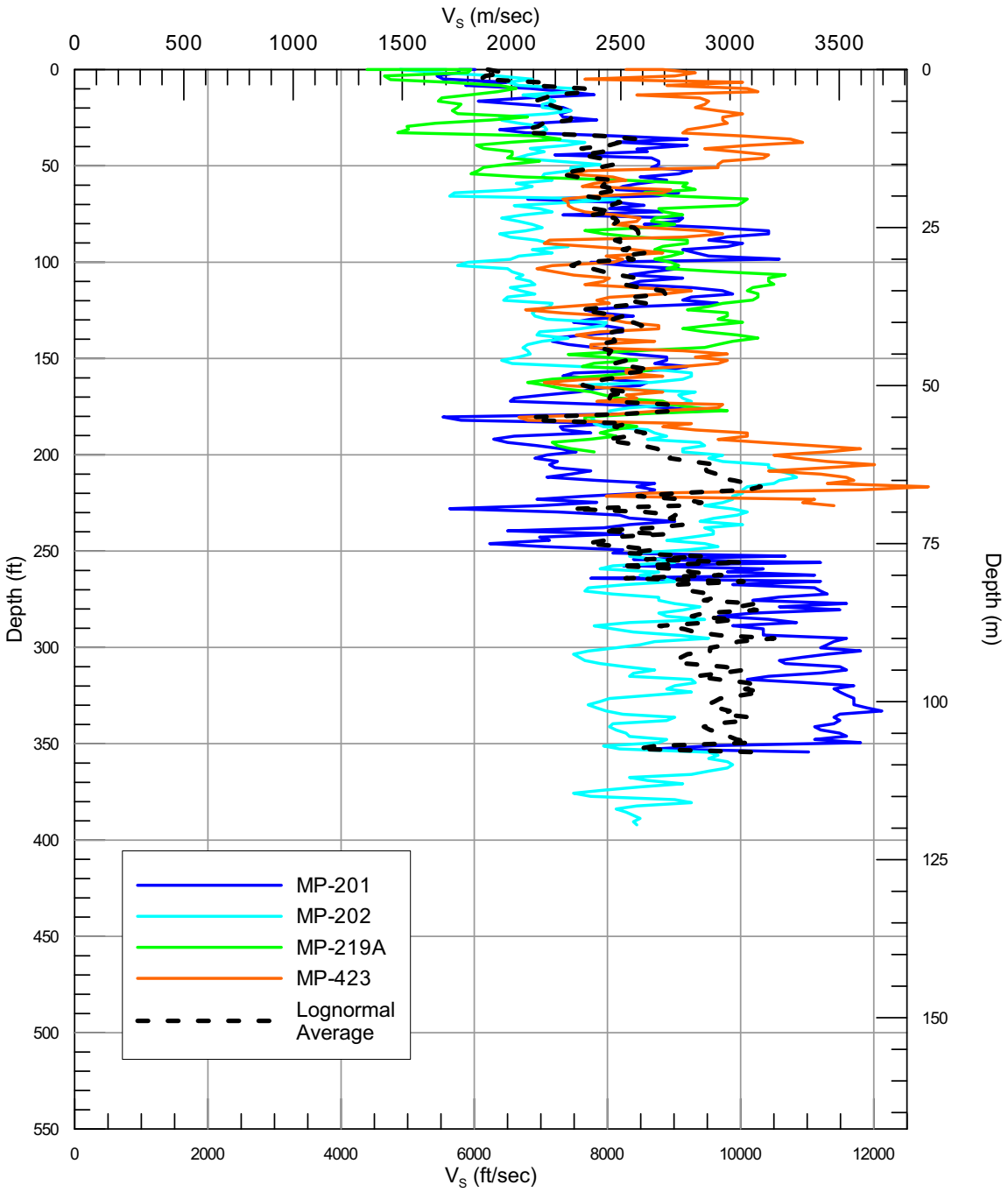

Notes: Data from P-S borehole logging
V_S based on receiver-to-receiver travel time

Figure 2.5.4-15. Shear Wave Velocity Profiles for Location B

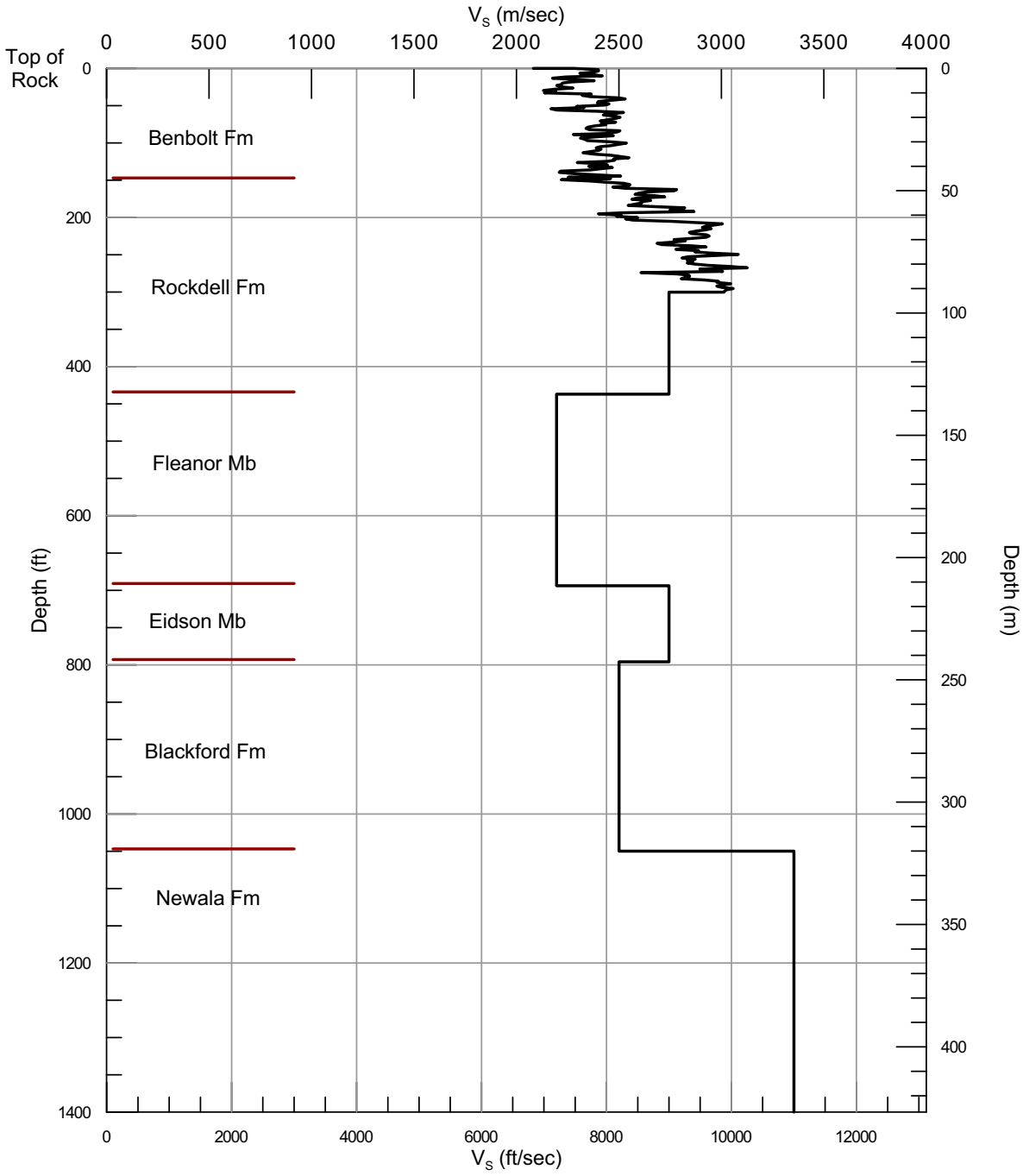

Figure 2.5.4-16. Shallow Shear Wave Velocity Profile for Location A

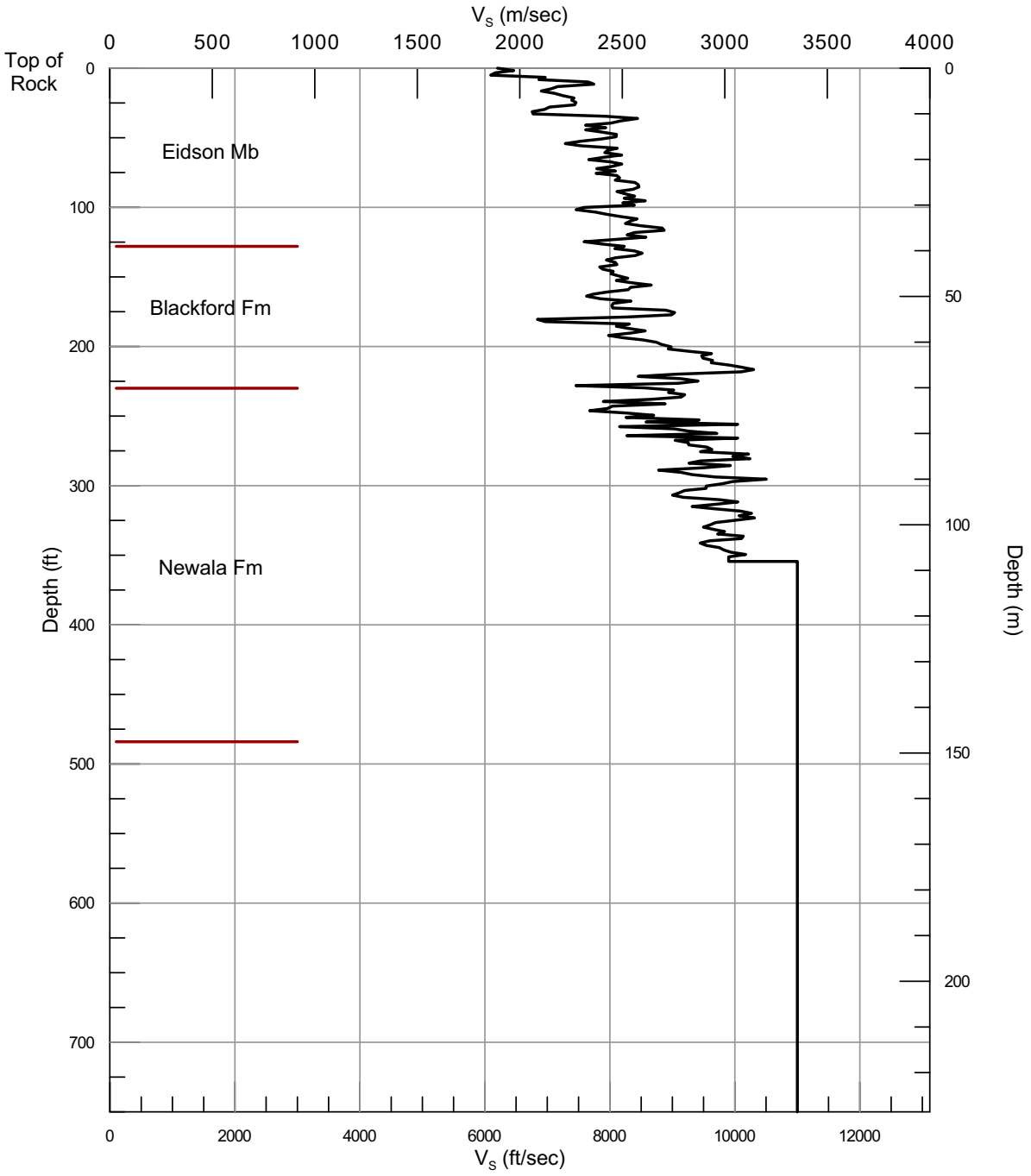

Figure 2.5.4-17. Shallow Shear Wave Velocity Profile for Location B

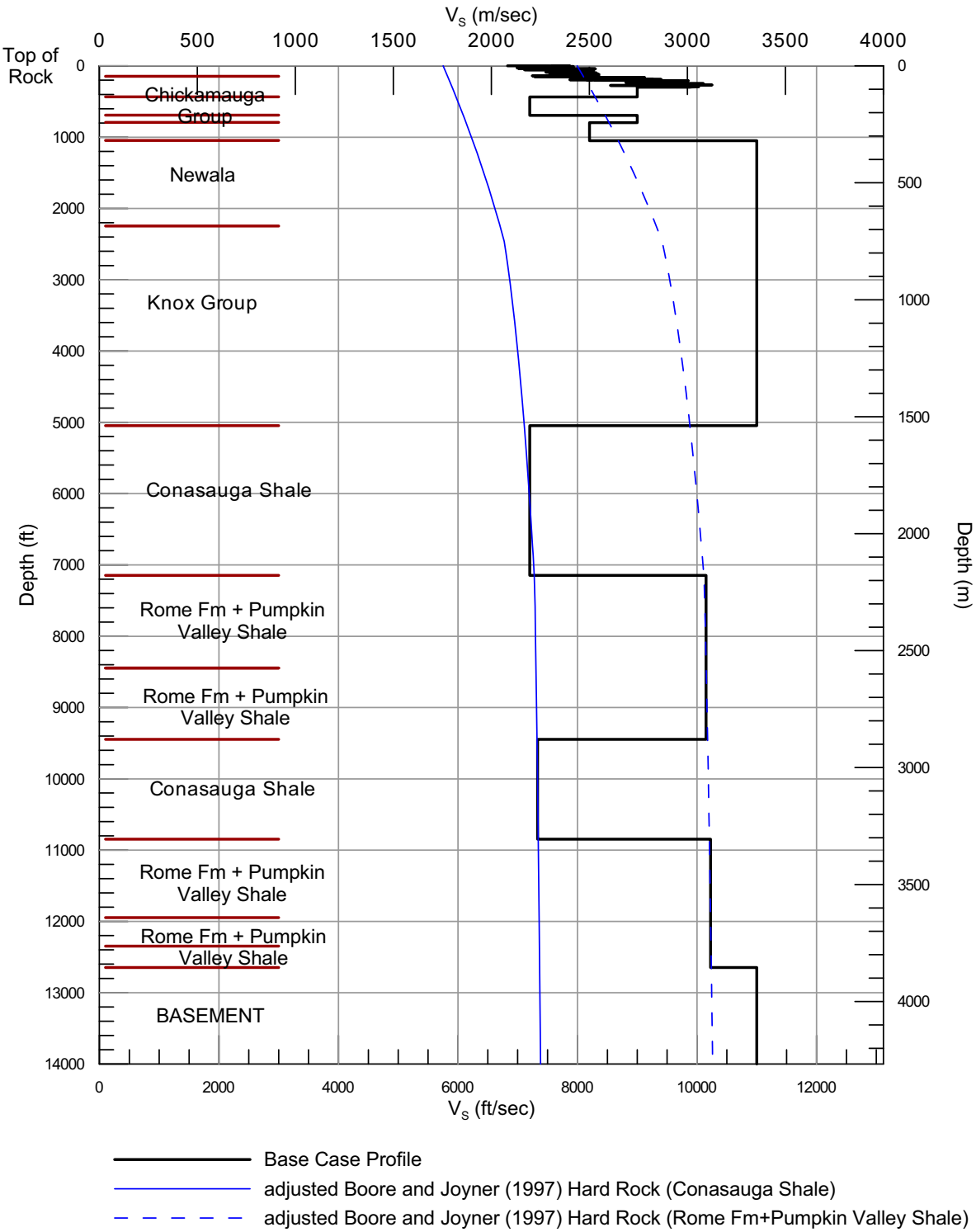

Note: Boore and Joyner (1997) is Reference 2.5.4-58

Figure 2.5.4-18. Geologic and Shear Wave Velocity Profile for Location A

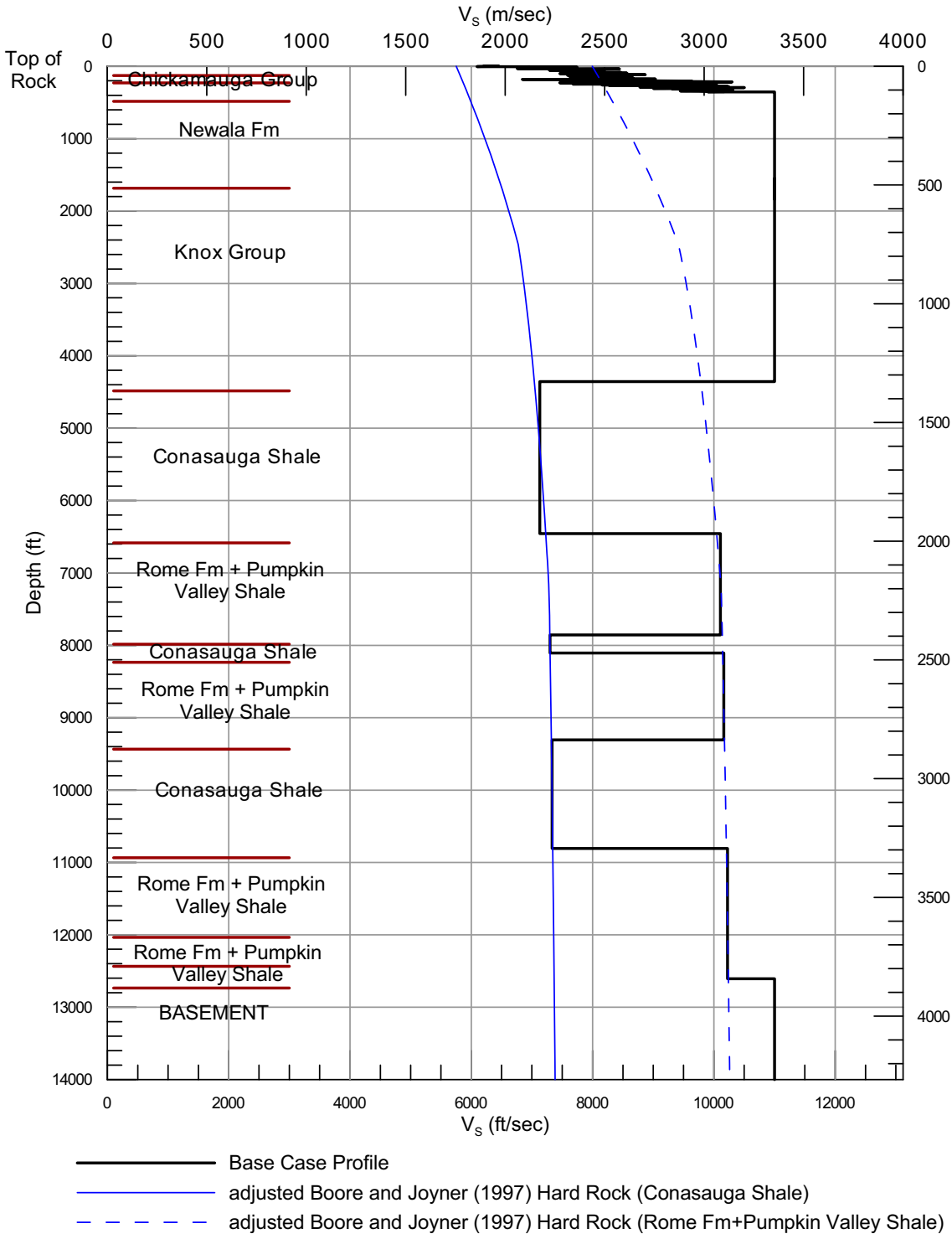

Note: Boore and Joyner (1997) is Reference 2.5.4-58

Figure 2.5.4-19. Geologic and Shear Wave Velocity Profile for Location B

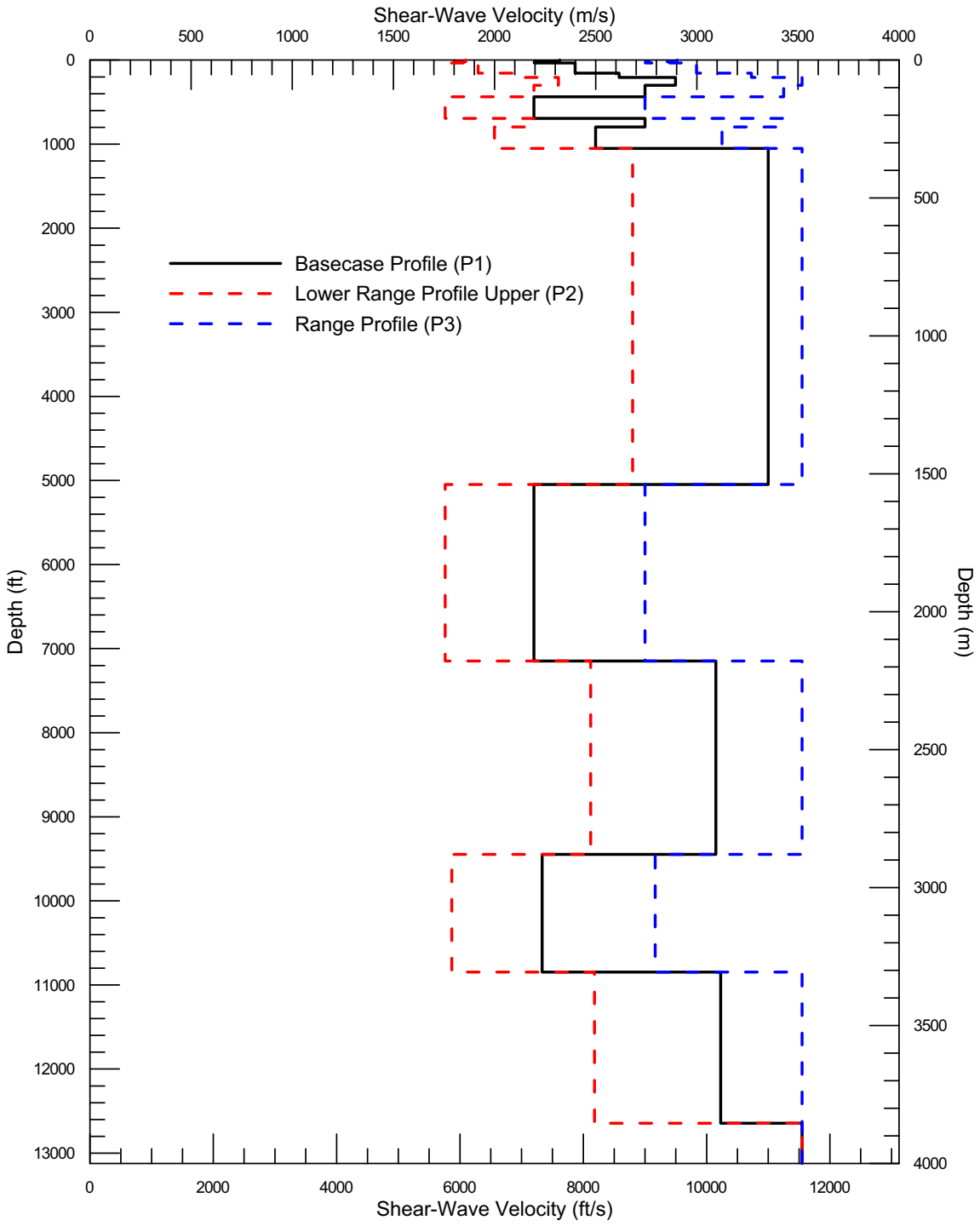

Figure 2.5.4-20. Basecase Shear Wave Velocity Profiles for Location A

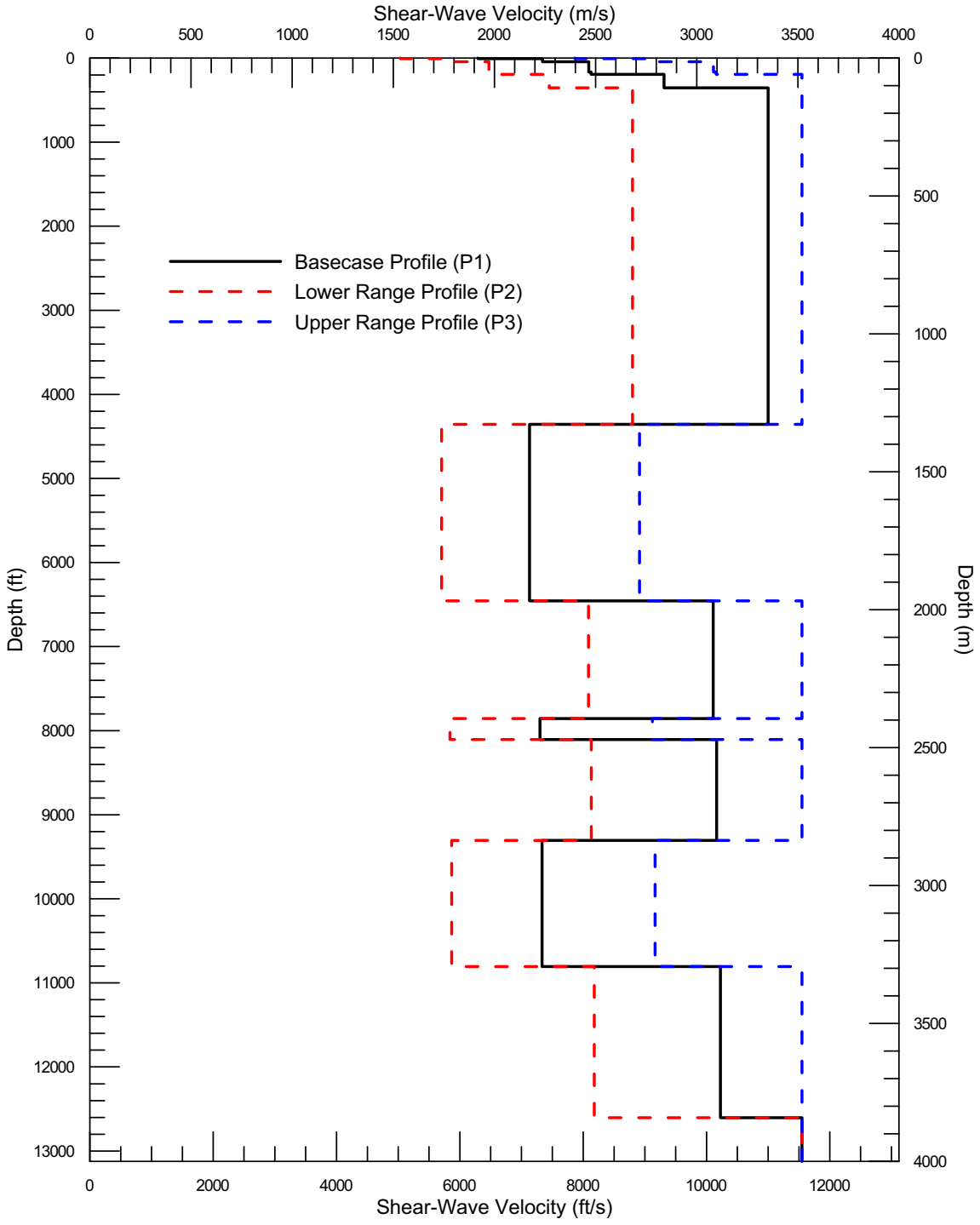

Figure 2.5.4-21. Basecase Shear Wave Velocity Profiles for Location B

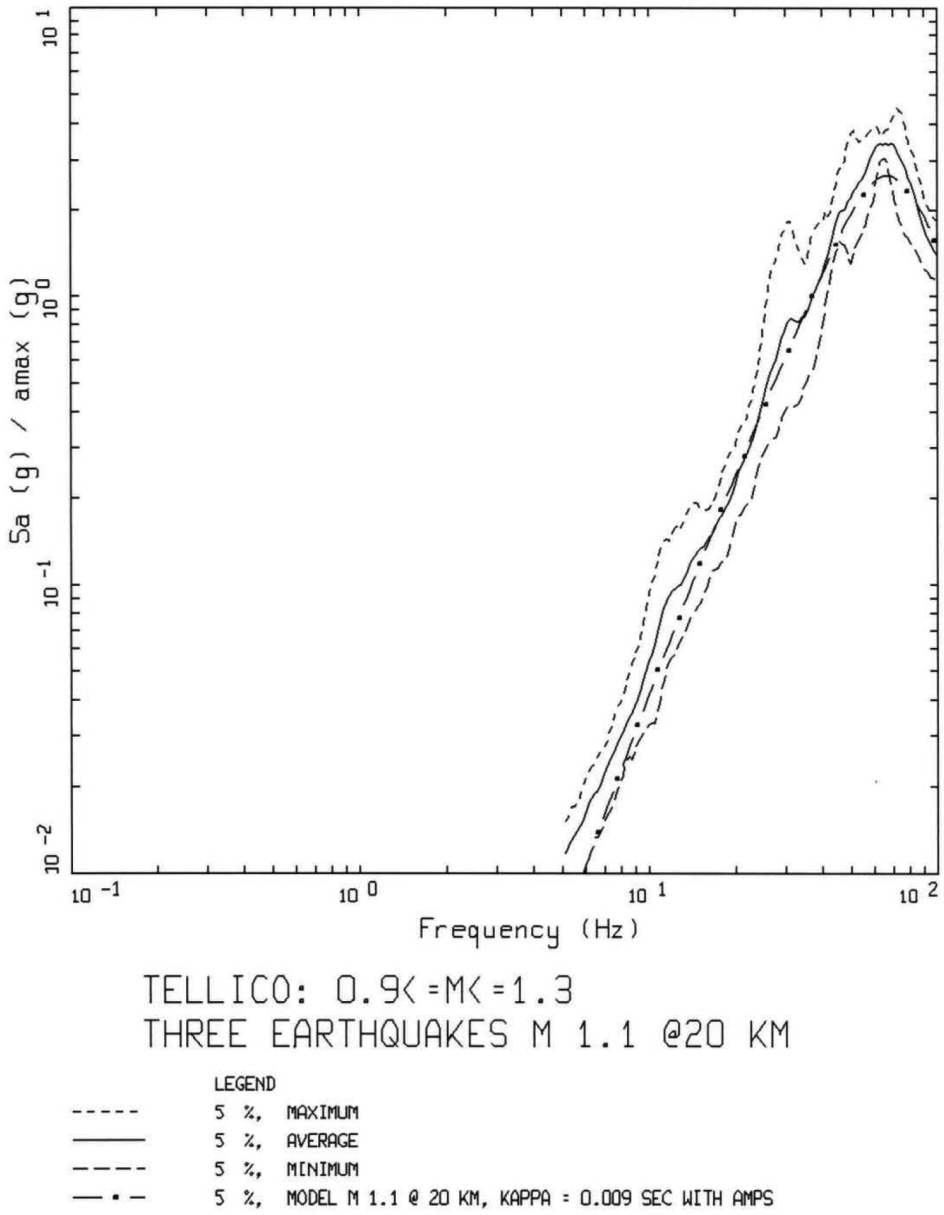

Figure 2.5.4-22. Response Spectral Shapes for Earthquakes at Tellico Dam Site (0.9≤M≤1.3)

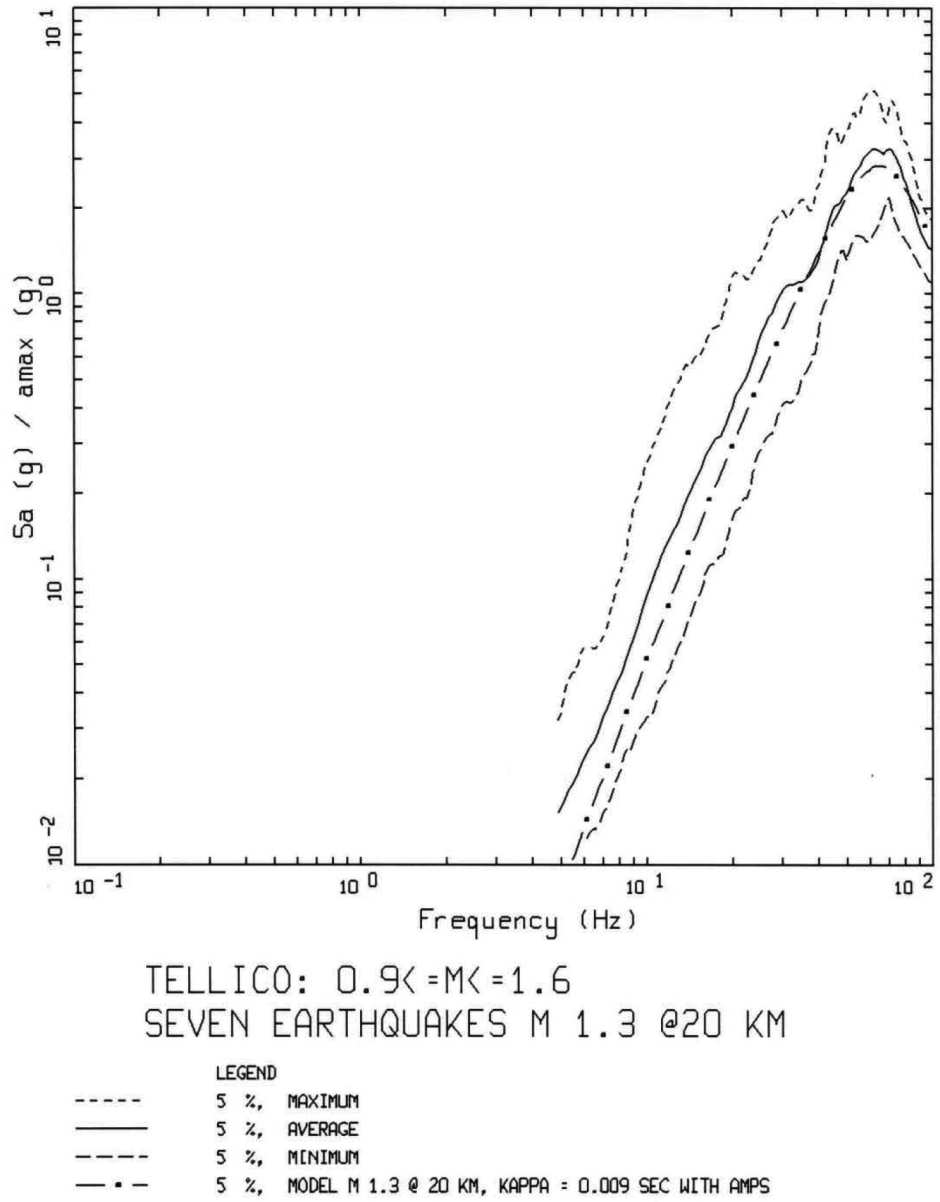

Figure 2.5.4-23. Response Spectral Shapes for Earthquakes at Tellico Dam Site (0.9≤M≤1.6)

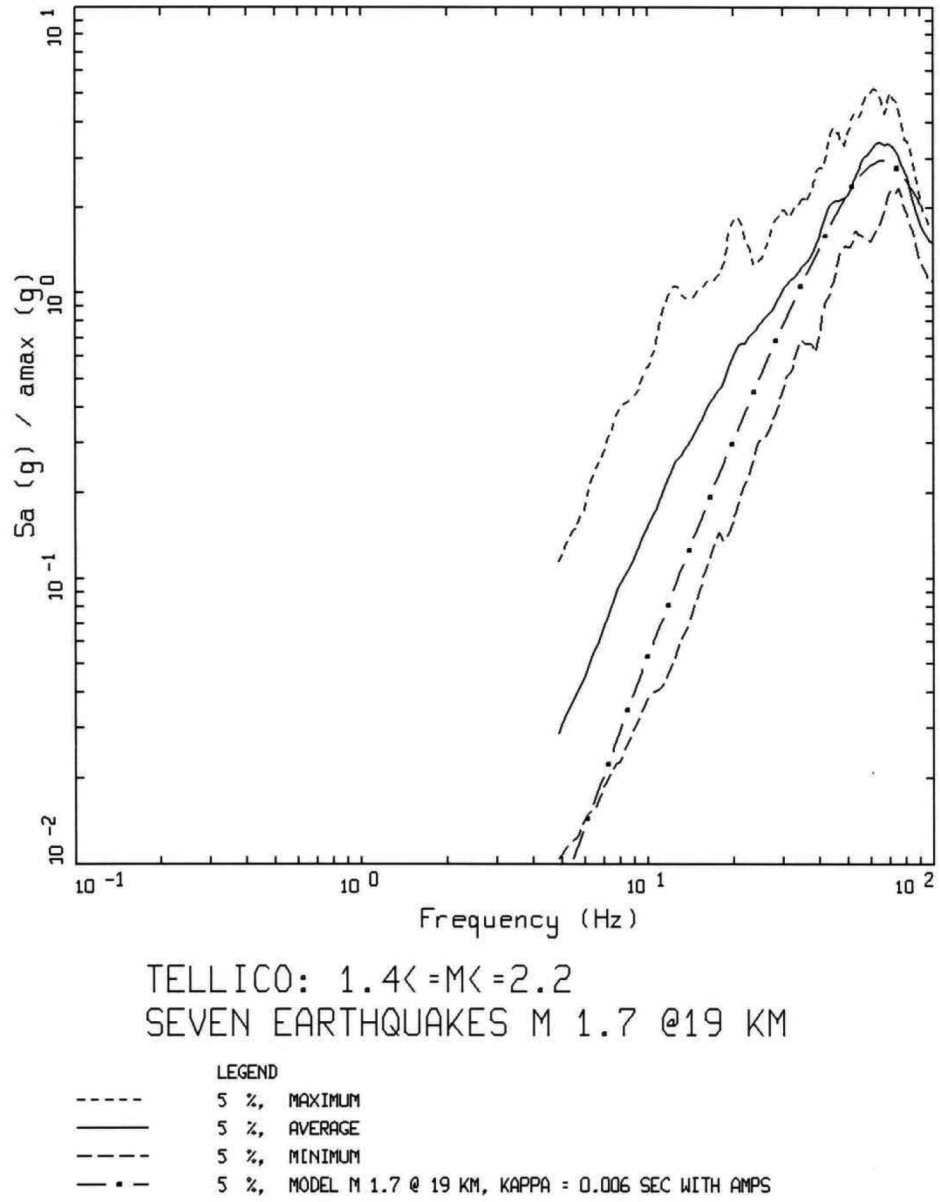

Figure 2.5.4-24. Response Spectral Shapes for Earthquakes at Tellico Dam Site (1.4≤M≤2.2)

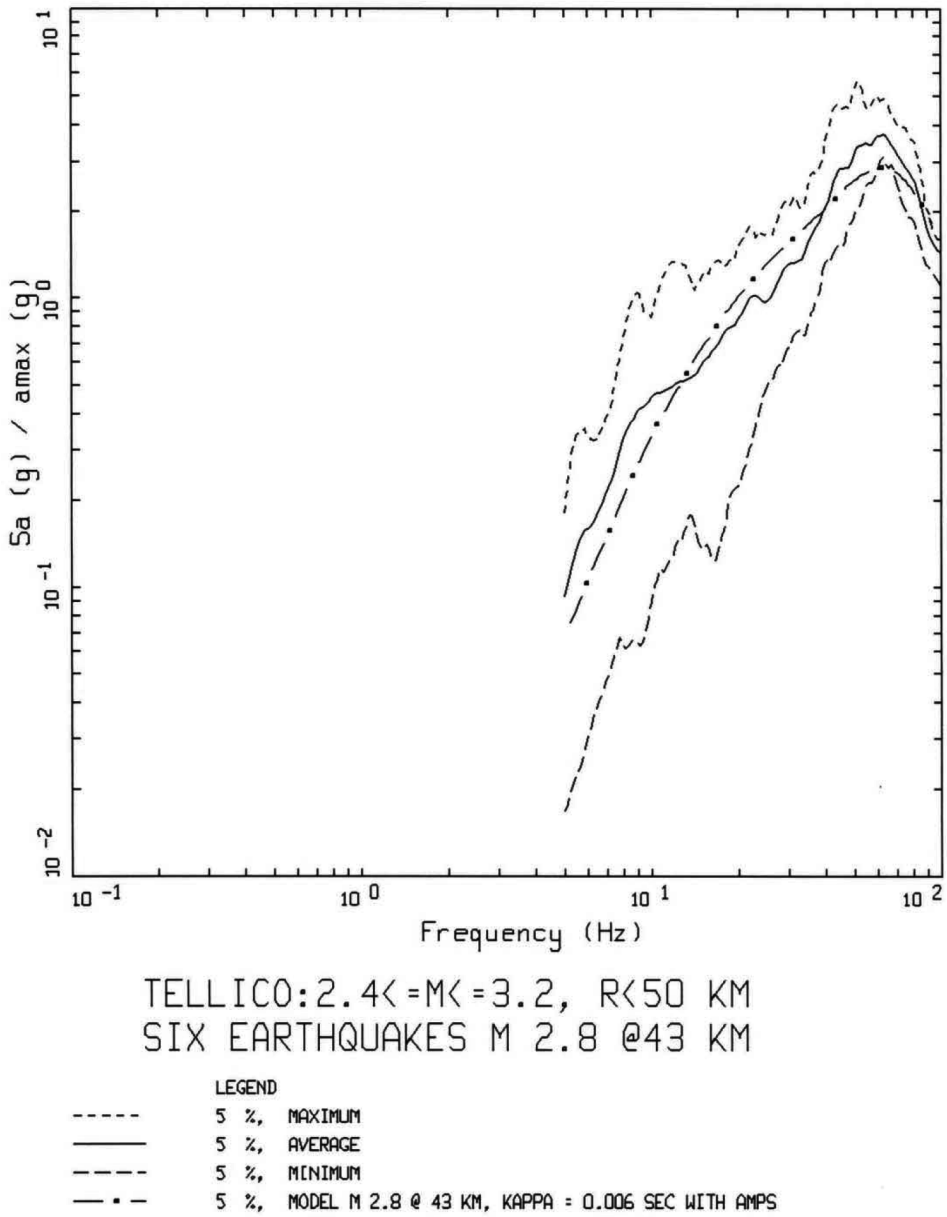

Figure 2.5.4-25. Response Spectral Shapes for Earthquakes at Tellico Dam Site (2.4≤M≤3.2)

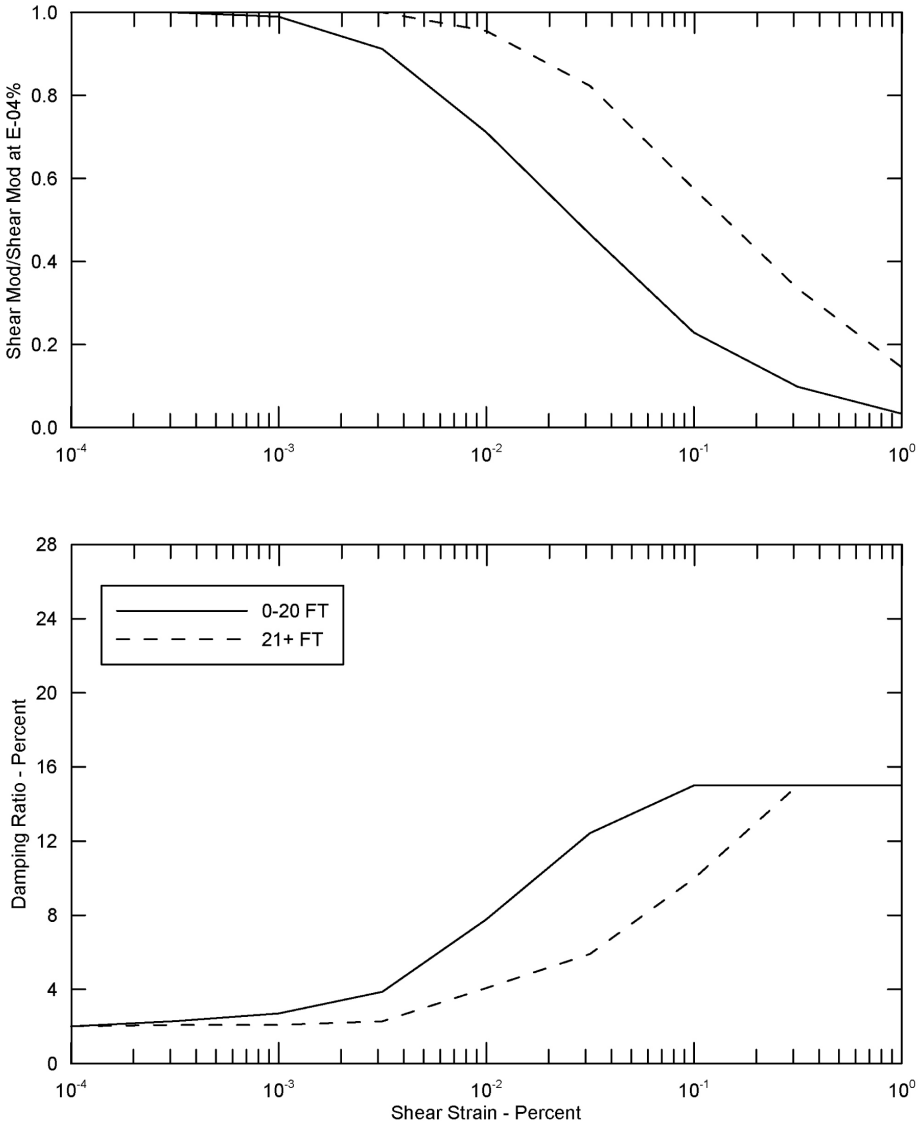

Figure 2.5.4-26. Shear Modulus Reduction and Damping Curves for Firm Rock

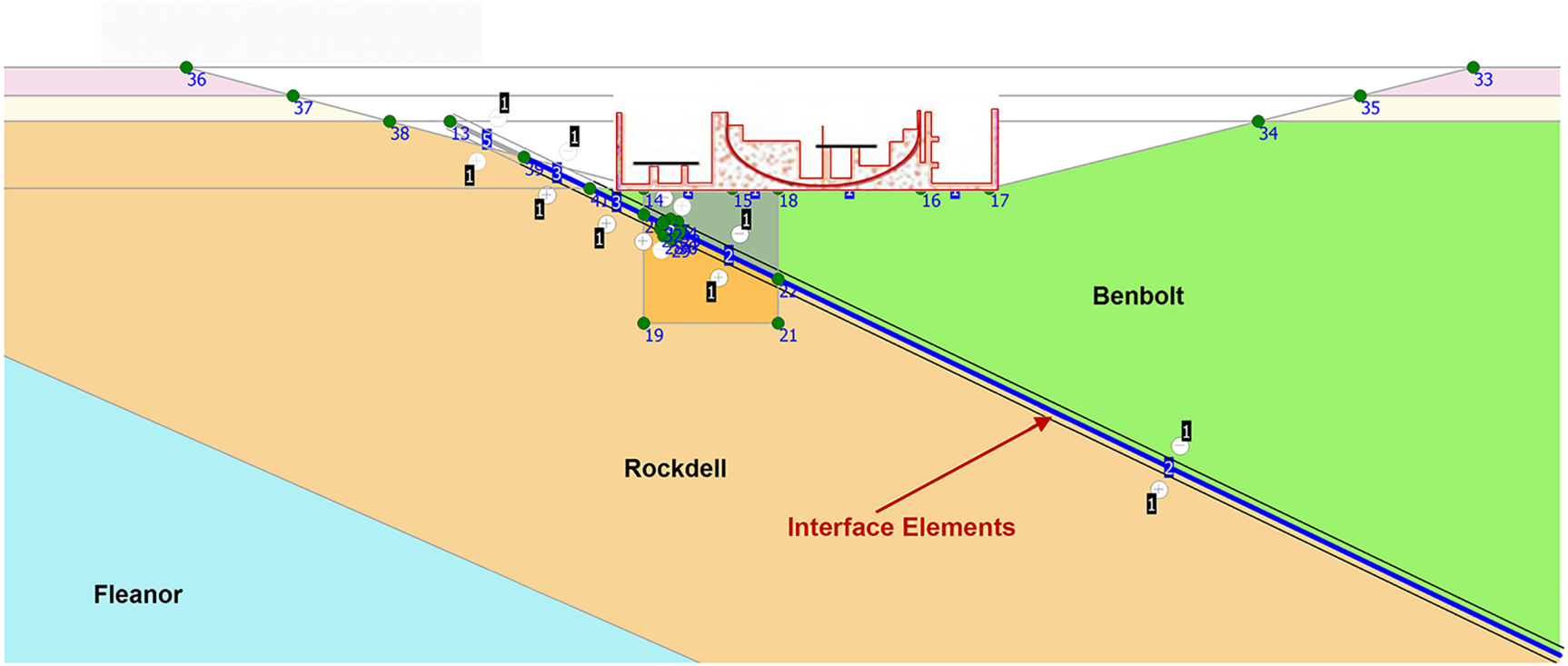

Note: Reference 2.5.4-59 Figure 2-14
Cavity Diameter: 15 ft
Embedment Depth: 90 ft
Cavity Location: 30 ft below Edge of Common Basemat
Interface Elements at Formation Contact

Figure 2.5.4-27. Finite Element 2D Model of Foundation Location A, Cross Section: A-A'

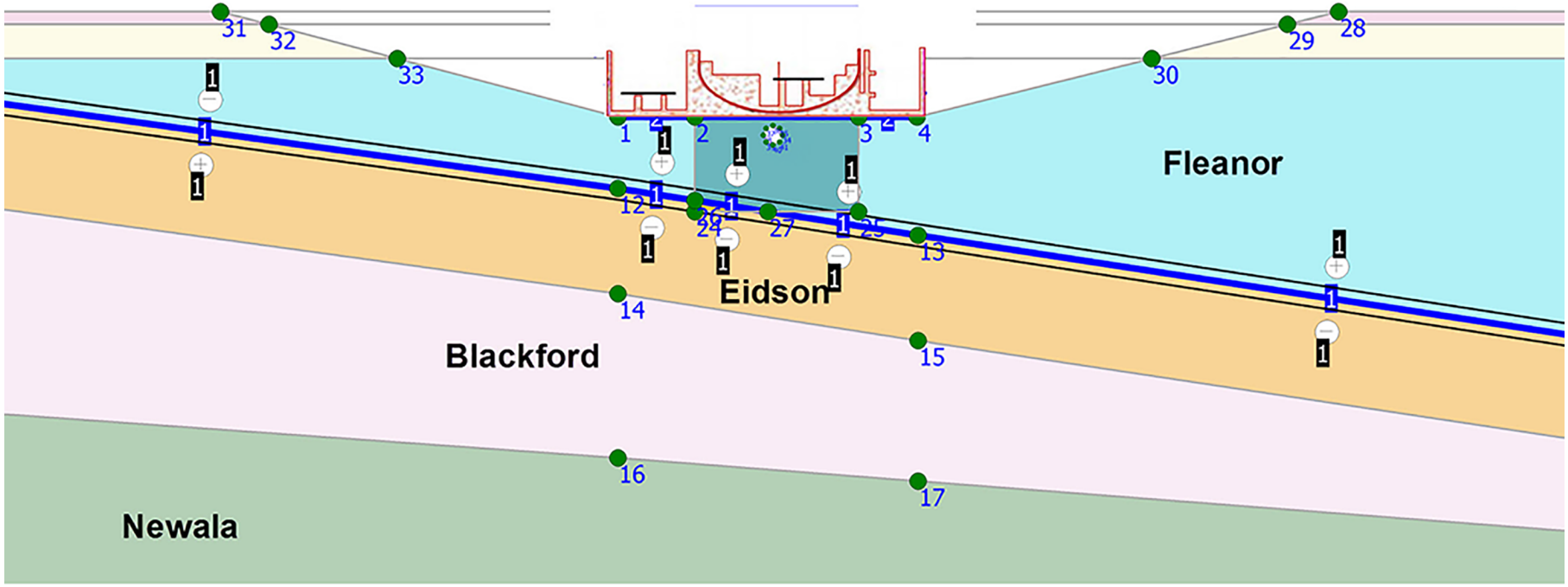

Note: Reference 2.5.4-59 Figure 2-29
Cavity Diameter: 15 ft
Embedment Depth: 90 ft
Cavity Depth: 5 ft Below Foundation
Cavity Location: Center of Common Basemat
Interface Elements at Formation Contact

Figure 2.5.4-28. Finite Element 2D Model of Foundation Location B, Cross Section: F-F'

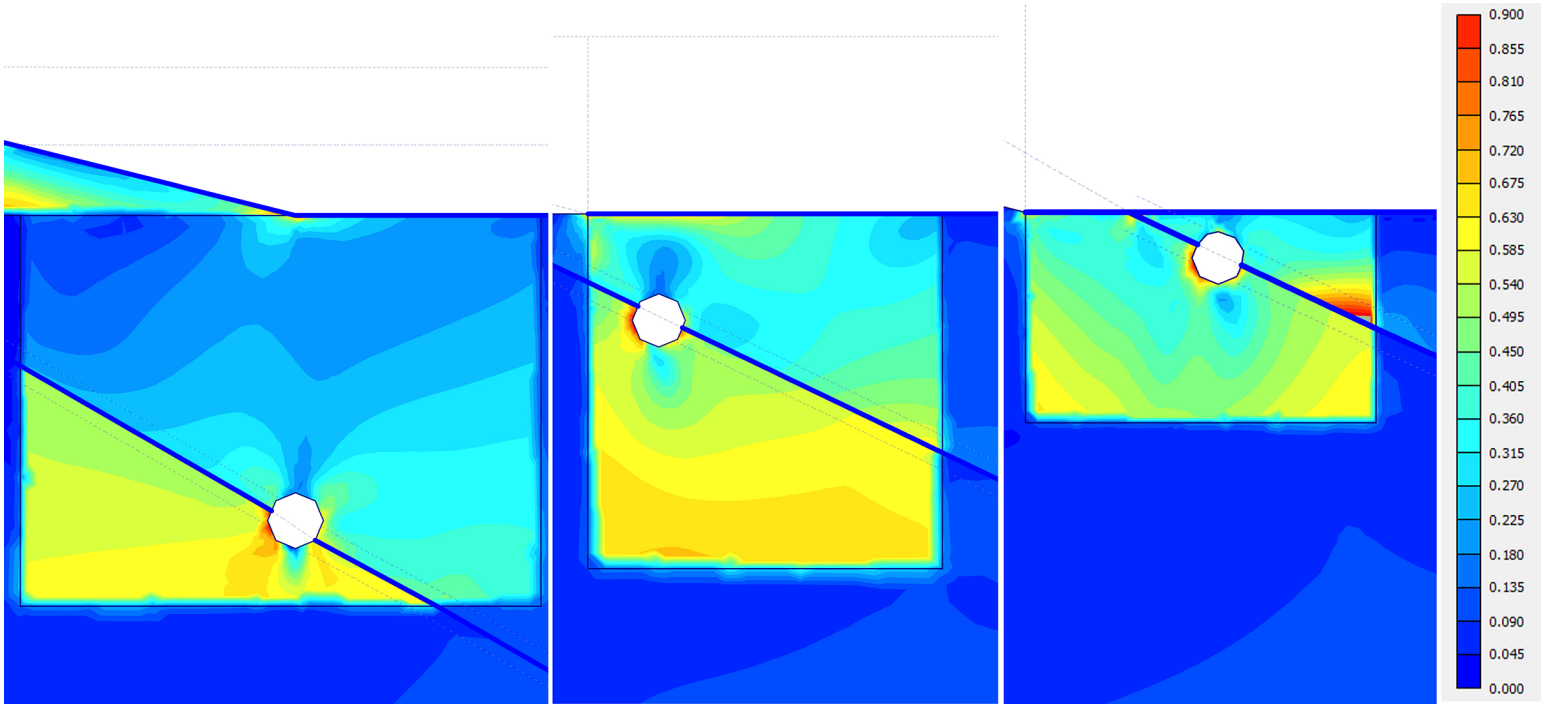

Note: Reference 2.5.4-59 Figure 3-7

Figure 2.5.4-29. Example Relative Shear Value Results for Foundation Embedment Depths of 140 ft (Left), 90 ft (Center), and 40 ft (Right)

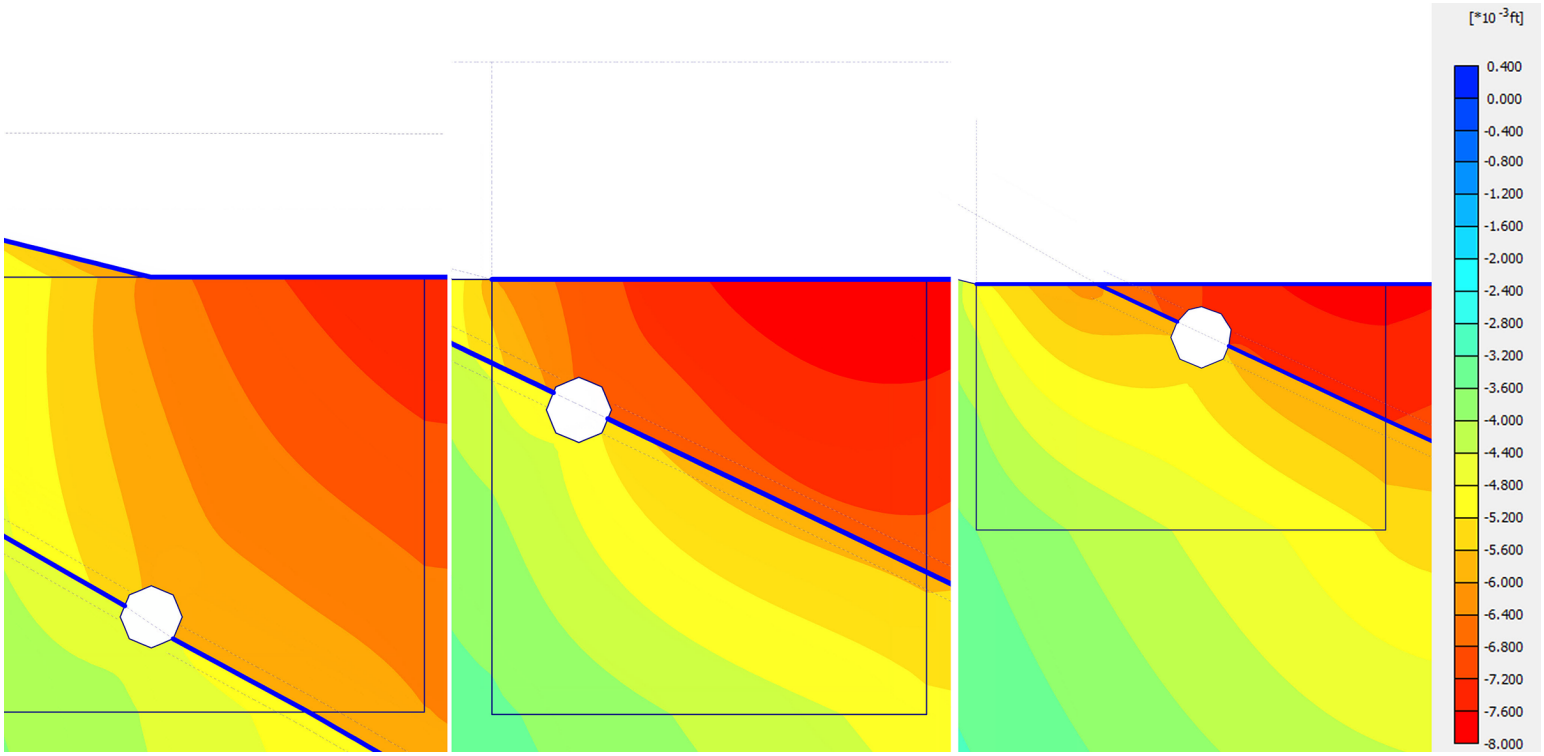

Note: Reference 2.5.4-59 Figure 3-8

Figure 2.5.4-30. Example Results for Vertical Deformations for Foundation Embedment Depths of 140 ft (Left), 90 ft (Center), and 40 ft (Right)